Raven SAR Rotorcraft

Advanced Rotor Control Concept

Alfred Gessow Rotorcraft Center
Department of Aerospace Engineering
University of Maryland, College Park
Maryland, 20742

University of Maryland

Alfred Gessow Rotorcraft Center
Department of Aerospace Engineering
University of Maryland, College Park
Maryland, 20742

Raven SAR Rotorcraft

In response to the 2001 Annual AHS International
Student Design Competition – Graduate Category
21 June 2001

Matthew Tarascio – Team Leader

Dr. Inderjit Chopra – Faculty Advisor

Marc Gervais

Gaurav Gopalan

Tim Gowen

Kristi Kleinhesselink

Jun Ma

Kiran Singh

Yong-sheng Zhao

Acknowledgements

The Terp Works design team would like to thank all of the people that assisted us during the 2001 AHS design competition. First and foremost, we would like to express our sincerest thanks to the faculty members that graciously offered their support throughout the entire project, including Dr. Marat Tishchenko, Dr. Alfred Gessow, Dr. V. T. Nagaraj, and Dr. Inderjit Chopra. We would also like to thank our fellow students who offered us their support, particularly Taeoh Lee, Jayanarayanan Sitaraman and Harsha Prahlad. And finally, we would like to send a special thanks to the SAR operators who took the time to respond to our questions, including Philip Hogan (Senior Helicopter Paramedic – Victorian Air Ambulance), Chris Snyder (Director of Coast Guard and Federal Programs – Agusta Westland), Daniel Tyler (SAR/EMS Senior Pilot – Care Flight Services), Lieutenant Strumm (Pilot – NAS Patuxent River SAR), Lieutenant Gancayco (Pilot – NAS Patuxent River SAR), AMHC Robert Mirabal (Crew Chief – NAS Patuxent River SAR), AT1 Jason Van Buren (Rescue Swimmer – NAS Patuxent River SAR), and HM2 Jason Owen (Medical Technician – NAS Patuxent River SAR).

Table of Contents

Executive Summary

Introduction

The Raven is a dedicated Search and Rescue (SAR) helicopter that has been designed in response to the 2001 AHS International Request For Proposal (RFP) for 'Advanced Rotor Control Concepts'. The objective of this student design competition, which is cosponsored by Boeing, is to develop a conceptual design of a modern civil SAR VTOL rotorcraft that incorporates new and innovative methods of controlling the pitch of the rotor blades. The primary challenge outlined in the RFP is the development of an advanced, high performance, rotor control mechanism that is not only affordable, but also capable of being developed to meet flight safety qualification and airworthiness requirements. It is anticipated that launch of the configuration will lead to delivery of the first aircraft in the year 2015 and therefore the new system is to provide dramatic improvements in performance over existing SAR configurations.

Mission Requirements

The primary mission of the Raven is to provide search and rescue service in IFR conditions out to a range of 300 nautical miles. The mission details are loosely based upon the mission flown in the "The Perfect Storm" and include fly-out, loiter, perform a rescue of two people and return to base, with two flight crew and two pararescuers onboard. The adverse conditions in which the rescue is to be performed include crosswinds gusting up to 45 knots, with large 60 knot headwinds specified during the return segment. The design is further constrained by a stringent One Engine Inoperative (OEI) requirement that stipulates a OEI Hover-Out-of-Ground-Effect (HOGE) capability at 60% fuel and full payload capacity, using no more than emergency power at sea level, ISA+20°C conditions.

Optimum SAR Configuration

The Raven was developed to be responsive to the unique requirements of search and rescue missions and presents an optimum SAR design solution. An optimum configuration was arrived at by developing a set of fundamental design drivers that were based upon mission requirements and operator suggestions. This approach allowed the key SAR design requirements to be highlighted at an early stage, allowing the team to focus its efforts on the issues that most heavily impact upon SAR mission success. A comprehensive configuration study was undertaken based on these drivers, to enable the best configuration to be selected from a large number of potential SAR candidates. In order to downselect the most promising candidates, their relative 'goodness' was established by a measure of both design attributes and performance, with attributes assessed on a qualitative basis and performance on a quantitative one. The results of the qualitative analysis concluded that a helicopter configured with a fan-in-fin anti-torque system would provide the best SAR design solution to the specified mission requirements. In fact, during the trade studies a new measure of SAR mission effectiveness was developed to ensure that the best configuration was indeed selected. This enabled a direct comparison to be made of the SAR potential of the three primary configuration types; helicopter, tiltrotor, and compound. The resulting quantitative analysis once again concluded decisively in favor of the helicopter, which was able to outperform the tiltrotor and compound configurations in virtually all aspects of the mission.

Raven Design Features

The Raven is a twin engined, SAR helicopter with a fan-in-fin anti-torque system. It incorporates high value technologies in the main rotor, airframe, flight controls and crew station that enable it to offer the customer unsurpassed mission performance. The primary design features of the Raven are displayed in the foldout on page xii and are discussed in greater detail below.

Swashplateless Main Rotor

The advanced swashplateless, five bladed, bearingless main rotor system of the Raven was designed to offer a safe, reliable and efficient means of providing pitch control to the rotor blades. The system, which was the result of a comprehensive design study into swashplateless technologies, uses trailing edge moment flaps to generate the required pitch inputs and provides an optimum design solution in terms of reliability, performance and cost effectiveness. The salient design features of the main rotor are summarized below:

- The swashplateless control system consists of trailing edge moment flaps embedded into torsionally soft rotor blades and actuated by a revolutionary smart material known as magnetic shape memory alloy.
- The blade design incorporates advanced airfoil sections and optimized blade tips to enhance performance in both hover and forward flight. Furthermore, the blades are indexed at the root to minimize flap deflections in hover and forward flight, resulting in much improved drag characteristics.
- Each blade incorporates twin trailing edge flaps that are both capable of providing primary control should the other fail. A redundant system was developed in order to minimize future certification costs and ensure a high level of system reliability.
- There are two flap actuators in each blade (one per flap) located behind the main spar. This design improves the weight distribution of the blade by locating smaller flap actuators at multiple spanwise locations.
- The actuators are designed from a magnetic shape memory alloy which is capable of providing the desired flap deflections and frequency throughout the entire flight envelope.
- Each actuator is readily accessible through access ports that have been designed into the blades. Additionally, the design incorporates the ability for manual blade folding to enhance mission flexibility and minimize hangar space.
- The hub design is bearingless, which produces a clean aerodynamic surface and results in low hub drag. Furthermore, simple dual operation compression pitch springs are incorporated into the hub design, in place of conventional pitch links, to accommodate the low blade torsional frequency requirement of the moment flap design.
- To transition the required power from the fixed frame to the blades, a contactless slip-ring was incorporated into the design, ensuring reliable and frictionless electrical transfer.
- Flap actuation is controlled via the Flight Control System (FCS), which gets feedback from sensors integrated into the blade. The status of the actuators and flaps are monitored by the HUMS, which ensures that the flaps are operating correctly and provides data to the pilot in the event of a failure.
- Active vibration and noise reduction is incorporated into the design by introducing higher harmonic pitch inputs at the embedded trailing edge flaps. A benefit of using flaps for primary control is that vibration and noise can be reduced without requiring any additional features to be added. Due to a large reduction in vibratory loads, the maintenance requirements of the Raven are expected to be significantly reduced.

- The swashplateless control system integrated into the Raven, which includes the on-blade actuators, cables, balance weights, additional blade structure (to stiffen the ribs around the actuators) and springs at the hub, is approximately 50% lighter than a conventional swashplate design. Furthermore, the design reduces operating costs by doing away with maintenance intensive hydraulic systems.

Crew Station

The Raven incorporates high value technologies in human factors engineering to allow it to interface seamlessly with the crew. The cockpit and cabin stations were specifically designed to enhance the SAR mission performance of the crew through improved situational awareness and reduced workload. The salient design features of the crew station are summarized below:

- The cabin is designed with large doors to facilitate rapid ingress and egress. Furthermore, the Raven incorporates an oversized fuselage to ensure ample space is available for efficient crew operations and extensive SAR/EMS equipment.
- An advanced digital 'glass' cockpit with large multi-function displays is provided to reduce crew workload and enhance mission flexibility. Crew workload is further reduced via the cockpit management system, automatic GPS search patterns, and cabin crew hover control.
- The large multi-function displays, powerful searchlight, FLIR and helmet mounted displays all serve to increase the situational awareness of the crew throughout the entire SAR mission.
- The crew stations were designed after extensive consultation with SAR pilots, pararescuers and crew station design experts to ensure the unique requirements of SAR missions were thoroughly addressed.

Flight Control System

The Flight Control System (FCS) for the Raven is a triple redundant, digital, Fly-by-Wire (FBW) system that ensures a predictable response, enabling helicopter pilots to fly the vehicle without requiring special training. The salient design features of the FCS are summarized below:

- The FCS maximizes safety and reliability by partitioning flight-critical and mission-critical control laws into a Primary Flight Control System (PFCS) and Automatic Flight Control System (AFCS).
- The PFCS has three separate redundant processors resulting in large improvements in safety and reliability. Other safety and reliability design features include redundancy in system processing, minimization of sensor inputs, reduced control law complexity, and isolation of the AFCS in the event of multiple system faults.
- The AFCS was designed with several features and modes to assist the flight crew to accomplish the mission by reducing workload and improving performance. In addition to stability augmentation functions, the AFCS will provide the pilot with the ability to switch to pure attitude command for operations in degraded visual conditions.
- The Flight Control Computers (FCC's) provide digital algorithms for fault detection as well as reconfiguration routines that provide redundancy management capability.
- Similar flight control systems in the RAH-66 Comanche have demonstrated a flight safety reliability of 0.9999998 for a one hour mission, fault detection of 97% and isolation of 96% effectiveness.

- The Raven was designed to the bandwidth and phase delay requirements depicted in ADS-33E-PRF for utility helicopters to ensure optimum handling qualities.

General Configuration

The Raven incorporates many other innovative design features that help to improve system performance and reduce costs. The primary design features of the Raven include:

- A fan-in-fin anti-torque system which enhances safety in flight and on the ground by housing the rotor in a shroud. Furthermore, the design is offloaded by the vertical fin in forward flight which reduces dynamic strains, resulting in reduced maintenance costs. An added feature of the design is the asymmetrically spaced blades which reduce noise.
- A hybrid composite/metal airframe which offers superior crashworthiness and corrosion resistance whilst facilitating ease of construction and repairability.
- A retractable undercarriage which minimizes drag, thereby enhancing cruise performance.
- A retractable FLIR and searchlight, which also serve to minimize drag and enhance cruise performance (special consideration was given to reducing the drag of the SAR equipment to limit the impact on mission performance).
- Extensive medical/EMS equipment to enable critically injured patients to be treated as soon as the rescue is performed, instead of making them wait until the vehicle returns to a hospital.
- Advanced, light weight, high performance engines, with a high emergency rating and low cruise specific fuel consumption.
- A split-torque transmission which enhances reliability and reduces repair times by elimination of complex planetary gearing.
- Advanced, lightweight avionics and equipment that incorporate MicroElectroMechanical Systems (MEMS) technology.
- Remove and replace modular avionics with robust avionics modules installed in highly accessible and easily opened avionics bays.
- An advanced diagnostic and prognostic system to assist maintenance personnel in isolating aircraft faults and diagnosing problems. A Health and Usage Monitoring System (HUMS) is also integrated into the design, enhancing maintenance predictability.

System Performance and Affordability

The Raven provides significant improvements in performance and operating costs over existing SAR rotorcraft. The salient performance, cost and general design characteristics of the Raven are summarized in Table 1 (displayed on page xi).

Conclusion

The Raven SAR design solution, as presented, offers prospective customers a revolutionary rotor control system that is affordable, reliable and easy to maintain. Furthermore, it is responsive to the unique demands of SAR operators by offering unsurpassed mission performance at an affordable price. The end result is a vehicle that meets or exceeds all of the performance requirements and expectations specified in the RFP. The Raven provides an innovative SAR design solution in a safe and reliable package that is capable of meeting all of the demands of current and future customers well into the 21st century. Put simply, the Raven is the perfect helicopter for the perfect storm.

Methodology and Approach

The design of the Raven by the Terp Works (University of Maryland) team was conducted in conjunction with the Spring 2001 helicopter design course (ENAE634), from February to May 2001. The design course was aimed at providing the team members with a fundamental understanding of design related issues in rotorcraft design. To this end, no commercial design codes were employed in the preliminary design stage, with in-house analysis tools being developed to gain insight into the primary issues involved. This design approach enabled us to develop some unique tools that are specially adapted to the SAR mission requirements expressed in the RFP. The performance analysis was based on a specially developed servo-flap rotor model (undergoing elastic flap and elastic twist) and the recently modified comprehensive code UMARC was used for further detailed design. The rotorcraft was modeled with IDEAS CAD software.

Note: The foldouts that are referred to throughout the report are located at the end of the relevant sections.

Table 1 – Raven Performance, Cost & General Design Specifications

General Details	
Designation	TW-258 Raven
Type	Twin turboshaft SAR helicopter
Accommodation	4 crew / 2 passengers
Acquisition cost	US $ 4.35 million (2000)
Direct operating cost[1]	US $ 423 per flight hour (2000)

Weights & Loadings	
Design gross weight	8330 lb (3778 kg)
Maximum takeoff weight	8680 lb (3937 kg)
Empty weight	4323 lb (1961 kg)
Fuel weight	1710 lb (776 kg)
Payload weight[2]	1432 lb (650 kg)
Disk loading, maximum	7.1 lb/ft^2 (34.7 kg/m^2)

Main Rotor Specifications	
Diameter	39.2 ft (11.9 m)
Number of blades	5
Chord	1.08 ft (0.329 m)
Tip speed[3]	695 – 725 ft/s (212 – 221 m/s)
Twist	-12.5 deg (linear)
Sweep (leading edge)	25 deg (from 90% radius)
Anhedral	8 deg (from 95% radius)
Shaft tilt	4 deg (forward)
Root cutout	30%
Airfoil sections	RAE9648 (root - 60%) VR-12 (60% - 90%) SSC-A09 (90% - tip)

Fan-in-fin Specifications	
Diameter	3.7 ft (1.1 m)
Number of blades	8
Blade chord	0.39 ft (0.12 m)
Rotational speed	3320 RPM
Twist	-7 deg
Blade spacing	35/55 deg
Root cutout	38%
Airfoil sections	OAF102 / OAF117 / OAF128

Performance Specifications	
Nominal cruise speed (@ 500ft)	160 knots (296 km/hr)
Maximum cruise speed (@ SL)	170 knots (315 km/hr)
HOGE ceiling[4]	12730 ft (3880 m)
HIGE ceiling[4]	15327 ft (4672 m)
OEI, HOGE ceiling[5]	4224 ft (1287 m)
VROC[4], maximum	3071 ft/min (936 m/min)
Climb rate[6], maximum	2900 ft/min (884 m/min)
Range[7], maximum	776 nm (1437 km)
Endurance[8], maximum	5.7 hrs

Engine Specifications	
Number of engines	2
Emergency power	1082 hp (807 kW)
Takeoff power	866 hp (646 kW)
Intermediate rated power	800 hp (597 kW)
Maximum continuous power	685 hp (511 kW)

Dimensions	
Length (overall, rotors turning)	44.5 ft (13.6 m)
Height (overall)	13.9 ft (4.24 m)
Fuselage width (maximum)	6.5 ft (1.98 m)
Horizontal stabilizer span	6.5 ft (1.98 m)
Wheelbase	24.1 ft (7.34 m)
Wheeltrack	6.4 ft (1.95 m)
Cabin width (maximum, internal)	5.5 ft (1.68 m)
Cabin length (internal)	8.9 ft (2.71 m)
Cabin height (internal)	5.7 ft (1.74 m)
Cargo compartment volume	130 ft^3 (3.68 m^3)
Cabin door height	5.1 ft (1.55 m)
Cabin door width	4.5 ft (1.37 m)

[1] – Direct operating costs include fuel, flight crew and maintenance only.
[2] – Including MEP weight
[3] – Hover and cruise setting
[4] – ISA, takeoff power
[5] – ISA, emergency power
[6] – ISA, maximum continuous power
[7] – Standard reserves at 500 ft PA, ISA+15°C
[8] – Standard reserves at 500 ft PA, ISA

Foldout

Section 1 – Introduction

This proposal presents the design of the TW-258 Raven – a vehicle that has been developed in response to the 2001 AHS International Request For Proposal (RFP) for "Advanced Rotor Control Concepts". The objective of this competition, as outlined in the RFP, is to develop a conceptual design for a modern civil Search And Rescue (SAR) Vertical Takeoff and Landing (VTOL) rotorcraft that incorporates new and innovative methods for controlling the pitch of the rotor blades. The primary challenge outlined in the RFP is the development of an advanced, high performance, rotor control mechanism that is not only affordable, but also capable of being developed to meet flight safety qualification and airworthiness requirements.

The primary method by which pitch control is transferred to the rotor in existing helicopters is through a swashplate, which was introduced in the late 1920's. Although it has proven to be reliable over time, the physical constraints of the mechanism limit it to providing cyclic inputs at a frequency of once per rotor revolution. Given that there is widespread interest in improving the vibration and noise characteristics of rotorcraft, alternate efficient means of providing cyclic inputs at higher frequencies should be sought. The main barrier that has until now impeded the implementation of a swashplate alternative is cost effectiveness – whether the potential benefits outweigh the higher development and certification costs. This is a quandary faced by all aircraft manufacturers; however with the extensive research that has been carried out in the fields of smart materials and controls over the last 20 years, the question is no longer is it feasible, but what is the best design solution to adopt.

In terms of mission requirements, the demand for a dedicated SAR platform capable of offering high levels of performance is evidenced by the lack of available options. In fact no existing design has been developed specifically with the civil SAR mission in mind, with all current SAR rotorcraft being adapted from utility variants – which has to date given mixed results. This is due primarily to the degradation in performance that inevitably arises as a result of the addition of extensive SAR equipment, which in turn results in large weight and drag penalties. This means that current civil SAR operators have to select from rotorcraft that do not fully meet their needs, with severe limitations having to be imposed on the SAR capabilities that they can offer. Given that the men and women who operate these vehicles courageously risk their lives day after day to save the lives of others, it is only fitting that a rotorcraft be developed that is capable of offering the high levels of mission performance that they require.

Therefore the overall objective of this design study is to develop a reliable and affordable civil SAR VTOL rotorcraft with an innovative and efficient method of controlling the rotor, and that is capable of offering unsurpassed SAR mission performance.

Section 2 – SAR Mission Responsiveness

In this section an outline of how the Raven was designed and developed to be responsiveness to the unique requirements of search and rescue missions will be presented. The general design philosophy that was adopted will first be briefly reviewed, followed by the results of a detailed mission study that looks in greater detail at the important factors that contribute most to SAR mission success. Finally, from the results of this study and the mission requirements expressed in the RFP, a list of the fundamental SAR design drivers will be presented.

2.1 – Design Philosophy

The general design philosophy, tailored for this specific design task, was established with two primary goals in mind; (i) System reliability and (ii) Mission capability. As a result the primary emphasis of this design task was placed upon the design of a reliable SAR rotorcraft that is capable of unparalleled mission accomplishment.

2.2 – SAR Mission Study

A detailed mission study was performed early in the design process to identify the primary elements of SAR missions that impact most upon mission success.

2.2.1 – General SAR Mission Requirements

SAR missions for which rotorcraft are employed typically consist of two main segments:

1. ***Search*** – in which the objective is to locate the position of the people requiring assistance as quickly as possible. The search segment usually requires large areas to be covered at relatively low speeds to ensure that the victim is not overlooked. Critical to the success of this segment is long endurance and advanced mission equipment capable of searching and locating people in adverse conditions.
2. ***Rescue*** – in which the objective is to load the located parties onboard as quickly as possible and return them safely to base. The rescue segment can require hovering for extended periods and usually requires a low downwash environment under the main rotor/s. Critical to the success of this segment is hover efficiency, low disk loading and extensive onboard Emergency Medical Service (EMS) equipment.

The relative importance of each segment is dependent upon the specific mission (i.e. if the location of the parties are known then the search segment may not be required). However since civil SAR operators generally operate with limited resources, they are usually not in the position to send out a second vehicle, such as a fixed wing aircraft, to locate the victim/s prior to sending out a dedicated rescue vehicle. It is also important to recognize that for long range SAR missions, speed can become a crucial factor. This is of particular importance when the victims are located in adverse environments with minimal survival equipment (i.e. if the victims are in cold water without life rafts or life vests).

2.2.2 – Mission Profile (RFP Defined)

The RFP specifies the need for a modern civil SAR VTOL rotorcraft that can provide SAR service in IFR conditions at a range of 300 nm. The primary SAR mission, which consists of the rescue of 2 people, is summarized below (Table/Figure 2.1).

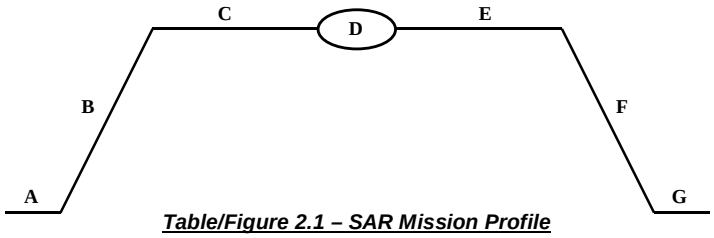

Table/Figure 2.1 – SAR Mission Profile

Segment	Description	Distance / Time	Altitude	Power required	Speed / Climb rate	Flight conditions
A	warm up	10 min	0 ft, ISA	idle	~	~
B	takeoff & climb	~	0-500 ft PA	climb	MROC	max fuel
C	cruise	300 nm	500 ft PA	cruise	99% best range speed	appropriate or max fuel
D	loiter	15 min	varies	hover	~	hover in 30 knot cross winds with 50% gusts (at 60% fuel) while evacuating 2 from a sinking boat
E	cruise	300 nm	optional	cruise	optional	headwind = 60 knots for 0-10K, 40 knots for 10K-15K (appropriate or 50% fuel)
F	descend & land	~	optional	descend	optional	land with 15 min IFR reserve @ 500 ft PA
G	shut down	~	0 ft, ISA	idle	~	~

2.2.3 – Mission Launch Requirements

An important factor in any SAR mission is the 'reaction time' of the SAR rotorcraft that is responding to the distress call. For the purposes of this design study, reaction time will be defined as the total mission time required from the time that the distress call is received, to the time that the rescued parties are returned to safety (if extensive medical equipment is onboard then this may coincide with the time that the parties are lifted into the vehicle). As a result, the time spent preparing the rotorcraft and crew for takeoff is critical and should be minimized to enhance mission performance. A typical pre-launch procedure for a SAR mission is listed in Table 2.2 on the following page.

Table 2.2 – Pre-launch Mission Requirements*

Segment	Segment Description	Elapsed time
Inform crew	Once the distress call is received by a dispatcher, the crew will be contacted immediately (provided that the crew is on standby).	10 sec
Equip crew	From the time the crew receives the call it takes approximately one to two minutes for the crew to don the flight gear (i.e. helmet, gloves, survival vest, etc.).	2 min
Strap in	It takes the crew approximately one minute to run to the rotorcraft and get strapped in.	1 min
Start engines	It takes approximately another 10 minutes to start a twin engine rotorcraft (based on H-3 and H-60 flight experience).	10 min
Takeoff / taxi	After the engines are started takeoff/taxi is immediate.	0 min
	TOTAL	**~ 13 min**

* - Based on current US Navy practice outlined by Lieutenant Commander Greg Sauter, HCS4, Norfolk Virginia.

Usually navigation data is uploaded or 'punched-in' whilst the rotorcraft is en-route to the rescue area (to save time). The table shows that the primary way to reduce the elapsed ground time is to reduce the time required to start the engines. This is difficult to do with existing engines, however it is something that could be discussed with engine manufacturers if a new engine was going to be used. If the engine start time could be reduced by about 50%, it would have the same effect as increasing cruise speed by 7.5 knots (for a 160 knot vehicle traveling 300 nm). Such a large improvement in mission performance would be highly desirable and would help to justify development of a new engine. Note that for the purposes of this study it was assumed that the crew is on standby (which is not unreasonable, especially when severe weather conditions are forecast).

2.2.4 – Mission Constraints

SAR mission success relies upon the ability of the crew to perform a quick and efficient rescue, once the victims have been located. The general role that the SAR vehicle should play in the rescue is to assist the crew as much as possible by providing a low downwash environment, a stable hovering platform (particularly in adverse conditions) and enhanced situational awareness (primarily through advanced communication devices and onboard sensors). All of these attributes are important, however only the first one is an inherent vehicle attribute that cannot be remedied by an advanced flight control system or mission equipment. As a result it was deemed necessary to establish a downwash limit above which SAR mission success could be jeopardized.

SAR missions necessitate relatively benign downwash environments that do not severely impair crew operations beneath the rotorcraft or cause excessive problems for the parties being rescued. As the disk loading increases, the ability to land at unprepared sites (which is necessary for a SAR VTOL aircraft) becomes proportionally more and more difficult due to ground erosion and wake interaction with personnel. In an effort to establish a set of disk loading limits a number of sources were consulted (refer to [Scot91], [TREC64], [Scha67], and [Mich71]). Based on the test results and conclusions in these reports, the general limits listed in Table 2.3 were established. Note that personnel can only tolerate a certain amount of force and overturning moment before balance is lost, whereas surface failure is a function of downwash velocity and occurs at different velocities for different types of surface.

Table 2.3 – Downwash Environment Limitations

Surface Type	Personnel Limits		Surface Failure Limit
	Moment (ft.lbs)	Force (lbs)	Disk loading (lb/ft^2)
Firm Surface[1] Operations	300	100	50
Loose Surface[2] Operations	225	75	15

[1] – Firm surfaces are defined as wet sand or dirt, packed dirt, sod and prepared surfaces.

[2] – Loose surfaces are defined as sand, loose dirt, gravel, and water.

As can be seen in Table 2.3, surfaces that can be considered loose start to fail at disk loadings greater than 15 lb/ft^2. Although these results provide some guidance as to a set of downwash limits, they do not specifically consider the requirements of a SAR mission performed over water (as specified in the RFP). In view of the fact that SAR missions must also consider the state of the victims in the water, and the possibility that they may be in a life raft, then it appears that the limit displayed in Table 2.3 is not sufficient. To establish a more practical limit, we consulted Marat Tishchenko whom suggested, based on his experience as the former Mil Design Bureau General Designer, that the maximum disk loading for SAR missions involving light flotation devices over water should not be greater than 35 kg/m^2 (7.2 lb/ft^2).

Table 2.4 – SAR Downwash Environment Limitation

Downwash Environment	Disk Loading (lb/ft^2)
SAR mission limit	7.2

This estimate of the maximum tolerable downwash for SAR rotorcraft is of specific interest for high speed concepts (such as tiltrotors and tiltwings) that are designed with relatively high disk loadings to minimize size and weight. In fact, given that the smallest existing manned production tiltrotor is the BA609, which has a disk loading of approximately 16.9 lb/ft^2, it appears unlikely that fixed diameter tiltrotors will make suitable SAR platforms. This is in line with the findings of Scott [Scot91] who states; "Successful high speed rotorcraft will have disk loadings between 15 and 45 psf, values below 15 do not look feasible."

2.2.5 – SAR Operator Suggestions

With competition in the rotorcraft industry at an all time high, it is essential to not only address the specific mission requirements expressed in the RFP, but also to consider additional user driven requirements that may help to enhance the attractiveness of the proposed design solution. This is of particular importance in the design and development of a new airframe, in which there lies an opportunity to incorporate desirable features that are not available on existing SAR platforms. Our team recognized the importance of being responsive to our customers needs, and as a result we conducted a survey to determine the specific design attributes and factors that operators considered to be important to the successful accomplishment of SAR missions. What follows is a brief selection of some of the feedback we received;

- ***Anti-torque safety –*** *"My dream machine would either be a NOTAR, a coaxial, or a multiple main rotor design to avoid the problem of mixing a tail rotor with obstacles and to allow loading and unloading of stretcher patients by untrained hospital porters in safety."*
- ***Speed –*** *"Many situations will not be survivable no matter how fast the SAR resource, but all other things being equal, quicker has got to be better. The problem is you generally can't realize the full speed advantage of a faster helicopter in the rescue role because of the drag generated by the rescue equipment – nightsuns, FLIR units, rescue hoist, antennae, etc."*
- ***SAR equipment*** *– "Because you seldom get the full story when dispatched on a SAR mission, it is necessary to carry a range of rescue/medical equipment in order to keep available a suite of response techniques appropriate to the situation."*
- ***Internal volume –*** *"… That means carrying more equipment on launch on all missions than will eventually be used. Where carrying capacity is equal, speed obviously prevails. However, where carrying capacity is unequal, larger internal volume usually prevails – that consideration prevailed over speed the last time we had to make that decision."*
- ***Launch time –*** *"Having all of the equipment on board all of the time to respond to any scenario reduces launch times, which counts toward rescue time far more than increased cruise speed."*
- ***Medical equipment*** *– "A problem that is usually encountered in SAR missions is that the patient/s can often expire during the return journey, which makes having extensive medical equipment onboard very desirable, even though it increases weight. With extensive EMS equipment onboard, the speed of the return segment becomes much less critical because the patients can be treated as soon as they are rescued."*

2.3 – SAR Design Drivers

A set of fundamental design drivers were established from a combination of the design philosophy, the design requirements expressed in the RFP and the operator suggestions outlined in the previous section. These design drivers are listed below in Table 2.5, together with a brief description. In the final column of the table the source of each driver is identified, either RFP specific ('RFP'), SAR mission specific ('SAR') or user defined ('User').

Table 2.5 – SAR Design Drivers

Driver	Description	Source
Compact design	Inherent ability to fit inside a standard size hangar without the requirement for significant folding. Ability to land, take-off and operate from confined locations – increasing operational flexibility.	RFP
High speed cruise	Ability to reach the rescue site as quickly as possible – increasing the effectiveness of the vehicle in the SAR role.	User
Range	Capable of ranges in excess of 600nm without the need for in-flight refueling – to improve mission capability.	RFP
Endurance	Capable of endurance in excess of 5 hours at speeds no greater than 120 knots without the need for in-flight refueling.	RFP
Adverse weather capability	Ability to operate at night, in storms, in icing conditions, in hot and high conditions, or a combination thereof – a critical requirement is the ability to operate in 45 knot crosswinds.	RFP
Hover efficiency	Ability to hover efficiently (high power loading – lb/hp).	SAR
Hover downwash	Ability to hover with low downwash velocities (disk loading) – improves SAR mission capability and enables rotorcraft to land at unprepared sites.	SAR
CG range	Inherent ability to enable large operational CG travel – when winching people to safety, or unloading crew, it is desirable to have a large CG range (both lateral and longitudinal).	User
Operational safety	Inherent vulnerability to mission hazards - SAR rotorcraft operate in close proximity to other objects - configurations without exposed tail rotors and angled main rotors are more desirable.	User
Availability	Ability to respond quickly – SAR vehicles must be available to respond quickly to a distress call, hence they must be reliable and easy to maintain.	SAR
Affordability	For a design to be affordable it must have low operating costs and a low acquisition cost (low operating costs are generally more important).	~
Design complexity	High risk technologies will impact adversely on system reliability and affordability.	SAR
Survivability	The vehicle must be crashworthy such that in the event of a crash, the crew and passengers survive - the vehicle must also have good autorotative characteristics.	RFP
Large internal volume	A large internal volume will enable the vehicle to carry extensive mission equipment and rescue as many people as possible.	User
Rear loading capability	Ability to offload patients quickly and efficiently.	User
Unique vehicle attributes	The potential of a new SAR vehicle to incorporate unique attributes that are not available in existing rotorcraft will enhance future sales prospects.	RFP
Acoustic signature	External and internal cabin noise should be minimized to enhance mission flexibility.	RFP
OEI performance	The ability of the rotorcraft to hover out-of-ground-effect (HOGE) with one-engine-inoperative (OEI) is a critical performance parameter.	RFP
Handling qualities	The inherent responsiveness of the vehicle to pilot control inputs during rescues in adverse conditions.	SAR
Multimission capability	The inherent capability of the vehicle to be adapted to perform a variety of other VTOL missions (such as VIP transport) to improve future sales prospects.	~
Swashplateless technology	The inherent ability of a configuration to incorporate swashplateless technology.	RFP

It is these SAR specific design drivers that provided the fundamental justification for all decisions made throughout the design process, thereby enabling us to develop a SAR vehicle that is truly responsive to our customers needs.

Section 3 – Configuration Design and Development

The objective of this section is to justify and rationalize the decisions made in the selection of the proposed configuration. In order to demonstrate that an optimum configuration was indeed selected, a detailed description of the methods employed to arrive at the Raven design concept will be presented.

3.1 – Design Methodology

The general methodology that was adopted can be split into two main parts:

1. ***Initial concept selection*** – involves the conceptual evaluation of potential configurations based on the design drivers. In this first order analysis, no formal calculations were performed – assessments were made based on design experience and information contained in the literature. The objective of this *qualitative* analysis was to asses the relative attributes of each configuration in order to determine SAR mission potential.
2. ***Configuration trade studies*** – involves performing trade studies on the selected configurations. This analysis was based upon an original design code developed from first order rotorcraft sizing techniques and tailored specifically for the assessment of SAR configurations. The objective of this *quantitative* analysis was to assess the relative performance of each of the three general classes of rotorcraft identified in the initial concept selection stage.

In order to downselect the most promising concepts, their relative 'goodness' was determined by a measure of both attributes and performance – with attributes assessed on a qualitative basis and performance on a quantitative basis. The final objective was to highlight an optimum configuration to form the foundation of a new SAR rotorcraft design.

3.2 – Initial Concept Selection

In this stage of the configuration design the relative attributes of a large number of configurations were assessed, with the objective of qualitatively ranking the concepts in order of their inherent SAR mission potential.

3.2.1 – Candidate Configurations

A wide range of potentially suitable configurations were included in the initial analysis to ensure that no concept was prematurely eliminated. The candidate configurations (displayed in Table 3.1 on foldout) were selected based on their inherent ability to perform a basic SAR mission. Note that only 15 of the 17 configurations are displayed in Table 3.1.

3.2.2 – Evaluation Criteria

Evaluation criteria were formulated to enable an assessment of the various configurations to be performed. The criteria, displayed in Table 3.3 (foldout), were taken directly from the design drivers listed in Table 2.6; however only those drivers that were deemed to be relevant to the selection of a suitable configuration were used.

3.2.3 – Weighting Factors

The weightings for the evaluation criteria were established by making an assessment of the relative importance of each to the successful completion of the desired mission. Therefore a higher weighting was assigned to those criteria that were judged to more strongly impact upon SAR mission accomplishment (refer to Table 3.2).

Table 3.2 – Weighting Factors

Weighting factor	Description
3	Major impact
2	Minor impact
1	No direct impact

Table 3.4 – Configuration Ratings

Rating	Description
3	Good
2	Fair
1	Poor

3.2.4 – Concept Evaluation

A configuration matrix was developed to enable a concise evaluation to be made of the 17 candidate configurations. The configuration matrix (Table 3.3 on foldout) presents the results of this first order qualitative configuration evaluation. Each configuration was assessed relative to the 'best' and 'worst' configuration for each criteria and was given a rating of good, fair or poor as a measure of this assessment (refer to Table 3.4 on the previous page). To provide greater flexibility, half point ratings were allowed. Therefore a configuration that ranked best in a given category received the highest rating (allowing for ties) and that value was then multiplied by the appropriate weighting factor, with the resulting totals displayed in the matrix. One hundred and eight points represents the maximum possible score. As explained earlier, the evaluation procedure did not include a quantitative analysis, but instead relied upon the qualitative evaluation of each concept based on design experience and information contained in the literature.

3.2.5 – Preliminary Concept Assessment

The rotorcraft configurations displayed in Table 3.3 can be broadly grouped into four main types:

1. *Helicopters* – which includes the conventional, NOTAR, fan-in-fin, VDR, tandem, coaxial, ABC, and synchropter.
2. *Compounds* – which includes the compound and VTDP.
3. *Tiltrotors* – which includes the tiltrotor, VDTR, and tiltwing.
4. *Experimental* – which includes the reaction drive, CRW, verticraft and folding tiltrotor.

The results displayed in Table 3.3 identify the helicopter type as being the most suitable SAR configuration. Since the evaluation was somewhat subjective in nature, this result does not automatically eliminate the other configuration types from being considered, however it does indicate that helicopters tend to have more desirable SAR attributes. Furthermore, the results do provide a sound rationale for the elimination of the reaction drive, folding tiltrotor, tiltwing, CRW and verticraft configurations, due primarily to issues arising from their complexity and unproven track record. Since the RFP requires swashplateless technologies to be incorporated into the design, any added complexity that arises from general configuration attributes will tend to magnify affordability and reliability problems, in turn adversely impacting upon SAR mission accomplishment. In fact, even though the VDR and VDTR ranked higher than the aforementioned configurations, they too can be eliminated as potential configurations due to the added complexity of the relatively unproven variable diameter mechanisms.

3.3 – Configuration Trade Studies

The elimination of seven configurations provided the opportunity to look at the best candidates in a more formal quantitative manner. It also ensured that none of the most promising concepts were prematurely eliminated, especially since only a conceptual subjective evaluation was initially performed. The remaining configurations that survived the initial concept evaluation, in order of preliminary ranking, include: fan-in-fin, NOTAR, tandem, coaxial, ABC, conventional, synchropter, VTDP, compound and tiltrotor. Based on the remaining concepts it is apparent that only three configuration types remain, with the experimental type being completely eliminated. Therefore in this stage of the configuration design, the relative performance of the remaining configuration types (i.e. helicopter, compound and tiltrotor) will be quantitatively assessed, with the objective of highlighting the most effective SAR design solution.

3.3.1 – Historical Database

Prior to starting the configuration trade studies, an extensive survey of existing rotorcraft was carried out. In the existing rotorcraft fleet there are very few dedicated SAR vehicles, with most being modified from basic utility variants to perform specialized SAR missions. A selection of utility and SAR rotorcraft that are in a similar weight class to the Raven are displayed in Table 3.5 on the following page (the data is from Jane's 2000/2001 edition [Tayl00]).

Table 3.5 – Existing Rotorcraft Performance Survey

Rotorcraft	Type	Crew / Passengers	W_{TO} (lb)	W_{EMPTY} (lb)	W_{FUEL} (lb)	DL (lb/ft^2)	D_{MR} (ft)	Range (nm)	V_{CR} (knots)
MD902	NOTAR	2/6	6250	3375	1078	7.12	33.83	257	134
EC135	fan-in-fin	1/7	6250	3284	1182	7.29	33.46	340	138
A109K2	tail rotor	2/6	6283	3638	1325	6.29	36.08	434	143
HH-65A	fan-in-fin	3/2	8928	5992	~	7.60	39.17	410	139
AS365N2	fan-in-fin	2/8	9369	5028	2008	7.97	39.17	464	150
MH2000	fan-in-fin	2/8	9920	5512	2001	8.08	40.02	421	135
412 EP	tail rotor	1/14	11900	6789	2209	7.34	46	402	122
BA609	tiltrotor	2/9	16000	10500	2476	16.9	26	750	275

3.3.2 – Mission Profile

The range and endurance missions specified in the RFP for use in sizing trade studies are summarized below (Table 3.6):

Table 3.6 – Configuration Trade Basic Missions

Mission	Requirement	Speed	Altitude	Conditions
Range	600 nm	None specified	500 ft PA	ISA $\pm$ 15°C
Endurance	5 hrs	60 kt $\leq$ V $\leq$ 120 kt	500 ft PA	ISA

The RFP also requires that the rotorcraft demonstrate a One Engine Inoperative (OEI), Hover-Out-of-Ground-Effect (HOGE) capability, which is summarized in Table 3.7:

Table 3.7 – OEI HOGE Requirement

Requirement	Weight	Available power	Altitude	Conditions
HOGE, OEI	60% fuel, full payload	Emergency power	Sea level	ISA + 20°C

3.3.3 – Methodology

The objective of the trade studies, as stated earlier, is to quantitatively compare the three configuration types such that an optimum SAR configuration can be selected for further detailed study. As a result, the trade study methodology that was adopted was based primarily upon first order analysis techniques. Such techniques are capable of capturing global vehicle design parameters, thereby enabling the primary configuration differences to be highlighted. The methodology developed is summarized in the flow chart displayed in Figure 3.1.

The primary input parameters comprise the rotorcraft configuration type (helicopter, compound or tiltrotor), disk loading, cruise speed and range. The weight of the crew and passengers are specified in the RFP and do not enter the trade study as independent variables. The Mission Equipment Package (MEP) weight is scaled from existing SAR rotorcraft (primarily the HH-65A and HH-60J) and then held constant as an independent variable. The performance models used are described in greater detail below.

Aerodynamic and Engine Performance

Hover performance was estimated via momentum theory which was modified to incorporate the effects of vertical drag, main rotor power conversion efficiency and transmission losses. Forward flight performance was estimated using the Braverman equation [Tish01] which identifies a relationship between the lift-to-drag ratio of a vehicle in cruise and the vehicle weight, cruise speed and engine power (the relationship also includes a number of empirical correction factors to account for main rotor propulsive efficiency and power conversion efficiency in cruise). Given that the range mission is specified at a pressure altitude

of 500 ft, the lift-to-drag ratio for each concept was adjusted to account for the reduction in lift-to-drag that occurs when the cruise segment is carried out at a sub-optimum altitude [Ruth91]. Engine performance was estimated from the scaleable IHPTET engine characteristics given in the RFP, with appropriate corrections incorporated to account for altitude, temperature, installation losses and ram power effects.

Figure 3.1 – Trade Study Methodology

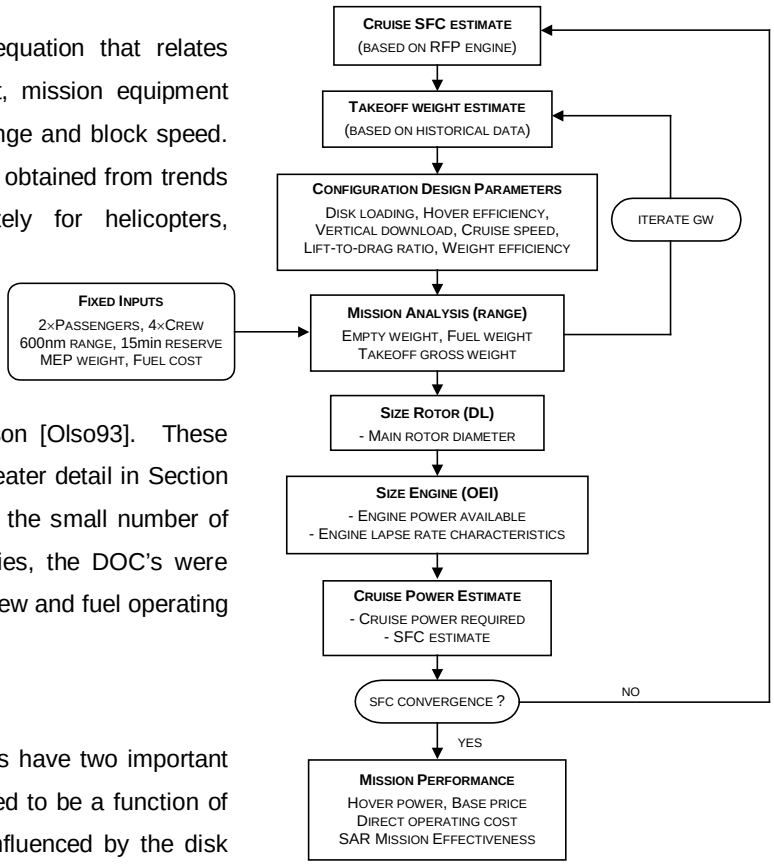

Weight and Cost Analysis

Takeoff weight was estimated from an empirical equation that relates vehicle empty weight fraction, payload, crew weight, mission equipment weight, specific fuel consumption, lift-to-drag ratio, range and block speed. The empty weight fractions and lift-to-drag ratios were obtained from trends of existing rotorcraft and were defined separately for helicopters, compounds and tiltrotors [Tish01]. The base purchase price was estimated from the Harris and Scully [Harr97] price estimating relationship and the Direct Operating Costs (DOC's) were estimated from the data presented by Leslie [Lesl96] and Olson [Olso93]. These simplified cost estimating techniques (discussed in greater detail in Section 14) were adopted for use in the trade studies due to the small number of required inputs. For the purpose of the trade studies, the DOC's were defined as consisting of only the maintenance, flight crew and fuel operating costs [Olso93].

3.3.4 – Analysis Limitations

The trade study methodology and analysis techniques have two important limitations. First, the empty weight fraction is assumed to be a function of takeoff weight only, whereas it is also significantly influenced by the disk loading. This effect is of particular importance for tiltrotors, which tend to suffer large weight penalties with decreasing disk loading – due primarily to the fact that larger diameter rotors require larger, stiffer wings for support. Second, the forward flight performance method is based on knowledge of the lift-to-drag ratios at optimum cruise altitudes and speeds. As a result, the technique is not directly amenable to study the effects of varying cruise speed and altitude, since the change in lift-to-drag ratio can be significant. Again this is of particular importance for tiltrotors, which operate over a wide range of altitudes and speed and therefore can suffer large penalties in lift-to-drag ratio at sub-optimum conditions. However, given that the primary objective of this trade study is to *compare* the different configuration types, it seems reasonable to utilize these first order analysis techniques.

3.3.5 – Design Parameters & Code Validation

The main design parameters used to model the three configurations were cruise speed, hover download, vertical download in hover, cruise lift-to-drag ratio and weight efficiency (which is defined as the ratio of useful load to the total weight of the vehicle). These design parameters were defined based on historical trends. To check the predictive capability of the methodology, the code was validated against a large number of existing rotorcraft. A comparison of the predictions made versus published data [Tayl00] for two existing rotorcraft configurations is displayed below in Table 3.8 (note that the performance data published in Jane's was used as a set of fixed inputs).

Table 3.8 – Code Validation

Parameter	HH-65A Dolphin		BA609	
	Estimate	Actual	Estimate	Actual
Gross weight (lb)	8924	8928	16033	16000
Fuel weight (lb)	1976	1956	2623	2476
Empty weight* (lb)	5967	5992	10129	10500
Installed power (shp)	1806	1478	4216	3880
Rotor diameter (ft)	39.17	39.17	26.01	26
Price (2000 US $ million)	4.79	N/A	10.72	8 - 10

* – Mission equipped empty weight

With reference to Table 3.8, the only notable difference between the estimated and the actual data is the installed power, which is overestimated due to the stringent OEI requirement specified in the RFP. This also has the effect of increasing the base price estimate, which is a function of installed power. Therefore, these results clearly validate the predictive capability of the methodology, which enables a high level of confidence to be formed as to the ability of the code to generate accurate performance estimates of the three configuration types under assessment.

3.3.6 – Measures of Effectiveness / Efficiency

To compare and assess the SAR potential of the three configuration types, a measure of design effectiveness is required. Such measures can be used to evaluate the concepts beyond the vehicle attributes of weight, speed, range and payload. Grouping these attributes together establishes parameters which can evaluate the overall vehicle effectiveness, allowing combinations of strong and weak attributes to further define the effectiveness and economy of a configuration. Examining the individual attributes of each concept independently may not resolve the problem, hence the need for a more refined comparative tool.

Commercial configurations are very sensitive to weight, range and time: how much can be moved how far, in what amount of time, and at what cost. As a result, for commercially driven rotorcraft there are two commonly used measures of effectiveness:

1. *Payload Delivery Efficiency (PDE)* – which is a measure of the efficiency of a vehicle to deliver payload from a cost perspective. It is defined as [(payload × range)/(fuel required)] – [Ruth91]. A higher value implies greater payload delivery for less fuel and hence less cost.
2. *Productivity (PR)* – which is a measure of the capability of the aircraft to deliver large amounts of payload in a given time, either by large amounts per sortie or by small amounts through a large a number of sorties. It is usually defined as [(payload × velocity)/(empty weight + fuel)] – [DeTo91].

These measures of effectiveness are suitable for assessing concepts whose primary mission is commercially driven (such as a civil short haul transport), since they are essentially a measure of the ability of a concept to generate revenue divided by direct expenses. However for a civil SAR rotorcraft, such measures do not give an indication of how well the rotorcraft will perform a SAR mission, due to the fact that mission success is not defined by the ability to generate revenue. Therefore a new mission effectiveness parameter was developed, based on the Bell defined measures of efficiency [DeTo91] and the SAR evaluation criteria defined in Table 3.3, that is better suited to the comparison of civil SAR configurations. The new measure of effectiveness is defined as:

$$SAR_{ME} = \frac{I_{VOL} E_{VEH} V_{CR}}{10 \cdot PL \cdot t_{MIS}} \left[\frac{W_{PAYLOAD} + W_{MEP} + W_{CREW}}{(1 + C_{DES}) W_{EMPTY} + W_{FUEL}} \right]$$

Parameter	Equation	Definition
W_{---}	~	Vehicle weights [lb]
I_{VOL}	$\frac{W_{EMPTY-BEST}}{W_{EMPTY-R/C}}$	Internal volume factor – for the same payload, crew and MEP, configurations with higher empty weights are less efficient transport vehicles
E_{VEH}	$\frac{(L/D)_{CR}\,\eta_{CR}\,\xi_{CR}}{SFC_{CR}}$	Vehicle energy efficiency – represents the distance by which a unit weight of a given vehicle travels per unit weight of fuel consumed (note that the two factors in the numerator define main rotor power conversion efficiency and main rotor propulsive efficiency in cruise) – [hp.hr/lb]
V_{CR}	~	Cruise airspeed [knots]
PL	P_{HOV}/T_{HOV}	Power loading in hover [hp/lb]
t_{MIS}	$\frac{Range}{Block\ Speed}$	Total average mission flight time [hr]
C_{DES}	0% - helicopter 5% - compound 10% - tiltrotor	Design complexity factor to account for reductions in system reliability and increased maintenance due to increased complexity

The units of SAR_{ME} are in nautical miles per hour or knots, which makes this parameter an 'effective' SAR velocity. A larger value of SAR_{ME} implies that the rotorcraft will be a more effective and efficient SAR design solution.

3.3.7 – Trade Study Results

Table 3.9 – Configuration Design Point

Configuration	V_{CR} (knots)	DL (lb/ft^2)
Helicopter	160	7.0
Compound	200	12
Tiltrotor	260	17

Disk loading, cruise speed and range were selected as the primary input parameters for the trade studies. However, given that the performance capabilities of each configuration type are constrained to different domains (i.e. helicopters have practical upper limits on speed and tiltrotors have practical lower limits on disk loading), a set of design points were established. The rationale for defining separate design points was to identify realistic input values for cruise speed and disk loading such that the configuration types could be compared at their optimum conditions, instead of comparing all configurations at similar conditions (which would unfairly benefit one over the other). The design points selected are based on existing rotorcraft and are summarized in Table 3.9.

Figures 3.2 – 3.8 show the trade study results for gross weight, fuel capacity, nominal (uninstalled) engine power, cruise power fraction, power-to-weight ratio, base price and direct operating costs as a function of disk loading. The rotorcraft types were sized to achieve the 600 nm range mission specified in the RFP (refer to Section 3.3.2).

Figure 3.2 – Gross Weight

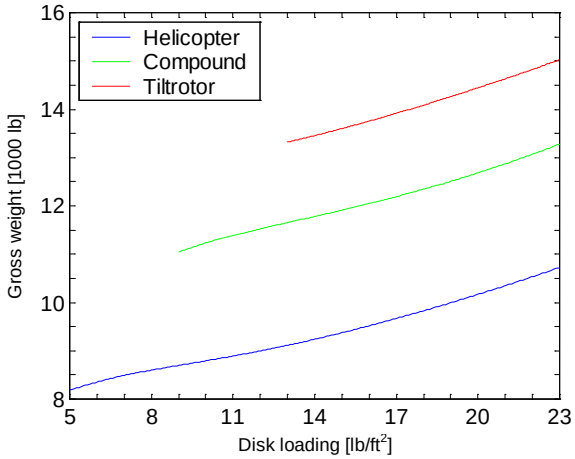

Figure 3.3 – Fuel Capacity

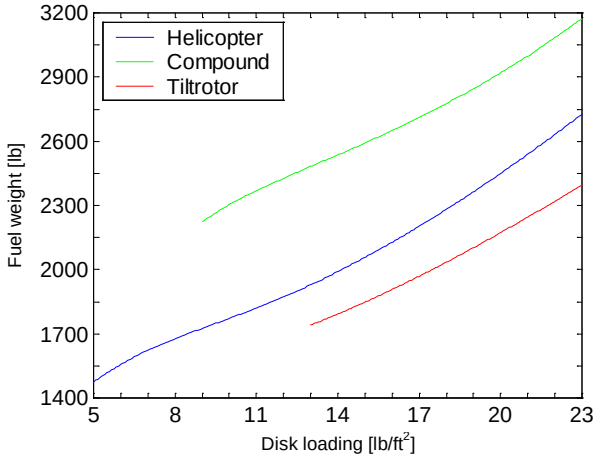

Figure 3.4 – Nominal Engine Power

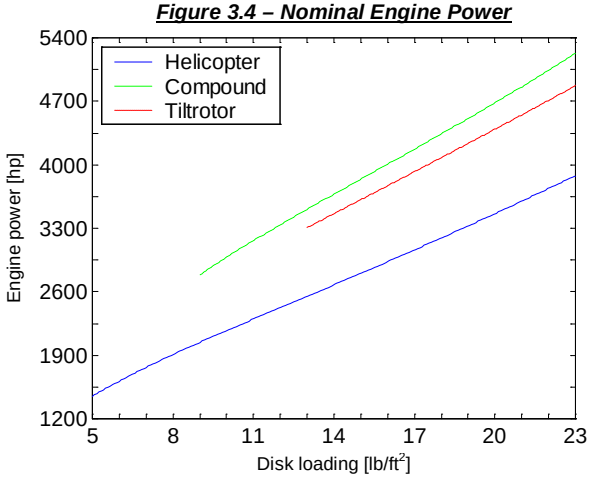

Figure 3.5 – Cruise Power Fraction

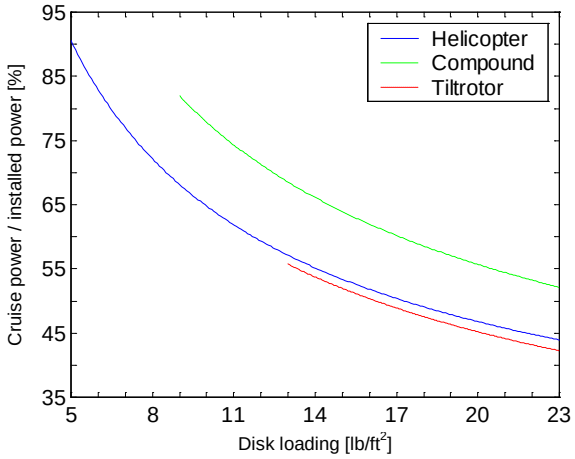

Figure 3.6 – Power-to-Weight Ratio

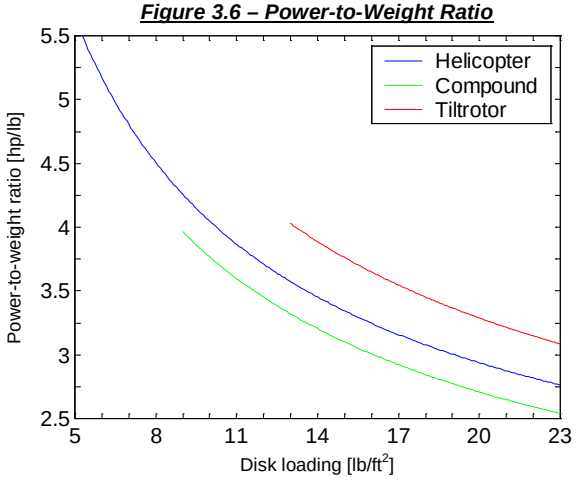

The dominant trend displayed in these figures is that with an increase in disk loading, the power-to-weight ratio decreases, resulting in lower fuel efficiency in cruise. This trend is directly attributable to the stringent OEI HOGE condition stipulated in the RFP, which tends to severely penalize high weight, high disk loading configurations. Therefore the tiltrotor, due to its larger weight and lower cruise power requirement, is most severely penalized by the OEI requirement, resulting in a very poor cruise fuel efficiency (identified by a low cruise power fraction). One would expect this trend to translate into a larger fuel requirement over the complete range of disk loadings, however it does not, which is primarily due to the higher speed and higher lift-to-drag ratio of the tiltrotor. However this trend is somewhat misleading, due to the fact that over the practical range of disk loadings that are applicable for each configuration (refer to Table 3.9), the helicopter requires less fuel and operates at a higher cruise power fraction than both the compound and tiltrotor.

Figure 3.7 – Configuration Base Price (2000)

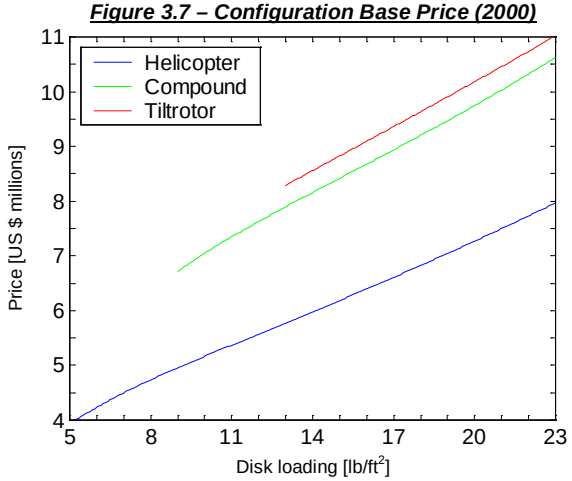

Figure 3.8 – Direct Operating Cost (2000)

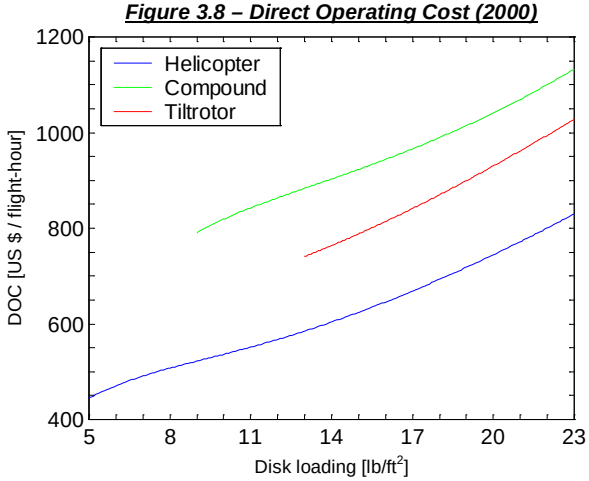

The two remaining figures, which show base purchase price and direct operating costs as a function of disk loading, further enhance the standing of the helicopter configuration relative to the compound and tiltrotor. Both plots show an increasing trend

with an increase in disk loading, which is not surprising since the base purchase price relationship is proportional to a combination of takeoff weight and installed power, whereas the DOC is proportional to fuel usage. What the plots demonstrate is that a high price is paid for the added speed capability of the tiltrotor and compound configurations. It again appears that the OEI requirement severely degrades the ability of the tiltrotor and compound to perform the specified mission in a cost effective manner. When considering the relatively limited resources of most civil SAR operators, cost is an unfortunate reality that can often mean the difference between a successful long term SAR operation and an expensive short term venture, with limited SAR capabilities.

Figure 3.9 – SAR Mission Effectiveness

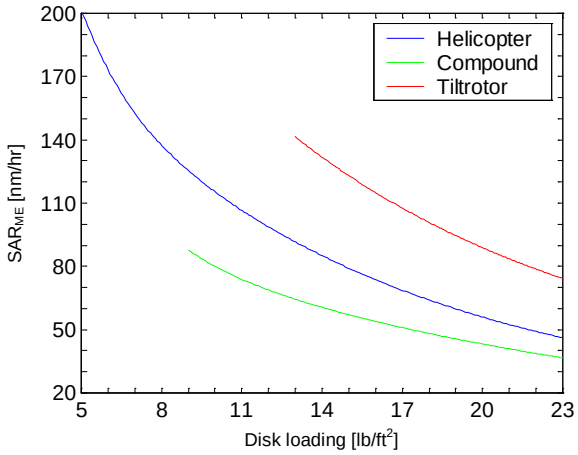

Figure 3.10 – SAR Mission Effectiveness

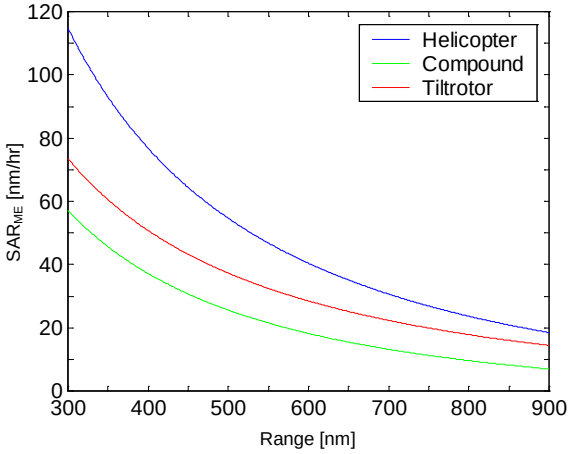

Figure 3.11 – SAR Mission Effectiveness

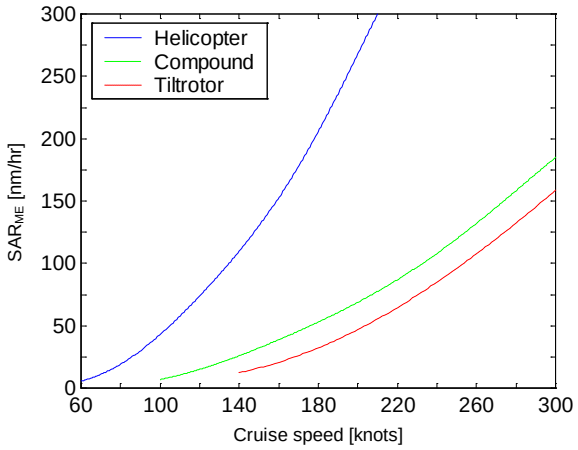

SAR mission effectiveness is displayed in Figures 3.9 – 3.11 as a function of disk loading, cruise speed and range. As explained in the previous section, this parameter provides a more realistic measure of SAR mission effectiveness, due to the fact that it enables an effective SAR velocity to be established that is based on a number of important SAR design parameters, not just cruise speed (this is important because regardless of how quickly a vehicle may arrive on scene, if the subject cannot be lifted into the vehicle or if the subject is severely injured during the rescue, then the mission will be considered a failure). What the figures clearly show is that the helicopter is a more effective SAR platform over the specified mission range, with the tiltrotor improving as range increases. In all cases, the helicopter is a more effective SAR design solution, followed by the tiltrotor and then the compound. It is of no surprise that the compound is least effective, since the helicopter is more efficient in hover, and the tiltrotor is more efficient in cruise.

These trends are further highlighted by tabulating the results of each trade conducted at the optimum design points (specified earlier in Table 3.9). The compound and tiltrotor are compared to the helicopter, with the percentage difference denoted in brackets next to each value (refer to Table 3.10). These results demonstrate the superior performance of the helicopter configuration over the compound and tiltrotor. The helicopter has a lower takeoff weight (higher weight efficiency), lower fuel requirement, lower installed power requirement and higher power loading. The base purchase price of the helicopter is significantly lower than both the compound and tiltrotor, with a similar trend displayed in DOC (which is attributable to the higher maintenance costs associated with more complex designs). Furthermore, the results show that although the compound and

tiltrotor can complete the cruise mission segments in less time, the helicopter is still far more effective at completing the entire mission, which includes performing a rescue over water, whilst hovering in adverse conditions.

Table 3.10 – Trade Study Results at Design Point

Parameter	Helicopter	Compound	Tiltrotor
Gross weight (lb)	8490	11525 (36%)	13912 (64%)
Fuel required (lb)	1624	2427 (49%)	1969 (21%)
Rotor diameter (ft)	39.8	35.8	24.2
Nominal engine power[1] (hp)	883	1670 (89%)	1961 (122%)
Cruise power (hp)	1194	2148 (80%)	1826 (53%)
Power loading[4] (lb/hp)	8.82	6.40 (39%)	3.67 (140%)
Base price[5] ($ million)	4.50	7.63 (70%)	9.36 (108%)
DOC[2] ($/fh)	491	864 (76%)	841 (71%)
DOC[2] ($/mission)	1841	2591 (41%)	1943 (5.5%)
SAR_{ME} (nm/hr)	**152.7**	**68.8** (122%)	**107.7** (42%)
Mission time[3] (hrs)	1.88	1.50 (26%)	1.15 (64%)

[1] – Uninstalled engine power available at sea level, ISA from each engine
[2] – Cash DOC in 2000 US dollars per flight hour and per design mission (600 nm)
[3] – Average flight time required to reach objective (300 nm)
[4] – Inverse power loading in hover
[5] – Base price in 2000 US dollars

3.4 – Final Configuration Selection

The results of the trade study identify the helicopter configuration type as the most effective SAR design solution, in terms of both mission performance and cost. Therefore these results provide a sound rationale for the elimination of both the tiltrotor and compound configuration types from further consideration. This assessment is in direct agreement with the initial qualitative evaluation, which highlighted the helicopter as the configuration type with the most desirable SAR attributes. In fact the seven highest ranked configurations from Table 3.3 were all helicopter types, providing a fundamental justification as to the soundness of the original assessment. Of the remaining concepts, the fan-in-fin single main rotor configuration (ranked 1) was selected as the optimum SAR rotorcraft (due to its good all-round attributes) and was therefore subjected to further detailed analysis. The primary reasons for not selecting the other remaining helicopter configurations are listed separately below:

- *NOTAR (ranked 2)* – Although the NOTAR configuration had good all-round attributes, it was eliminated due to concern that the anti-torque system, which relies on the Coanda effect in hover, would not be capable of functioning efficiently in a 45 knot crosswind, as required by the RFP.
- *Tandem (ranked 3)* – The tandem was primarily eliminated due to the fact that swashplateless technology would have to be implemented on two main rotors, as opposed to only one for a single main rotor configuration. The tandem was also deemed to be an inefficient design solution for this weight class.
- *Coaxial (ranked 4)* – The coaxial was primarily eliminated due to the higher level of complexity that would be involved in developing a swashplateless control system for two contra-rotating rotors, instead of one single main rotor. A similar argument was used to eliminate the ABC concept, which is more complex than a coaxial due to its rigid rotors.
- *Conventional (ranked 6)* – One of the main concerns expressed by SAR operators was the danger posed by an exposed tail rotor, and therefore the conventional design was primarily eliminated for this reason.
- *Synchropter (ranked 7)* – The synchropter was eliminated due primarily to safety concerns over the intermeshing rotors impeding ingress and egress from the vehicle. Safe ingress and egress is vitally important for a SAR vehicle, which must be capable of loading people whist the main rotor/s are still turning.

Foldout 3.1

Section 4 – Raven Design Features and Performance Summary

Foldout 4.1

Section 5 – Main Rotor and Hub Design

The main rotor is a key component that required careful design in order to ensure that the Raven could meet its performance objectives. In this section the salient design features of the main rotor and hub will be addressed including the hub configuration, rotor sizing, tip speed, blade configuration, autorotation characteristics, blade dynamic and aeromechanical characteristics, and the innovative swashplateless pitch control system.

5.1 – Baseline Rotor Design

The main rotor design was carried out as part of an iterative process in which the primary design parameters were selected to ensure adequate hover and forward flight performance. In the procedure adopted, a main rotor with a conventional swashplate was designed in order to provide a baseline for all subsequent swashplateless designs to be compared with. Therefore in this subsection the salient design features of the baseline main rotor will be presented and the selections made will be justified. A summary of the baseline main rotor design is shown in Table 5.1.

Table 5.1 – Main Rotor Design Parameters

Parameter	Value
Diameter	39.2 ft
Number of blades	5
Chord	1.08 ft
Solidity	0.088
Twist	-12.5 deg (linear)
Sweep	25 deg (from 90%)
Anhedral	8 deg (from 95%)
Tip speed	695 – 725 ft/s

5.1.1 – Diameter

There are several conflicting factors that influence the selection of the main rotor diameter, with larger diameters resulting in lower disk loadings, lower induced power requirements and better autorotational characteristics, and smaller diameters resulting in lighter hubs and lower drag. Hence the objective is to determine the smallest diameter that can produce the required performance without violating the maximum disk loading. With this in mind, the diameter was sized based on the maximum specified disk loading (defined in Table 2.4), the design gross weight and the vertical download in hover. Due to the fact that the vehicle weight and drag estimates were continuously refined throughout the design, the sizing of the main rotor was carried out in an iterative fashion. The final diameter was determined to be 39.2 ft, which corresponds to a disk loading of 7.1 lb/ft^2.

5.1.2 – Tip Speed and Tip Shape

The selection of tip speed is also influenced by a number of conflicting requirements including compressibility effects, blade stall, autorotation characteristics, and noise. Furthermore, optimum hover performance requires a low tip speed whereas optimum forward flight performance requires a high tip speed. Therefore in order to optimize flight in both regimes, a tip speed was selected that varies from 695 ft/s in hover to 725 ft/s in cruise (the change is effected at 70 knots). The hover tip speed setting was selected to ensure acceptable autorotation characteristics (lower limit) whereas the cruise tip speed setting was selected to ensure acceptable noise characteristics (upper limit based on an advancing tip Mach number of 0.87). In order to further minimize the effects of noise and compressibility in high speed cruise, a swept/tapered tip geometry was selected. A tip sweep of 25 degrees (for the outer 10% of the blade) and an anhedral of 8 degrees (for the outer 5% of the blade) was selected. The anhedral helps to improve the figure of merit and reduce the BVI noise characteristics of the rotor.

5.1.3 – Solidity

The selection of rotor solidity requires careful consideration of blade stall limits. As flight speed increases, a larger portion of the rotor operates in a stalled condition, which manifests itself as an increase in power and vibration. Therefore a solidity of 0.088 was chosen such that the stall boundary of the rotor at 170 knots (maximum cruise speed) was not exceeded during a standard rate one turn (corresponding to a 30 degree bank turn), under ISA, sea level conditions (refer to Section 13.3.2). The effect of solidity on hover performance was also studied, however it was found to be relatively minor over the range of solidities investigated.

5.1.4 – Twist and Taper

A moderate linear blade twist of approximately 12.5 degrees was selected to improve hover performance, delay retreating blade stall, minimize vibration and blade loads in forward flight and improve hover performance in ground effect. Furthermore, the blades were tapered over the last 10% of the blade to improve vertical climb and hover performance. A small amount of taper improves performance by unloading the tips to achieve a more uniform induced velocity distribution across the rotor disk. The effects of linear blade twist and taper on hover performance were studied by using blade element momentum theory with empirical corrections to account for tip loss and compressibility.

5.1.5 – Number of Blades

A five bladed main rotor was selected for the baseline Raven rotor design. Five blades were selected in preference to four in order to reduce the vibration and noise levels of the vehicle in forward flight and to reduce the weight of the vehicle. The effect of increasing the number of main rotor blades on the design gross weight of the vehicle is displayed in Table 5.2.

Table 5.2 – Main Rotor Weight Comparison

Weight component	4 Blades	5 Blades
Main rotor blades	300 lb	256 lb
Main rotor hub	225 lb	177 lb
Swashplateless control system	61 lb	76 lb
Design gross weight	8425 lb	8330 lb

5.1.6 – Airfoil Sections

The choice of airfoil sections was given special consideration due to the fact that significant improvements in rotor performance can be realized with optimal selection of airfoil shapes. Factors that were considered in the selection of the airfoils include lift-to-drag ratio, maximum lift coefficient, drag divergence Mach number, and pitching moments. In order to optimize the performance of the rotor, three different airfoil sections were selected to be distributed along the span. The main lifting airfoil is the VR-12, which is located on the blade from 60% to 90% radius. This airfoil was primarily selected because of its high maximum lift coefficient. However, this amount of lift is obtained at the expense of higher pitching moments. These higher pitching moments were offset by the RAE9648 airfoil, which is reflexed and located inboard of 65% radius where the demands of high maximum lift are not so important. The tip region uses the SSC-A09 airfoil, which has a relatively low thickness-to-chord ratio to give high drag divergence Mach number. The SSC-A09 airfoil is also cambered in such a way as to give a weak shock wave, relatively high maximum lift and low pitching moments.

5.2 – Swashplateless Rotor Design Study

5.2.1 – Feasibility Study of Rotor Control Concepts

A comprehensive assessment of a wide range of potentially suitable swashplateless rotor control concepts was carried out with the aim of establishing an optimum swashplateless design solution (refer to [Chop01], [Chop00], [Stra95], [Siro01], [Fink00], [Chen96], [Roge98], [Chop92], [Tish01], and [Garf75]). The concepts studied were classified into categories according to their method of operation and are discussed briefly below (refer to Table 5.3 for more elaborate details):

- *Blade camber control* – achieved by cyclic excitation with embedded material that is applied differently on the top and bottom surfaces of the blade sections. Based on the lack of availability of a suitable smart material, this concept was found to be infeasible (refer to [Stra95]).
- *Blade twist control* – enables blade twist to be generated from embedded active materials and via the application of a cyclic differential voltage over the span of the blade.
- *Blade pitch control* – actuates individual blades in pitch using hydraulic or smart material actuators.
- *Tilting shaft concept* – effects a tilt of the control mast in order to reorient the direction of the rotor thrust. This concept was found to be infeasible due to the unacceptably large actuation forces and strokes required, and due to the inherent

complexity and weight of the actuation mechanism.

- *Active trailing edge flaps* – flaps integrated with the main lifting section of the blade are deflected cyclically in order to change the lift and/or moment characteristics of the blade section (refer to Table 5.3).
- *Active servo flaps* – auxiliary airfoil sections that are located behind the main blades (adopted by Kaman for primary control) and are actuated in a similar manner to the trailing edge flaps. This concept was found to generate large drag at high speed and was therefore eliminated.

Table 5.3 – Swashplateless Rotor Control Concepts

	Control concept	Control action	Response achieved	Evaluation
Controllable twist blade	Embedded piezo-ceramic actuators [Chen96]	Piezo-actuators oriented at ±45° under skin, produces pure twist	Tip twist ~ 0.5°	Suitable for partial vibration suppression, high weight penalty
	Embedded, distributed piezo-fibers in composite blade [Roge98]	Piezo-fibers embedded at ±45° induce linear blade twist along length of spar	±2° tip twist expected at 1.7 kV	High voltage slip ring, weight penalty, structural integrity issues
Pitch control	All-movable blade [Stra95]	Piezo elements on spar twist a torsion tube causing feathering	Strain requirement ~ 0.4%	Expected strains infeasible with current materials
	Pitch case actuator [Stra95]	Torque tube embedded with SMA fibers at 45° for collective control	Strain requirement ~ 13%	Strain requirement is too large
	Flex-beam actuator [Chop92]	Piezo-strips attached at ±45° on flexbeam surface for active control	Twist less than 1°	Full range of feathering motion at root not achievable with current materials
	Servo actuator [Tish01]	Actuator cyclically operates pitch link at 1/rev	Desired pitch inputs possible	Weight penalty, complexity due to hydraulic slip ring, higher costs and maintenance requirements
Flap actuation	Piezobimorph [Kora00]	Pure bending of bimorph deflects trailing edge flap	±4° @ 1/rev	Multi-layered actuators, significant weight penalty
	Piezostacks [Chop00]	Requires stroke amplification such as LL or X-frame	±3° @ 3-5/rev	Potential for vibration control, infeasible for primary control
	Piezoelectric hydraulic pump [Siro01]	New concept power harnessing at high frequency and stroke amplification with hydraulic system	Achieved large steady stroke/force	Barriers due to high frequency valving and actuator heating
	Piezoceramic actuated bending-torsion composite tubes [Bern00]	Piezo actuators generate spanwise induced twist	Active tip of 10% span – 2.5° @ 1/rev	Potential for vibration reduction
	Electromagnetic actuators [Fink00]	Electromagnet motor drives trailing edge flap	±8° flap deflection	High power required, high weight and temperature penalties

Most of the swashplateless technologies investigated require the use of active 'smart materials' for actuation. Therefore an assessment of current smart materials was carried out in order to find a suitable material (Table 5.4 – [Chop01]).

Table 5.4 – Smart Material Properties

Material	Max. Strain	Block force	Response	Operating voltage	Considerations
Piezobimorphs	Low ~ 0.13%	Low ~ 8-10 lb	Fast: 0-100 kHz	8 layers; 290V_{rms}	40 or more layers required for primary control
Piezoceramic	Low ~ 0.13%	Low ~ 2 lb	Fast: 0-100 kHz	120 V	Embeddable in skin/spar for controllable twist blade
Piezostacks	Low ~ 0.1%	Large ~ 1000 lb	Fast: 0-100 kHz	100–1000 V	Feasible for vibration reduction
Shape Memory Alloys (SMA)	High ~ 6-8%	Large	Slow <1 Hz	Low, 12 V	Low frequency applications such as rotor tracking
Electrostrictive	Low ~ 0.1%	Low ~ 2 lb	Fast: 0-100 kHz	120 V	Low range of operating temperature: 0-40°C
Magnetostrictive	Low ~ 0.2%	Moderate ~ 500-600 lb	Fast: 0-10 kHz	Low, 120 V	Bulky, high weight penalty
Electromagnet	Moderate	Large torque ~ 50 ft-lb	Moderate: 0-36 Hz	High – 215 kV	Thermal management required – 405°F, weight penalty

5.2.2 – Analysis of Active Flap Technologies

Based on the concept feasibility study it was determined that the use of active flaps would provide the best swashplate replacement in terms of performance, cost, weight and reliability. As a result these technologies were studied in greater detail.

Lift and Moment Flap Actuation

Smart active on-blade control surfaces such as trailing edge flaps and smart active tips are the subject of ongoing research that is primarily aimed at achieving vibration control and noise reduction (refer to [Bern00], [Shen00], [Shen01], and [Stra99]). An extension of these concepts for primary control provides the potential to efficiently eliminate the swashplate and associated hydraulic actuation systems [Ormi01].

To further investigate these concepts a propulsive trim model of a helicopter with active trailing edge flaps was developed and an extensive parametric study of various flap configurations was undertaken. In this model the rotor blades were assumed to be rigid, with concentrated torsional and flapwise springs at the hub. The coupled pitch-flap equations were solved using the harmonic balance method and tip losses were ignored. For the purposes of the preliminary analysis, NACA 23012 airfoil section characteristics were used for the entire blade. The cyclic pitch inputs at the flap were defined as:

$$\delta(\psi) = \delta_0 + \delta_{1c}\cos\psi + \delta_{1s}\sin\psi \quad \text{and} \quad \delta_c = \sqrt{\delta_{1c}^2 + \delta_{1s}^2}$$

where $|\delta|$ is the maximum flap deflection and δ_c is the maximum cyclic flap deflection. A coupled propulsive trim code extended this analysis to include the effect of blade flexibility (flap bending and elastic twist) and higher harmonic pitch-flap dynamics.

Trailing edge flaps can be implemented to control blade flapping in two distinct ways, either as a lift flap or as a moment flap. Deflecting a flap will change the sectional lift and pitching moment characteristics of the blade section, which is equivalent to a change in camber and/or a change in angle of attack. The relative chordwise extent of the flap primarily determines its effectiveness in changing these sectional properties. Therefore based on the size of the trailing edge flap as a percentage of blade chord, and the fundamental rotating torsional frequency of the blade, the flap will predominantly act as either an effective lift flap or an effective moment flap. Both of these flap 'types' are discussed in greater detail below.

Lift Flaps

Flaps that are relatively large as a percentage of chord (> 35% chord) on torsionally rigid blades (torsional frequencies higher than 4/rev) will act primarily as lift flaps. A positive flap deflection (defined as trailing edge down) corresponds to an increase in sectional lift and can have the same effect on blade flapping as a positive pitch input at the blade root. However, a positive flap deflection also increases the effective camber of the section and therefore results in a nose down pitching moment. This effect reduces as the flap chord is increased from 25% to 100% of the chord. Furthermore, a relatively high blade torsional frequency suppresses the tendency of the blade to pitch down in response to the change in pitching moment. Therefore a trailing edge flap would act as a lift flap if its primary effect was to change the lift characteristics of the airfoil section, without significantly altering the pitching moment characteristics of the section and pitch dynamics of the blade. By ignoring the effect of the blade pitching moments, a 'best case' preliminary estimate of the effectiveness of lift flaps for primary control was determined.

Under the conditions described above, the most effective lift flap would be an all-moving blade section on a torsionally rigid rotor blade. However, the requirement to maintain structural blade integrity restricts this concept to an all-moving blade tip (<25% of the outboard blade span), which has been previously investigated for vibration control [Bern00]. In such a design, pitch control inputs can be directly traded between the root and the tip flap based on the relative span of the tip section. Providing a collective index angle at the blade root reduces the collective pitch requirements from the flap, without significantly impacting upon cyclic requirements. Figure 5.1 shows the cyclic control deflections required from an all-moving tip section as a function of

forward speed, with collective control actuation being provided entirely at the blade root. Tip sections of 25%, 20% and 15% of the radius were considered. The discontinuity in control deflection requirements at 70 knots corresponds to a change in tip speed (refer to Section 5.1.2). The control deflections required to provide primary control were found to be excessively large, with large deflections at the tip also resulting in high profile drag losses.

Figure 5.1 – Control Deflections for an All Moving Tip

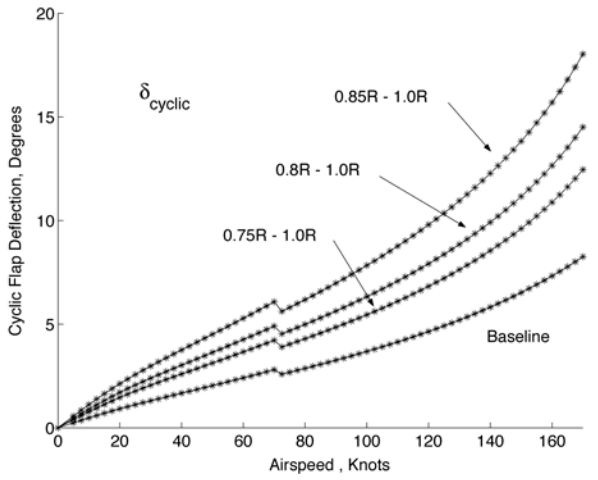

Figure 5.2 – Control Deflections for a Lift Flap

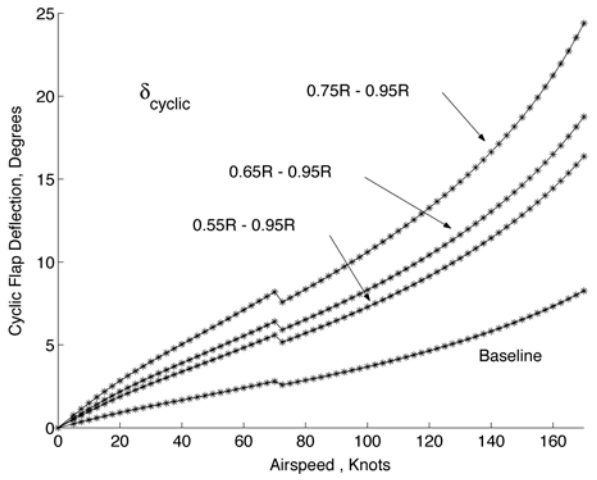

Trailing edge lift flaps, such as those currently used for vibration reduction, were also investigated. Figure 5.2 shows the cyclic control deflections required from a 40% chord trailing edge flap as a function of forward speed, with collective actuation provided entirely at the blade root. Flaps centered at 75% radius with 20%, 30% and 40% spans were considered. The results show that a 30% span trailing edge flap requires cyclic pitch inputs in excess of 16 degrees at a forward speed of 160 knots. Such a requirement was considered to be infeasible in terms of current state-of-the-art actuators (the large deflections also result in large profile losses).

Moment Flaps

Flaps that are relatively small as a percentage of chord (15% - 25% chord) will act primarily as moment flaps. These type of trailing edge flaps are considered to be the most effective in changing the pitching moment of the blade section [Abbo58] and generally have a relatively small impact on the sectional lift characteristics. Coupled with a torsionally soft rotor blade, the moment flaps can be used to generate a significant elastic twist response, resulting in primary pitch control of the rotor. Kaman uses this concept for primary control, by employing an external servo-flap.

Figure 5.3 – Control Deflections for a Moment Flap

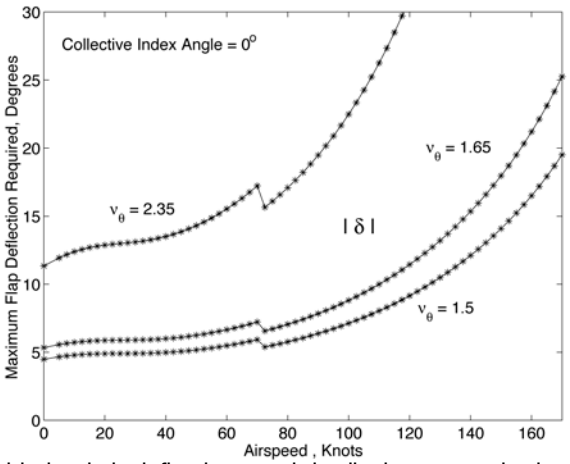

A parametric study was carried out on embedded moment flap configurations of 20% chord (optimum value). Figure 5.3 shows the maximum flap deflections required for a moment flap extending from 65% to 85% radius for different blade torsional frequencies. Torsional frequencies (rotating) were varied from 1.5 to 2.5 per rev, avoiding frequencies close to 2 per rev due to resonance considerations (a torsional frequency lower than 1.5 per rev was considered to be infeasible due to aeroelastic problems). The results do not show any improvement in the required flap deflections when compared with lift flaps, with torsional frequencies in excess of 2.3 per rev resulting in excessively large control deflections. Furthermore, it was also observed that for torsional frequencies between 1.75 and 2.3 per rev, the blade pitch deflections and tip displacements had a

pronounced 2 per rev vibratory component. Therefore as a result, a blade torsional frequency of 1.65 per rev was selected for further study.

Although the deflections required are reasonably small at low speed, at higher speeds they become quite large. Therefore the effect of collective indexing was studied to determine if the deflections could be reduced, particularly at higher speeds. Figure 5.4 shows the longitudinal cyclic and collective flap deflections required in forward flight for collective index angles of 0, 10 and 18 degrees. The results clearly show that for a flap extending from 65% to 80% radius, the required flap deflections to trim the helicopter in level flight reduce dramatically with an increase in collective indexing. Therefore unlike lift flaps, collective indexing has a significant effect on the cyclic deflection requirements. In fact the results show that with a collective indexing of 18 degrees, the maximum collective and cyclic flap deflections required reduce to 5 degrees (up to 160 knots).

The additional lift produced by the flap usually works against the lift produced by the blade pitching motion, and as a result a slightly larger blade pitch is required with a moment flap. However, the collective flap deflection remains positive up to 160 knots with an 18 degree collective index, and both the lift and pitching moments associated with the collective flap deflection work together in producing the blade flapping and feathering required for trim. The collective flap deflection required increases as the pitching moment coefficient of the blade changes from 0 to –0.01, as shown in Figure 5.5. Therefore a low pitching moment coefficient would be beneficial in terms of reducing the required flap deflections. As previously mentioned, the use of reverse cambered airfoils inboard of 60% blade span ensures low blade pitching moments.

Figure 5.4 – Longitudinal Cyclic and Collective Flap Deflections

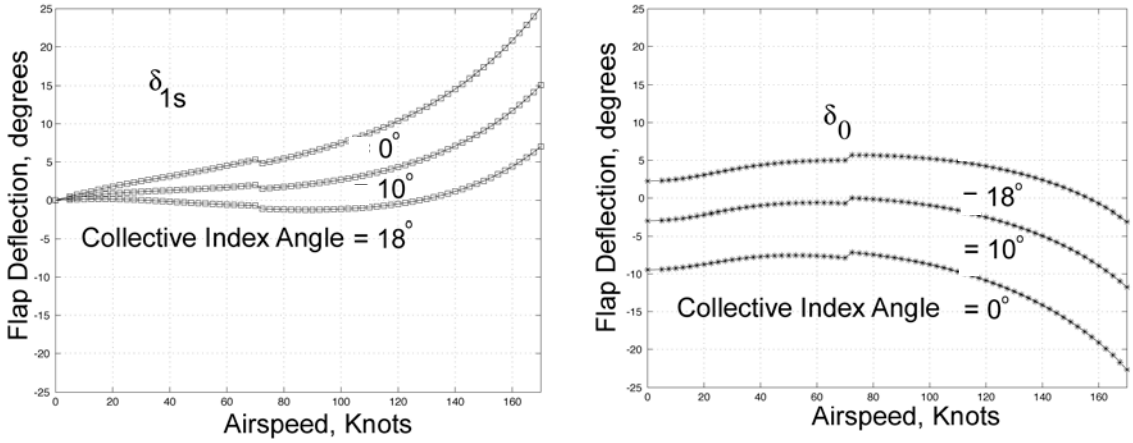

Figure 5.5 – Effect of Pitching Moment

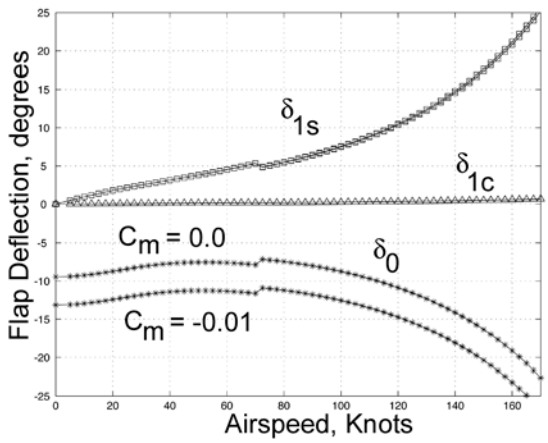

Figure 5.6 – Coupled Trim / Rigid Trim Comparison

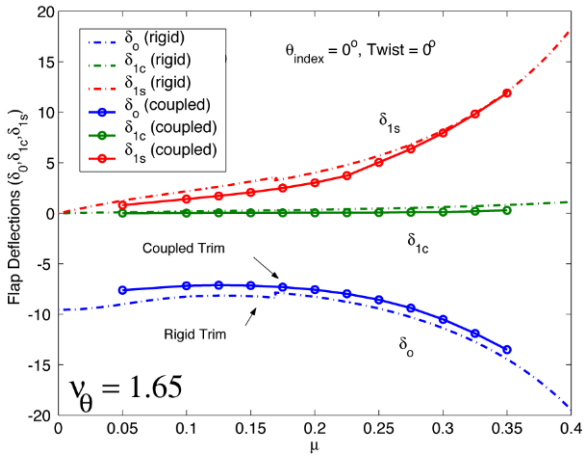

To build confidence in the analysis techniques used, the results obtained from the rigid blade trim model were compared with results from a coupled trim model that incorporates flexible blades (refer to Figure 5.6). The results show excellent correlation between the two methods which ensures that the primary features of the flap designs were captured and that the correct trends were predicted. Therefore based on this preliminary study, the moment flap concept, in conjunction with collective pitch indexing, was identified as the most promising candidate to provide swashplateless pitch control of the rotor blades.

5.3 – Flap Configuration Selection

The swashplateless design solution that is incorporated into the Raven is a revolutionary "next-generation" servo-flap – consisting of an integral moment flap mechanism that is actuated via smart materials. This innovative on-blade control mechanism is employed for primary rotor control, vibration reduction, noise reduction, and in-flight tracking of the rotor. As a result, this optimized design solution improves vehicle performance and reliability whilst also reducing maintenance and weight. The salient design features of the proposed system are presented in this section.

5.3.1 – Moment Flap Design Parameters

Based on the preliminary analysis, a nominal 'plain' moment flap configuration with a flap overhang of 2.6% of the section chord was selected. A detailed study of the effects of various parameters on the flap deflections required to trim over a range of flight speeds was carried out in order to optimize the configuration. The effects investigated included collective index angle, linear blade twist, flap spanwise location and spanwise flap length. Furthermore the effects of these parameters on the associated flap hinge moments and actuation power requirements were also studied.

Flap effectiveness was found to be the highest for low rotating torsional frequencies (1.5 to 1.7 per rev), high blade aspect ratios and low blade feathering moments of inertia. The required flap deflections were also found to reduce as the flap is increased in spanwise length and as it is placed further outboard along the blade (refer to Figures 5.7 and 5.8). However, these considerations were somewhat offset by aeromechanical stability considerations and hinge moment requirements. For example, the likelihood of pitch-flap flutter and pitch divergence increases as the rotating torsional frequency approaches 1 and as the aspect ratio of the blade increases. Furthermore, as the flap is moved outboard the actuator weight contribution to the blade flapping moment of inertia increases, thereby reducing the Lock number and increasing the possibility of pitch-flap flutter. Hinge moment requirements also increase as the flap is increased in spanwise length and moved closer to the tip. Another issue that arose in the system optimization study was the requirement for larger collective index angles (due to the torsionally soft hub) to obtain the same reduction in flap deflections as predicted earlier. Therefore an attempt was made to optimize the flap configuration by addressing all of these issues.

Figure 5.7 – Effect of Varying Flap Location

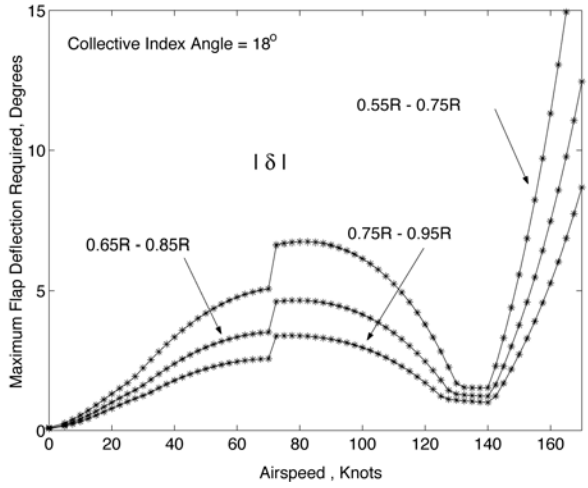

Figure 5.8 – Effect of Varying Flap Span

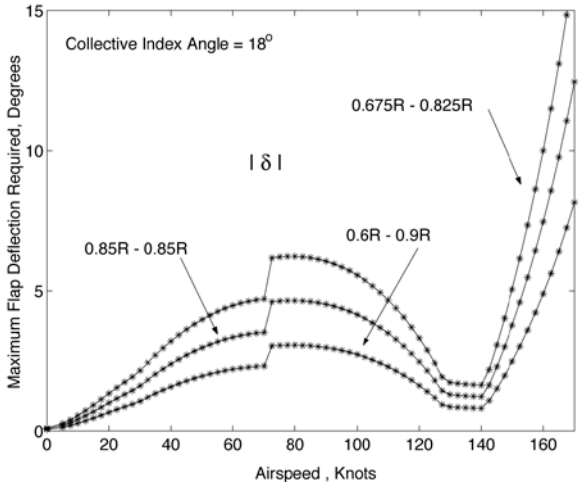

The primary design parameters of the final optimized configuration are displayed in Table 5.5. As can be seen from this table, the configuration consists of two separate flaps, each of 10% radius, that were selected to provide greater flexibility in blade pitch control. Furthermore, this twin flap configuration results in smaller actuators and provides inherent system redundancy. The collective index angle of 22 degrees was selected as a compromise based on flap actuation power requirements (refer to Figure 5.9), flap deflection requirements, blade root elastic deflections (refer to Figure 5.10) and flap hinge moments. The design also corresponds to a low actuation power requirement at 160 knots (Figure 5.9). Figures 5.11 to 5.13 show the hinge moments, flap deflections and pitch deflections required to trim at forward flight speeds up to 170 knots. The results displayed in these figures provide a clear indication of the excellent performance of the proposed configuration. Finally, Figure 5.14 shows a comparison between the rigid trim and coupled trim results. Once again the simplified analysis shows good correlation with the coupled code.

Table 5.5 – Swashplateless Rotor Design Parameters

Parameter	Value
Torsional frequency (rotating)	1.65
Lock number (sea level)	8.37
Blade feathering moment of inertia	5.84×10^{-4}
Flap chord	0.216 ft
Flap spanwise extensions (% radius)	63-73% : 75-85%
Blade sectional pitching moment coefficient	-0.006
Blade twist	-12.5 degrees
Collective index angle at blade root	22 degrees

Figure 5.9 – Flap Actuation Power

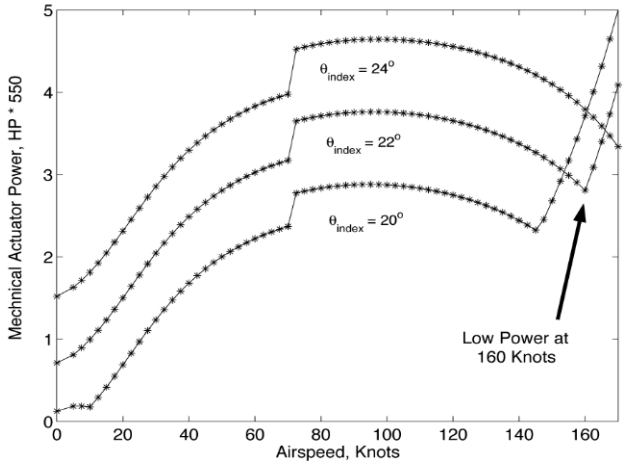

Figure 5.10 – Blade Root Elastic Deflections

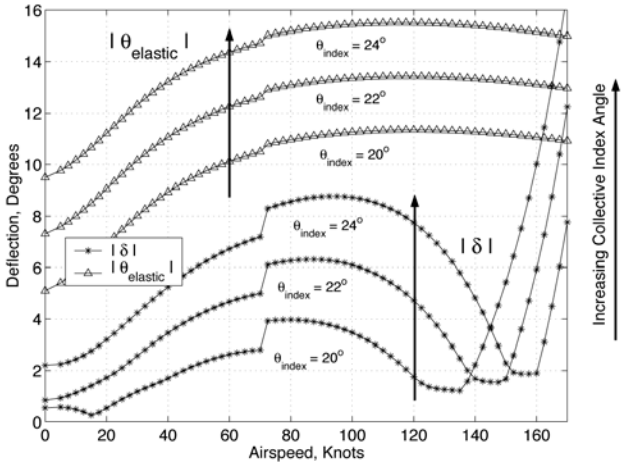

Figure 5.11 – Flap Hinge Moment

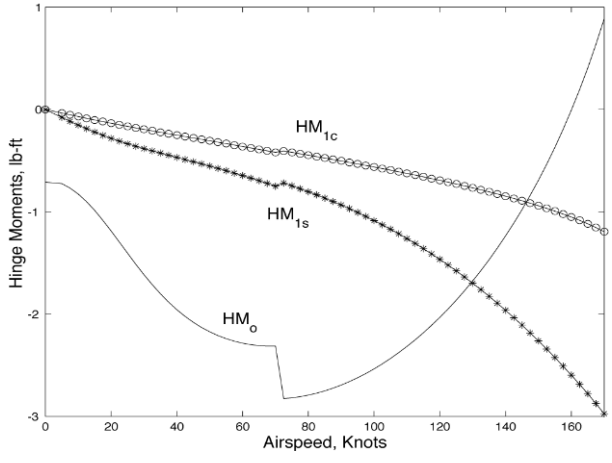

Figure 5.12 – Flap Deflections for Trim

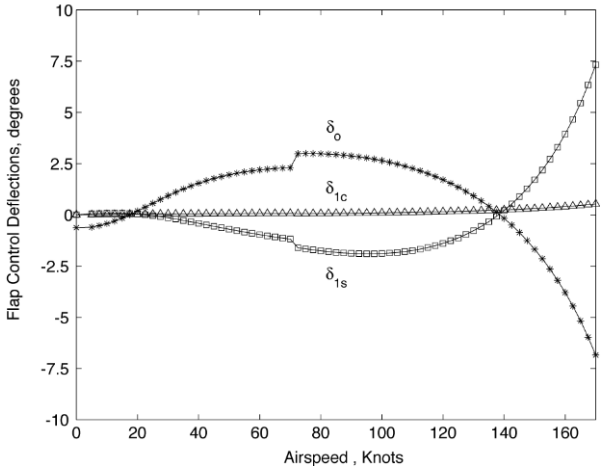

Figure 5.13 – Pitch Deflections for Trim

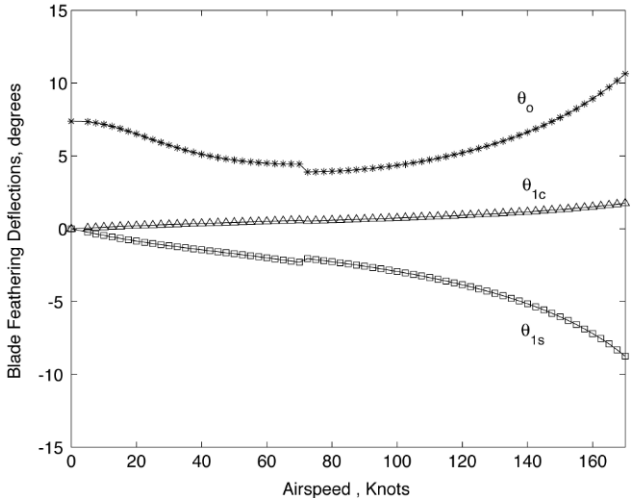

Figure 5.14 – Coupled Trim / Rigid Trim Comparison

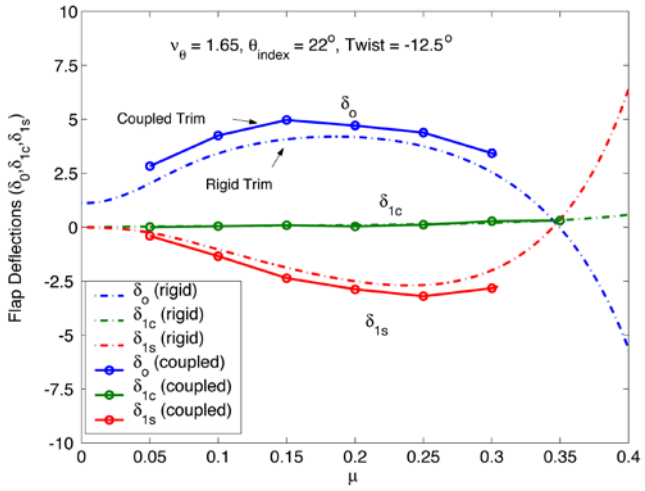

5.3.2 – Actuator Design

Figures 5.11 and 5.12 show the hinge moment and flap deflection requirements for the actuators. Considering these requirements in conjunction with the properties displayed in Table 5.4, it becomes readily evident that existing smart materials are not suitable for use in primary control applications. Based on the data displayed in Table 5.4, the only suitable option would have been to use conventional electromagnetic actuators, resulting in high power and weight penalties. These penalties were judged to be unacceptable and therefore in light of the fact that delivery of the first vehicle is not expected until 2015, the use of a new smart material, referred to as a Magnetic Shape Memory Alloy (MSMA), was proposed (refer to [Adap01] and [Pago01]). The properties of this revolutionary new smart material are displayed in Table 5.6. As can be seen from this table, the maximum strain and operating bandwidth of MSMA's are well beyond the capability of current smart materials and as a result are better suited to providing primary rotor control.

Table 5.6 – Properties of Magnetic Shape Memory Alloys

Parameter	Value
Maximum strain	6%
Maximum stress-by-strain	26.1 psi×in/in
Young's modulus	1117 ksi
Compressive strength	101.5 ksi
Curie temperature	103 °C
Maximum operating temperature	70 °C
Relative permeability	1.5 – 40
Maximum cycle energy density	1.5 ft-lb/in
Field strength for maximum strain	10 kA/in

On-Blade Actuator Design

The on-blade actuators were primarily designed to meet the stroke and hinge moment requirements that were displayed in Figures 5.11 and 5.12. In addition, a number of system related requirements were also considered ([Prec98] and [Lee98]). These additional requirements include:

- *Accessibility* – The actuator must be easily accessible for routine maintenance.
- *Pre-stress* – The flap hinge must be constantly under a pre-stress such that the active material, which is unidirectional in nature, is always under compression. Furthermore, the flap should be equally stiff when actuated in either direction and the preload mechanism must allow for flap adjustment.
- *Centrifugal loads* – The actuator must react the centrifugal loads and the flap hinge must be designed to operate freely in the rotating environment.

Actuator Design Details

The primary actuator sizing parameters (i.e. width, thickness and length) were selected such that the resulting force and strain on the actuator would remain within the force-strain boundary displayed in Figure 5.15. This figure shows the azimuthally varying force acting on the actuator as a function of strain. As can be seen, the actuator was designed to operate well below the material limits for all flight conditions. To enable the actuator mechanism to be designed (a schematic of which is shown below) a mathematical model was developed that is based on the following equation:

$$M_H - I_\theta \frac{d^2\delta}{d\psi^2} + K_\theta(\delta - \delta_{bias}) - K_a \frac{e(\psi)}{r} - \frac{C_a}{r}\frac{de(\psi)}{d\psi} = 0$$

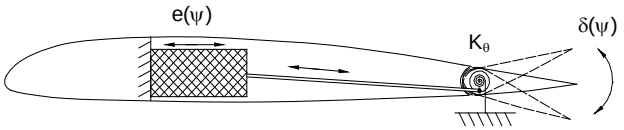

K_a	Actuator stiffness (lb-in)	M_H	Flap hinge moment (lb-in)	I_θ	Flap feathering moment of inertia (slugs-ft^2)
C_a	Actuator damping (lb-in)	δ	Flap angle of actuator (rad)	δ_{bias}	Spring bias angle (rad)
K_θ	Torsion spring stiffness (lb-in/rad)	e(ψ)	Actuator stroke (in)	R	Radius of hinge tube (~0.25 in)

The optimized actuator design consists of the following primary components (refer to Foldout 5.1):

- *Magnetic SMA* – MSMA is a unidirectional material that is only capable of actuation under compression. To enable bi-directional actuation of the flap, a spring was built into the design. The actuator and spring design parameters were chosen to ensure that the actuator is fully functional throughout the entire flight envelope.
- *Magnetization Material* – For actuation the required magnetic field varies from 200 to 400 kA/m [Pago01]. The design consists of a magnetic field bias generated by permanent magnets of field strength equal to 300 kA/m. Two coils provide a differential magnetic field of ±100 kA/m. Samarium-Cobalt permanent magnets are used because they have a much higher maximum energy when compared with conventional magnets [Jile00].

Figure 5.15 – Force Strain Curve for MSMA Actuator

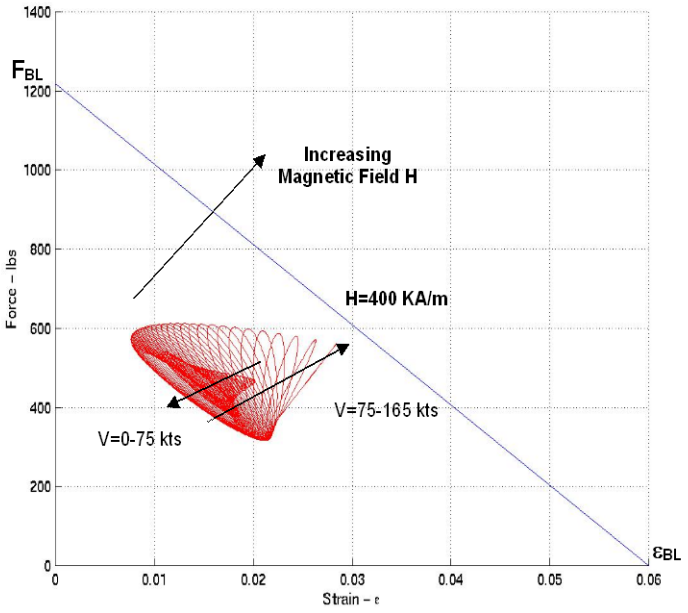

- *Spring Design* – A torsion spring was incorporated into the design to provide stiffness for effective control of the downward movement of the flap. The spring is biased to an initial angle to provide actuator pre-compression.
- *Housing and Support Structure* – The actuator is placed aft of the spar for easy access. The actuator is rigidly attached to the spar such that the centrifugal forces will not compromise the operation and safety of the blade. An elliptical access hatch is provided to prevent stress concentrations, whilst countersunk screws (with caps) are used to reduce aerodynamic interference.

The principle of operation of the system is relatively straight forward; the trailing edge flap rotates about a hinge tube, which attaches to the main blade through two spherical bearings (refer to Table 5.7 [McMa01]). The torsion spring is connected to the hinge tube and provides the required stiffness and pre-compression. The actuator push rod connects via a pitch horn to the tube and provides the necessary actuation moment to deflect the flap (refer to Foldout 5.1).

Table 5.7 – Bearing Design Features

Inner race diameter	Outer bearing diameter	Bearing thickness	Maximum static load	Maximum cyclic load per bearing
0.188 in	0.563 in	0.219 in	3975 lb	1002 lb

Wires to each coil (magnet) are required to carry a current of 4 Amperes at 43 Volts. These wires are routed from the slip ring (Section 5.4) to the actuators along the spar. Each actuator requires 4 sets of wires, with one pair added for redundancy. The electrical power requirements for this actuator (209 Watts) are much lower than that required for blade deicing, which for this blade was estimated to be 1.5 kW. The actuator design presented is therefore very economical in terms of power, weight and volume. The relevant actuator dimensions are displayed below in Table 5.8.

Table 5.8 – Actuator Dimensions

Component	Thickness (in)	Width (in)	Length (in)	Weight (lb)	Current (A)	Voltage (V)	Power (W)
MSMA	0.8	1.75	2.0	0.798	~	~	~
Electrical coils (×2)	0.8	1.0	2.0	0.311	4	42.4	210
Permanent magnet (×2)	0.8	0.5	2.0	0.226	~	~	~
Total actuator (includes housing)	0.9	5.0	2.3	1.9	4	42.4	210

The RFP states a requirement to measure the rotor states and therefore gyros will be placed on the rotating shaft to measure the flap, pitch and lead-lag motion of the blades. Hall-Effect sensors will be used to measure trailing edge flap deflections, with the sensor voltage being transferred through the slip ring to the data acquisition system. This feedback will then be sent into the flight control system and integrated into the HUMS, which will enable system status to be monitored at all times.

The actuator design as presented provides a low weight, low power system that is capable of actuation throughout the entire flight envelope, without compromising vehicle maintainability or accessibility. Future work is required for concept validation and system tuning that will consist of experimental testing in static, rotating and forward flight conditions. The University of Maryland, under the sponsorship of DARPA, is currently investigating primary on-blade control technology in greater detail. The results of this research should provide further insight into on-blade swashplateless control systems.

5.4 – Slip Ring

A slip ring is used to transfer power from the fixed frame to the rotating frame. Conventional slip rings usually consist of copper brushes and one or more rings through which electrical current is passed. Mechanical imperfections and wear due to friction may result in a loss of contact, which would cause a malfunction of the actuators. To enhance system reliability and safety, a different type of slip ring developed by NASA Ames was used in this design. The slip ring, referred to as a 'Contactless Magnetic Slip Ring' [Kuma97], is designed to transfer electric power between the stationary and rotating equipment without any mechanical contact. The mechanism consists of a primary and secondary coil. The primary coil is attached to the transmission housing where it receives current from the electrical generators. The wrapped wires of the secondary coil have first and second ends connected to the wires along the main rotor shaft, which supply current to the blade actuators. The amount of power that can be transferred is limited only by the heat dissipation scheme and the size of the device.

5.5 – Blade Structural Design

The structure of the Raven's main rotor blades must be designed to accommodate the onboard flaps, actuators and associated hardware. Furthermore, the blade is torsionally flexible, which imposes additional constraints upon the design of the blade chordwise CG location. The aft CG limit is imposed by the requirement to avoid pitch-flap flutter and pitch divergence, whilst the forward CG limit is imposed by the nose down pitching moments generated by the main lifting section of the blade.

5.5.1 – Blade Structural Details

The blade structure (displayed in Foldout 5.1) consists primarily of a D shaped spar and zero degree uni-axial fiberglass plies, enclosed in a graphite epoxy torsion wrap. Leading edge weights are placed ahead of the spar, with the remaining internal blade structure consisting of Nomex honeycomb. The outer skin is made from a glass/epoxy fabric. The spar cross section was designed to accommodate spanwise changes in airfoil shape, actuator placement and tip geometry. Tungsten mass ballast weights were used to move the center of mass of the blade to the quarter chord location and are placed locally in the inner cavity of the nose block at discrete locations along the blade. The erosion strip, which is mounted over the blade leading edge, consists of a stretch formed of a titanium sheet that is bonded to a sheet of neoprene, which is in turn bonded to the composite spar. Between the erosion strip and the spar is a de-ice blanket that is used to heat the leading edge. A cutaway of the blade section is displayed in Foldout 5.1, and shows the spar structure in greater detail. Table 5.9 summarizes the properties of the primary structural materials used in the design of the blades.

Table 5.9 – Actuator Dimensions

Material	Density (lb/in^3)	Young's Modulus (ksi)	Shear Modulus (ksi)	Nominal ply thickness (in)
0° Uniaxial Fiberglass Epoxy	0.067	6.3×10^3	0.52×10^3	0.009
±45° Graphite	0.055	2.1×10^3	4.55×10^3	0.018
Tungsten	0.669	40×10^3	19.2×10^3	~
Nomex honeycomb	0.00116	0.0105×10^3	0.0042×10^3	~

5.5.2 – Blade Folding

The rotor design of the Raven requires a collective indexing of 22 degrees at the blade root. Therefore to facilitate manual blade folding, an additional attachment was designed to connect the hub to the blade. This added component provides 19 degrees of twist between the hub and the blade and is attached at both ends with the help of two sets of wire-locked bolts. In order to fold the blades, one of the bolts on the hub mating piece is removed such that blade rotation can take place about the other bolt. The gearbox is indexed such that when the blades are folded one of the five blades will be aligned with the tailboom (zero degrees azimuth), two blades will be folded back and two folded forward (refer to Foldout 5.2).

5.5.3 – Lightning Protection and Electromagnetic Shielding

Most helicopter rotor blades are designed to withstand a 200 kA lighting strike and still permit the helicopter to land safely [Alex86]. In designing the blades for lightning protection it is preferred that the flow of current be passed through the exterior of the blade. In the Raven design, the actuators and slip ring are particularly vulnerable to any large flow of current. Additionally, the composite spar may be delaminated in the presence of high heat. Therefore in order to protect the vulnerable components, exterior doublers made up of a conductive material are bonded to the top and bottom of the blade sections containing relatively large internal masses of metal. These metal doublers were designed to conduct the stray electrical current to the metal abrasion strip, which in turn directs it along the span to the root end attachment of the blade. Furthermore, to prevent interference of the actuator from stray electromagnetic fields, the housing was wrapped with layers of nickel/iron alloy foil. This material consists of 48% nickel which is effective at providing low frequency magnetic shielding [Amun01].

5.6 – Hub Design

The hub was designed to ensure low parasite drag, low hub moment stiffness (for improved vibration characteristics, gust response and handling qualities), reduced maintenance requirements (through simplicity and reduced number of parts), and high fatigue life. Additionally, the unique moment flap design imposes a requirement for low torsional stiffness. In order to meet all of these objectives, a bearingless hub was selected. A bearingless design was selected primarily from the standpoints of structural simplicity, low weight, and reduced drag – which in turn result in improved reliability and maintainability. Furthermore,

bearingless rotors have greater control power compared to articulated designs, which results in better handling qualities ([Moui75] and [Bous83]).

5.6.1 – Bearingless Hub Design Details

The bearingless hub design developed for the Raven (refer to Foldout 5.2) consists of four primary elements: a flexbeam, a torque tube, a pitch spring and an elastomeric damper.

- *Flexbeam* – This is the primary structural component through which flap, lead-lag and pitch motion is achieved. The cross-sectional spanwise variation of the flexbeam was tailored to the required stiffness and material properties. The bearingless main rotor is a soft-inplane design and therefore a limit was imposed on the lead-lag frequency of the blade in order to avoid aeromechanical instabilities. The flexbeam is cantilevered at one end to the hub support structure and bolted at the other end to the blade indexing component.
- *Torque Tube* – In a conventional rotor design the torque tube transmits the pitch inputs from the pitch link to the blade. In this design however, the relatively stiff pitch link is replaced with a spring that provides flexibility in pitch. Additionally, the torque tube reacts against an elastomeric damper, which is used to augment rotor lead-lag damping. The pitch spring element is a compression spring that was designed to carry the 1/rev oscillatory loads and provide the necessary stroke to achieve the required blade pitch. The stiffness of the spring was determined using UMARC and was designed to allow a maximum blade pitch of ±20 degrees. The primary spring parameters are displayed below in Table 5.10.

Table 5.10 – Spring Design Features

Length (in)	Turns	Coil diameter (in)	Coil wire diameter (in)	Ultimate fatigue shear stress (psi)	Shear modulus (psi)
7.75	18	1.7	0.19	50×10^3	12×10^6

5.6.2 – Hub Manufacture

The flexbeam is fabricated from unidirectional S-glass/epoxy tapes. S-glass fabric is added to achieve the tailored shape along the span. The torque tube is fabricated from carbon fiber filaments. Unidirectional tape is added to provide high chordwise stiffness [Naka01]. The elastomeric damper is made up of layers of alternate elastomer and metal shims. SAR missions can require operation in high temperature and humidity, therefore a silicone rubber elastomeric damper was selected ([Lord01], [Hutch01], and [Paul01]).

5.7 – Autorotation Characteristics

Autorotation performance depends on several factors including the rotor disk loading, the stored kinetic energy in the rotor system and the flap control authority. An autorotation index is often used in main rotor design to provide a means of comparing the autorotative performance of a new helicopter design, with existing helicopters that exhibit acceptable autorotative characteristics. Table 5.11 lists the autorotative index (which is defined as the kinetic energy of the main rotor divided by the gross weight times the disk loading) of the Raven with that of several other helicopters of similar weight. As can be seen from this table, the Raven has good autorotation characteristics compared with the other helicopters.

Table 5.11 – Autorotation Index Comparison

Helicopter	GTOW (lb)	Polar moment of inertia (slug-ft^2)	Rotor speed (rad/sec)	Disk loading (lb/ft^2)	Autorotation index (ft^3/lb)
Raven	8330	1201	35.46 ; 37	7.10	12.8 ; 13.9
Bell 412	11900	2760	33.9	7.36	18.1
S-76A	10300	1890	30.68	6.96	12.4
SA365N	8818	1542	36.55	7.53	15.5

5.8 – Active Vibration Control

Helicopters are susceptible to high vibration levels because of the unsteady aerodynamic environment in which the flexible main rotor blades operate. High vibration loads degrade ride quality and result in accelerated fatigue of structural components. A low fundamental torsional frequency for the Raven main rotor makes the control of higher harmonic vibratory blade response even more critical, especially at higher forward speeds. High vibration loads at the blade root in the rotating frame as well as vibratory loads that filter to the non-rotating frame need to be addressed. For a tracked rotor, blade root loads are dominated by 2/rev pitch excitation, while non-rotating vibratory loads on the fuselage are dominated by 5/rev harmonics (for a 5 bladed rotor). At a torsional frequency of 1.65/rev, there is a relatively strong 2/rev blade pitch response in high speed forward flight conditions. Therefore a vibration reduction scheme is proposed for the Raven through higher harmonic excitation of the outer trailing edge flap. Based on flap performance studies on a typical bearingless 5 bladed rotor, a 10% span, 20% chord trailing edge flap centered at 80% radius (outer flap) was shown to maximize flap effectiveness and minimize the actuation power required for active vibration control [Milg97]. In order to completely minimize vibration, flap deflections of about ± 2 degrees were required.

A robust neural-network based adaptive control methodology will be employed to implement Individual Blade Control (IBC) on the Raven (refer to [Spen00] for control algorithm details). A radial basis neural network structure is used to approximate the command input to the trailing edge flaps. The controller is implemented in discrete time by sampling the hub loads and control inputs on a per rev basis. It performs both system identification and vibration reduction in real time. A time domain control algorithm formulation was designed such that vibration reduction is not limited to a specific harmonic, but may be performed at any integral multiple of rotor speed. Additionally, this controller was designed to control each blade independently [Roge01]. Recently this control methodology was demonstrated successfully in a Mach scaled rotor test in the Glenn L. Martin wind tunnel. It successfully minimized vibrations by up to 90% for steady as well as transient flight conditions [Kora00]. Therefore the trailing edge flaps on the Raven will not only be used for primary control and active in-flight tracking, but also for vibration and noise reduction. Several researchers are investigating BVI noise reduction using active trailing edge flaps ([Wang99] and [Stra95]). With focused research and continued advances in smart materials, the possibility of achieving the rapid flap deflection rates required for BVI noise control appears promising.

5.9 – Rotor Dynamics

The main rotor system is a soft inplane bearingless design with onboard servo-flaps and actuators. As a result the rotor dynamics were examined carefully to ensure proper placement of frequencies and a sufficient margin from aeromechanical instabilities.

5.9.1 – Unique Requirements

The constraints imposed on the dynamics of the rotor system proposed for the Raven include:

- *Rotor Operating RPM* – The rotor has two distinct operating speeds, which places an additional requirement that the blade natural frequencies be properly placed at both operating conditions to avoid resonance with rotor harmonics.
- *Bearingless Rotor System* – To avoid ground and air resonance instabilities with a soft inplane rotor system requires additional inplane damping. For a stiff inplane rotor system the chordwise loads become too high and therefore a soft bearingless rotor with a lag frequency of 0.65/rev was selected.
- *Torsional Stiffness* – In order to optimize the effectiveness of the advanced rotor control system, the fundamental torsional frequency was set at 1.65/rev.
- *On-blade Actuators* – The stiffness and mass distribution of the rotor blades was tailored to account for the presence of the onboard actuators. This was an important consideration in developing the finite element model for the blade section.

5.9.2 – Dynamics Analysis

To obtain the blade natural frequencies and the rotor fan diagram, the University of Maryland Advanced Rotorcraft Code (UMARC) was used. The blade was divided into 20 discrete elements with the flexbeam modeled with 4 elements, the torque tube with 3 elements and the blade section with 13 elements. The blade sections that incorporated actuators were discretized into individual elements. A code was developed to determine the blade stiffness and inertia of each of the blade sections. A frequency placement and stiffness optimization code was employed to develop a design to generate the desired key frequencies. The blade frequencies that were obtained after the final iteration in the optimization process are displayed in Table 5.12 and the blade stiffness and inertial distributions are displayed in Figure 5.16. In these plots the actuator and bearing locations can be identified by the spikes. The rotor fan diagram is displayed in Figure 5.17 and illustrates the regions of operation at the two distinct rotor RPM settings.

Table 5.12 – Rotor Natural Frequencies

	Hover Setting			Cruise Setting		
Mode	1st	2nd	3rd	1st	2nd	3rd
Flap	1.027	2.62	4.1	1.03	2.67	4.23
Lag	0.64	3.23	6.7	0.65	3.44	6.79
Pitch	1.64			1.65		

Figure 5.16 – Blade Stiffness and Mass Distribution

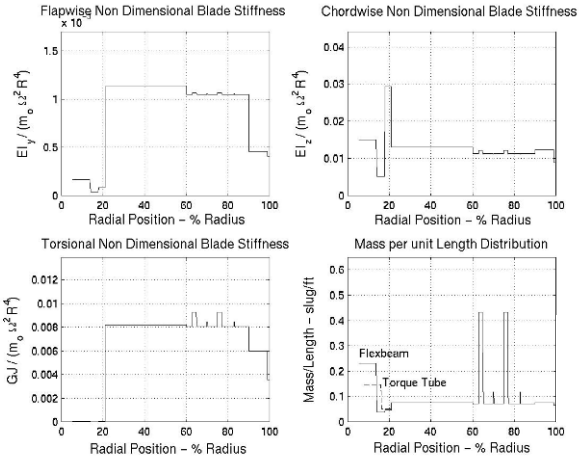

Figure 5.17 – Rotor Blade Fan Diagram

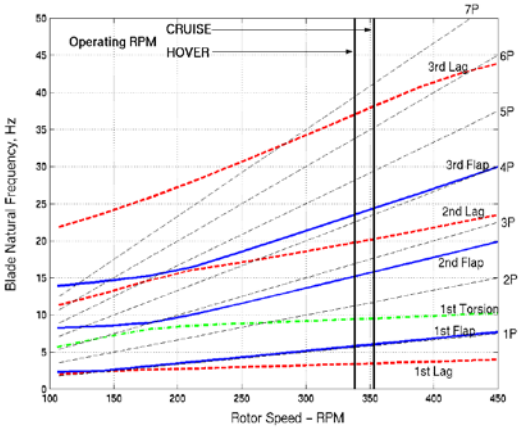

Figure 5.18 – Flutter and Divergence Stability

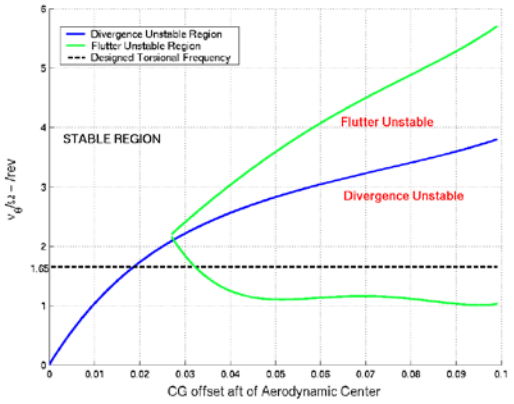

Figure 5.19 – Flap/Lag/Pitch Stability

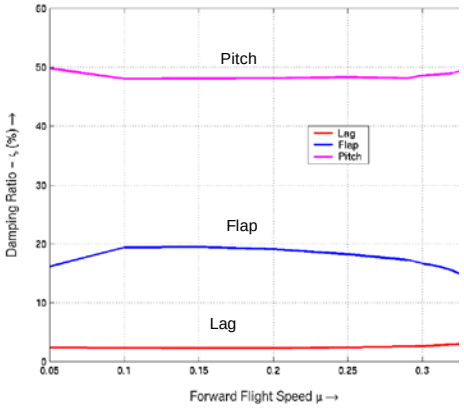

Stability Analysis

A stability analysis was conducted to assess whether the system enters into an unstable region during flight. In hover (Figure 5.18) the divergence criteria becomes critical at the operating torsional frequency of 1.65/rev, for a CG located 0.018 chord lengths aft of the aerodynamic center. An adequate margin of safety was maintained by placing the CG 0.01 chord lengths ahead of the aerodynamic center during the blade structural design. A comprehensive aeromechanical stability analysis in forward flight (Figure 5.19) showed that the pitch and flap modes are stable, with coupling having a stabilizing effect on the pitch mode. The flap mode damping reduces somewhat but remains stable. A similar analysis was carried out to ensure that the hover flap-lag instability modes were not excited. Figure 5.19 clearly shows that the lag mode is stable throughout the flight envelope.

Foldout 5.1

Foldout 5.2

Section 6 – Anti-Torque System Design

The primary purpose of the anti-torque system is to provide sufficient yaw control for the rotorcraft. This means that the system must not only be capable of generating an anti-torque force to counter the torque reaction of the main rotor, but also must be capable of providing the pilot with directional control. In this section the anti-torque design will be presented, together with the empennage layout and primary design features.

6.1 – Anti-Torque Configuration Selection

In Section 3 a fan-in-fin configuration was selected over a conventional tail rotor as the best anti-torque design for a single main rotor SAR helicopter. The primary reason given for the elimination of the conventional tail rotor was that the dangers imposed by the exposed tail rotor were unacceptable. Although this reason is valid, it is not entirely sufficient due to the fact that measures can be taken to reduce the associated dangers, such as positioning the rotor at the top of the fin. Therefore in order to further justify that the best anti-torque system was indeed selected, the characteristics of the two anti-torque configurations will be compared in terms of performance and operational considerations.

6.1.1 – Performance Comparison

The relative performance of the fan-in-fin (also referred to as 'fenestron' or 'fantail') and conventional tail rotors were compared in terms of their inherent hover, forward flight and handling qualities attributes.

- ***Hover performance*** – In hover the fan-in-fin configuration is a more efficient anti-torque design due primarily to the duct, which is capable of generating thrust. The negative static pressure on the duct inlet generates approximately 50% of the total anti-torque thrust, which in turn significantly reduces the power requirements. The fan-in-fin design also eliminates the fin blockage effect, which typically reduces the thrust capability of a conventional tail rotor by 10% [Vuil86].
- ***Forward flight performance*** – The power requirements of a fan-in-fin in forward flight are usually lower than that of a conventional tail rotor. In forward flight, a correctly sized vertical fin will be capable of significantly offloading the fan-in-fin such that its thrust requirements are small. Consequently the shaft power required by the fan-in-fin will be low and will primarily consist of the power required to overcome the profile drag of the blades. Power measurements in cruise flight on a fenestron tail shaft indicate a power requirement of less than 1 percent of the main rotor power, which has to be compared with a typical value of between 3 to 5 percent for a conventional tail rotor [Vuil89].
- ***Handling qualities*** – Helicopters equipped with a fan-in-fin anti-torque system have proven to have excellent yaw maneuverability and smooth handling [Vuil86]. Crosswinds from the left (effective descent) will have a tendency, as for conventional tail rotors, to oppose the fan flow, to create airflow recirculation around the duct and, if wind speed is sufficient, to develop into a vortex ring state. However since fan-in-fin induced velocities are generally much higher than for conventional tail rotors, this vortex ring state phenomena will usually take place at higher wind speeds (the structure surrounding the fan also helps prevent easy establishment of a recirculating airflow).

6.1.2 – Operational Comparison

A number of operational factors, including safety, reliability, noise, weight and cost, were also looked at in order to further compare the suitability of the two anti-torque configurations.

- ***Safety*** – A fan-in-fin design enhances safety both in flight and on the ground by housing the rotor in a shroud, which prevents the rotor from injuring personnel and striking obstacles. When the aircraft is on the ground, people can see the shroud and cannot be hurt by the rotor, which enables untrained hospital porters to load and unload stretcher patients in safety. Furthermore, the shroud prevents the rotating fan blades from striking the ground during landing or takeoff. In flight it is difficult, if not impossible, for the fan to be hit by debris detached from the airframe or main rotor blades (or to snag hoist

cables). The inherent safety features of the fan-in-fin are the reason why in more than two million flight hours that have been logged on helicopters fitted with fan-in-fin's, there has not been a single serious accident [Vuil89].

- ***Reliability*** – A fan-in-fin design can be significantly offloaded in forward flight, resulting in a considerable reduction in the dynamic strains on the rotating parts of the fan. Furthermore, a fan-in-fin is less sensitive to icing effects than conventional tail rotors. All of these inherent features serve to enhance system reliability, with experience showing that the mean time between removal for tail rotor blades on the entire Aerospatiale helicopter fleet is about three times higher for the fan-in-fin concept than for conventional tail rotors [Vuil86].
- ***Noise*** – The fan-in-fin design houses the fan in a shroud, which reduces radiated noise. Results have shown that a five to six decibel reduction is obtained in the plane of rotation of the blades due to the masking effect of the shroud, which can provide substantial noise reduction on the ground trace of a helicopter in forward flight [Moui86]. Furthermore, the fan-in-fin radiated noise decreases in forward flight as the fan thrust tends to zero.
- ***Weight and Cost*** – The fan-in-fin concept shows a substantial reduction in weight and cost, on the order of 20 percent [Moui86], when compared with a conventional tail rotor design. This is due primarily to the fact that a conventional tail rotor would have to be mounted at the top of a vertical fin (to reduce ground safety concerns), necessitating the use of an additional intermediate gearbox.

6.1.3 – Assessment

Considering the large number of performance and operational advantages that the fan-in-fin design has over a conventional tail rotor, it appears to be the best anti-torque configuration for a helicopter tasked with the specified SAR mission requirements.

6.2 – Fan-in-Fin Design

The fan-in-fin configuration is a unique anti-torque system whereby the fan and duct generate equivalent amounts of thrust. As a consequence, the design of a fan-in-fin anti-torque system requires special attention to be given to the design of the fan and the duct, in order to optimize system performance.

6.2.1 – Methodology

A relatively simple methodology was developed to enable a preliminary sizing of the fan-in-fin to be carried out. The method is based upon a momentum theory approach, with non-ideal effects being incorporated through the application of full-scale fenestron test results [Moui86]. These tests give the fan figure-of-merit as a function of mean blade loading and enable the effects of advanced airfoil sections and guide vanes to be incorporated into the analysis. This method is capable of capturing the effects of all the major blade parameters, such as blade chord, number of blades, diameter, and root cutout, however it is incapable of capturing the effects of changes in blade pitch, twist or thickness. Since fan performance is primarily dependent upon the global design parameters, then this method is sufficient for preliminary design purposes. Note that this analysis is incapable of directly considering the effects of the duct shape parameters (such as inlet lip radius, exhaust lip radius, duct width and duct aft closure shaping). The duct was however globally considered by setting a flow contraction ratio from the rotor disc to infinity (the contraction ratio was derived from tests and was taken as 0.95 [Vuil86]).

6.2.2 – Fan Design

The fan design parameters were selected to provide a design that is efficient, lightweight, durable, and easy to manufacture and maintain, whilst meeting the stringent crosswind requirements expressed in the RFP. The pertinent design parameters are summarized below in Table 6.1.

Table 6.1 – Fan Design Parameters

Parameter	Value	Parameter	Value
Tail rotor moment arm	22.3 ft	Fan rotational speed	3320 RPM
Fan diameter	3.7 ft	Blade twist	-7 deg
Blade chord	0.39 ft	Root cutout	38%
Number of blades	8	Fan rotation direction	top aft
Fan solidity	0.54	Airfoil sections	OAF102 / OAF117 / OAF128

The selections made include an eight bladed fan with untapered planform, OAF series airfoils and 7 degrees of linear twist. The advanced OAF airfoil sections were selected to provide optimum performance over a wide range of operating conditions. The untapered fan planform was chosen to simplify manufacturing and improve maximum thrust capability. The number of blades were chosen based on acoustic, reliability, and durability considerations. The fan tip speed was chosen as a result of acoustic considerations. The fan twist was selected to alleviate control reversals found in early Aerospatiale helicopters [Keys91].

Fan diameter – the fan diameter was sized to provide sufficient anti-torque thrust to enable the helicopter to hover in a 45 knot crosswind, whilst also giving the pilot sufficient yaw control to generate a maximum turn rate of 0.75 rad/sec (43 deg/sec). This last requirement comes from Lynn [Lynn69] who specifies a set of maneuvers that a helicopter must be able to perform at its critical ambient design condition. The total fan power required versus fan diameter is displayed in Figure 6.1. As can be seen from the figure, the selection of fan diameter represents a compromise between minimizing power requirements and minimizing weight. The stringent design condition specified above enables a maximum sideward flight speed of approximately 70 knots to be achieved (right sideward flight, design gross weight, ISA, sea level conditions).

Figure 6.1 – Fan Power Requirements

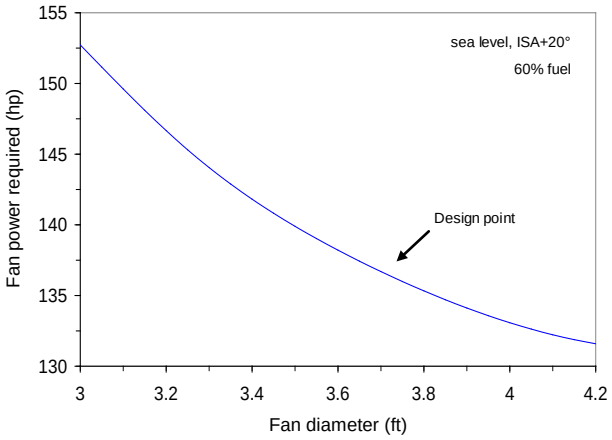

Blade Spacing – An unequal blade spacing with an asymmetry angle of 35/55 degrees was selected based on acoustic considerations (refer to Foldout 4.1). A spacing of 35/55 degrees was presented by Niwa as the optimum value based on experimental tests that were carried out on the OH-1 fan-in-fin design [Niwa98].

6.2.3 – Duct/Shroud Design

The design of the duct (or shroud) is critical in obtaining the desired anti-torque performance, due to the fact that it can support a thrust component as great as the fan itself (negative static pressure on the duct inlet produces approximately 50% of the total fan-in-fin thrust). The pertinent duct design parameters are summarized below in Table 6.2.

Table 6.2 – Duct Design Parameters

Parameter	Value	Parameter	Value
Inlet lip radius / fan diameter	0.075	Duct divergence angle	5 deg
Exhaust lip radius / fan diameter	0.075*	Duct width	1.20 ft

* - Refer to discussion below.

The duct includes a small collector with rounded lips, a small cylindrical zone at the blade passage and a conical diffuser accommodating the transmission tube, the gearbox, the guide vanes (which also function as transmission support arms) and the pitch control system. Eight stator blades (guide vanes) are placed in the diffuser replacing the gearbox support arms of earlier designs in order to recover the flow's rotational energy (Figure 6.2).

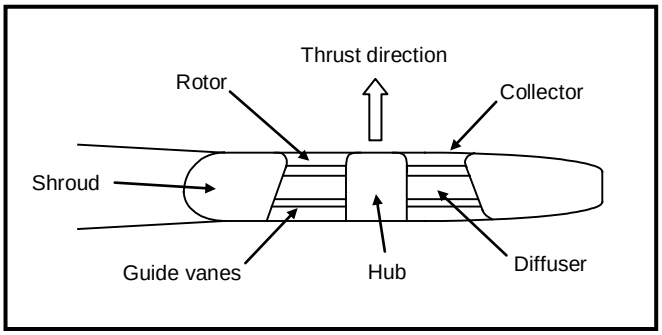

Figure 6.2 – Duct/Shroud Cutaway Layout (Plan View)

Scale tests performed at the UTRC showed that to obtain maximum hover performance, inlet lip radius to diameter values greater than 0.065 to 0.075 are required [Keys91]. Testing of scale RAH-66 models indicated that increasing the radius of the aft 1/3 of the exit lip to that of the inlet provided a measurable drag reduction and improved reverse thrust performance [Keys91]. The duct width was selected based on existing advanced designs that utilize guide vanes in the diffuser.

Stator blades – Tests conducted at Aerospatiale in the 1980's showed the benefits that could be achieved by recuperating the rotational energy that is usually lost in the flow. The tests showed that the maximum figure-of-merit could be increased by approximately 4 percent and the maximum thrust by 26% by incorporating guide vanes, or stator blades, inside the diffuser [Vuil86]. Furthermore, the use of stator blades also improves the pressure recovery, which reduces the required diffuser length, resulting in a narrower shroud and reduced parasite drag [Vuil86].

Diffuser Angle – The diffuser angle (or duct divergence angle) is limited to a practical value of approximately 5 degrees – with higher diffuser angles flow instabilities may occur due to adverse interaction with the main rotor wake [Vuil86].

6.3 – Empennage Design

The empennage consists of the vertical and horizontal stabilizers and the associated fuselage structure. In conventional helicopter designs the primary purpose of the stabilizers is to enhance stability about a particular axis. However, for a helicopter configured with a fan-in-fin anti-torque system, the vertical stabilizer is usually designed with a different purpose in mind – to offload the fan in forward flight. Therefore in this preliminary design study the vertical fin was primarily sized to offload the fan whereas the horizontal stabilizer was sized to provide sufficient stability about the pitch axis. The main stabilizer design parameters are summarized in Table 6.3.

Table 6.3 – Empennage Design Parameters

Parameter	Vertical Stabilizer	Horizontal Stabilizer
Area	17.1 ft^2	12.0 ft^2
Span	5.1 ft	6.5 ft
Chord (mean)	3.4 ft	1.9 ft
Aspect ratio	1.5	3.5
Sweep	32 deg @ L.E.	0 deg
Incidence	4.5 deg	-3 deg
Airfoil	NASA 63_3A618	SU3015

6.3.1 – Vertical Stabilizer

As mentioned above, the vertical stabilizer was designed to generate a large proportion of the thrust required to counteract main rotor torque in forward flight. Trimming in cruise flight with the fan results in a large drag penalty, which can be reduced by as much as 30% by unloading the fan with the fin. This drag reduction is due to the superior lift-to-drag ratio of the vertical tail over the fan, which enables it to generate the same thrust for less drag. The vertical tail incidence (which is set with respect to the aircraft centerline) was chosen to enable the fin to operate near minimum drag in cruise. A cambered NASA 63_3A618 airfoil section (the same airfoil section used on the RAH-66 Comanche) was selected, which provides a 4 degree effective incidence (through camber). The fin area, chord and span were then established to meet the specified design condition. The resulting

thrust and power requirements as a function of forward speed are shown in Figures 6.3 and 6.4.

Figure 6.3 – Fan power required in forward flight

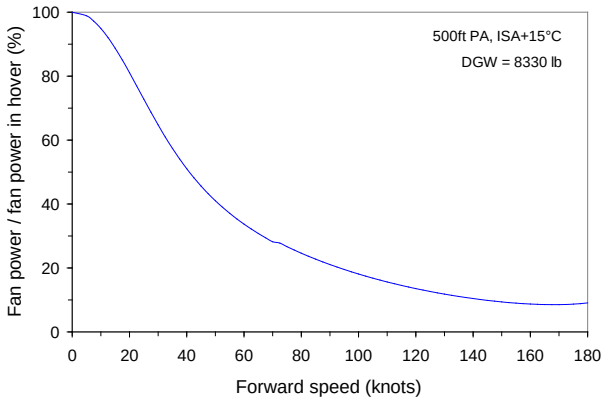

Figure 6.4 – Anti-torque thrust breakdown in forward flight

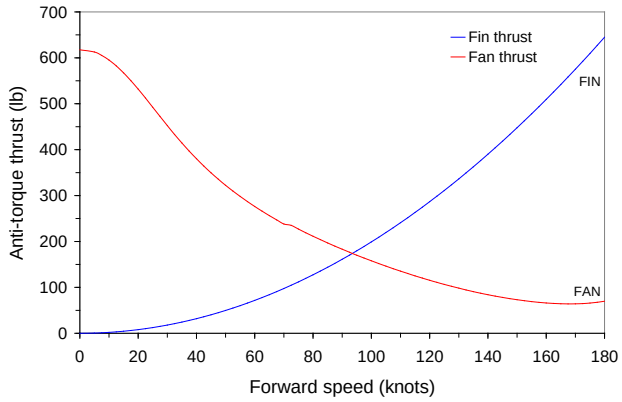

These results show that the power required from the fan-in-fin decreases sharply from 100% in hover, to approximately 10% in cruise. It is clear from the figures that the fan thrust required for yaw equilibrium is very much reduced in forward flight. This unloading of the fan has a number of very important benefits:

1. The dynamic strains on the rotating parts of the fan-in-fin are reduced, resulting in a significant improvement in fatigue life and a reduction in maintenance costs.
2. Instabilities that arise in the tail rotor with increasing forward speed, which have to be avoided on conventional tail rotors, do not normally occur with fan-in-fin designs.
3. A safe return to base can be performed with an inoperative fan. This has been proven in flight on a Dauphin which landed safely (running landing) after one hour of flight with a stopped fan [Moui86].

6.3.2 – Horizontal Stabilizer

The horizontal stabilizer was designed to provide sufficient stability about the pitch axis in forward flight. A SU3015 airfoil section (the designation for a Sikorsky uncambered 15% thick, 30 series airfoil) was chosen based on existing designs. The stabilizer sizing and design parameters that were presented in Table 6.3 were selected based upon stability and control considerations (refer to Section 10 for further details).

6.3.3 – General Arrangement

The general arrangement of the empennage (including the fan-in-fin) was displayed in Foldout 4.1. As can be seen from this three view diagram, the horizontal and vertical stabilizers were arranged in a 'T-tail' configuration. This arrangement was selected to minimize main rotor wake impingement effects and to improve ground clearance around the vehicle. Although the design is structurally inefficient, it was deemed to be the most suitable design configuration (in terms of handling qualities) due to the fact that the wake does not impinge on the horizontal stabilizer for most flight conditions.

6.4 – Fabrication

The fin and duct structure are to be assembled from two half-shells of graphite, Kevlar and Nomex honeycomb stabilized with composite frames and internal ribs to limit the structural deformations under load. The fan blades are to be made from graphite and are to be cantilevered at two stations on plastic self-lubricating pitch bearings and linked to the hub with a unidirectional Kevlar fiber spar providing low torsional rigidity for blade pitch variations. The stator blades in the diffuser will act as the primary gearbox support arms. The tail boom has a fairing accommodating the tail rotor transmission shaft, the directional control linkage, and the hydraulic system tubing.

Section 7 – Airframe Design

In this section the salient design features of the airframe and undercarriage are presented.

7.1 – Airframe

The airframe structural arrangement is displayed in Foldout 7.1. The airframe consists of five primary modules: a front section, a center fuselage, a rear fuselage, a tail section and an engine and transmission deck. The primary advantage of adopting a modular airframe design is that the individual modules can be produced separately and equipped with electrical wires, hydraulic lines, and subsystems before final assembly. The cross-section of the aircraft was designed with both aerodynamic and structural considerations in mind. The cross-sectional shape changes along the fuselage, from a rounded section at the cockpit (to improve aerodynamic flow characteristics) to a rounded/square shape under the transmission and engine deck. The decision to adopt a squarer main fuselage shape was made in order to reduce the bending moments in the bulkheads that support the gearbox and engine. This unique feature will serve to increase the fatigue life of the fuselage structural members and allow for lighter structural bulkheads to be used.

7.1.1 – Structural Details

The Raven airframe design (Figure 7.1) uses six lightweight, primary load bearing metal bulkheads and several secondary frames to help maintain structural shape. The first primary bulkhead is used to connect the nose and cockpit, and support the nose landing gear and avionics bay. The second primary bulkhead connects the cockpit and center fuselage and forms the front support for the engine and transmission deck. The third primary bulkhead forms an intermediate support for the transmission deck and supports the two front legs of the rotor mast support standpipe. The fourth primary bulkhead supports the main landing gear, the two aft legs of the rotor mast support standpipe and the front of the engine mounts. The fifth primary bulkhead is at the junction of the center and rear fuselage, and forms another support for the engine and transmission deck. And finally, the sixth primary bulkhead connects the tail section to the rear fuselage.

Figure 7.1 – 2 Dimensional Structural Layout Diagram

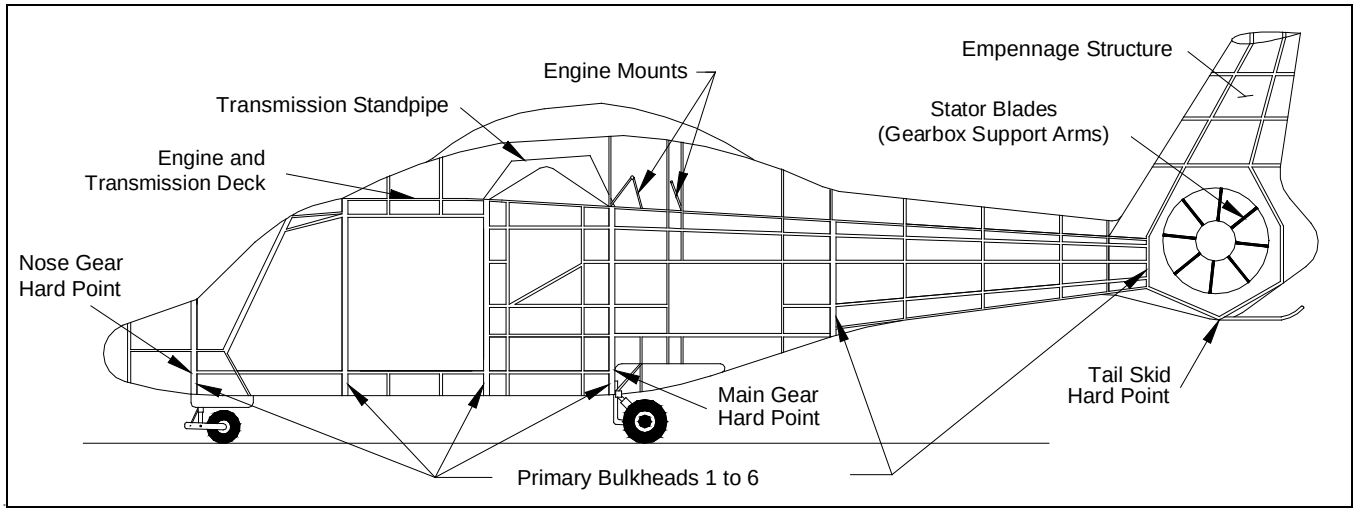

The keel beams are mounted to the primary bulkheads to support the structure. Two keel beams run between the first and fourth primary bulkheads to support the floor in the cockpit and cabin. Keel beam sections with sine wave webs exhibit good energy absorption characteristics and were therefore chosen to enhance fuselage crashworthiness. In addition, the sub-floor structure was designed to provide sufficient crashworthiness when the undercarriage is retracted.

7.1.2 – Engine & Transmission Deck

The engine and transmission deck is the primary structural interface for the main gearbox, engines, and electric lines. The deck is to be made from a Kevlar/graphite/epoxy sandwich panel that is bonded to a 'D' shaped bulkhead.

7.1.3 – Tail Section

The tail section includes the fan-in-fin anti-torque system and the horizontal and vertical stabilizers. The vertical stabilizer consists of a hybrid sandwich structure which uses Kevlar/epoxy face sheets and a honeycomb core to ensure light weight. The spars for the vertical and horizontal stabilizers are to be made from graphite/epoxy.

7.1.4 – Structural Material Considerations

In selecting the materials for the primary structure the following properties were considered: static strength efficiency, fatigue life, corrosion resistance, availability, producibility, and cost. According to these criteria, a hybrid composite-metal frame consisting of a composite skin laid up over a metal frame was selected. An aluminum-lithium alloy is to be used for the metal frame due to its superior strength-to-weight and stiffness-to-weight ratios (the material costs will decrease over the next decade as more manufacturers use aluminum-lithium components). The hybrid composite/metal airframe design proposed for the Raven has the advantage of superior crashworthiness and corrosion resistance whilst facilitating ease of construction and repairability.

7.1.5 – Manufacturing & Construction Issues

The manufacture of the Raven will employ 'lean manufacturing' practices to minimize costs. Lean manufacturing is a systematic approach to perform the minimum work necessary in production. The major benefits of this manufacturing philosophy are continual quality improvement, small production runs and the ability to reconfigure the production line for different products. Lean manufacturing is composed of many elements including: (i) elimination of waste, (ii) continuous flow and (iii) quality control. For the relatively small production run envisioned in the RFP, continuous flow is of primary importance. Continuous flow manifests itself as the ability to easily convert the production line from one product to another at the conclusion of a production run or between production runs so that manufacturing down-time is minimized. Additionally, facility overhead costs are spread over more products. Optimizing the manufacturing process for low rate production will keep the production costs low [Feld00].

As previously stated, the helicopter is made up of five modules. These five modules were developed such that they could be pre-assembled with the required components, hydraulic lines and electrical lines, which will serve to reduce the time required for final assembly. Six main manufacturing jigs are required to construct the vehicle: one jig for each module and a final assembly jig to help assemble the five modules.

7.2 – Landing Gear Design

In rotorcraft design there are essentially two main landing gear configurations commonly adopted; skids or wheels (fixed or retractable). For the Raven, a retractable wheeled tricycle undercarriage arrangement was selected. This selection came as the result of a design study into the relative benefits of skid versus retractable wheeled units. It was determined that although retractable wheeled units are approximately twice as heavy as skids (110 lbs heavier), the large reduction in parasite drag in forward flight (8% or 0.76 ft^2 reduction in flat plate area) more than compensates. This reduction in parasite drag leads to a significant reduction in fuel weight, operating costs and improves cruise performance, which is critical to mission effectiveness over long journeys. The wheeled units also help to improve the ground handling characteristics of the vehicle which is a desirable feature to improve shipboard compatibility.

7.2.1 – General Arrangement

The landing gear location was driven by three main requirements. First, the relative position of the rear wheels versus the vehicle CG is such that the main wheels support 88% of the aircraft weight and the nose wheel supports 12%, which provides

for good ground handling performance. Second, the main gear track (77 in) and wheelbase (289 in) dimensions give an overturn angle of 62 degrees and a tip back angle of 32 degrees for the worst design case. These angles are within the recommended limits of 63 degrees maximum turnover angle and 15 degrees minimum tip back angle [Raym00], which are specified to avoid aircraft turnovers and tip backs during a landing or ground maneuver. Finally, the landing gear arrangement was designed with crashworthiness as a primary consideration. Therefore in the event of a vertical crash with the wheels fully lowered, the nose gear was designed to penetrate through the cockpit floor beneath the large center instrumentation console located between the flight crew, whilst the main gear was designed to not penetrate the passenger cabin at all (as required by FAR 29). A detailed landing gear arrangement diagram is displayed in Foldout 7.1.

7.2.2 – Tire Sizing

Low pressure tires were selected to allow the helicopter to land at unprepared sites. At the maximum takeoff weight, each main tire must carry (static) approximately 3819 lbs. Therefore 17.5×5.75-8 type tires with a maximum load of 5000 lbs, 12 plies and an inflation pressure of 180 psi were selected for the main gear. The nose gear tire was sized to support the dynamic breaking loads and therefore a Type III 5.00-4 tire with a maximum load of 2200 lb, 12 plies and an inflation pressure of 55 psi was selected.

7.2.3 – Oleo Sizing

Oleo-pneumatic shock absorbers were used for both the main and nose gears due to their high shock absorbing efficiency [Curr88]. The stroke of the oleo was sized to meet FAR 29.727 which states that each gear must be able to withstand a 12 inch drop test, which corresponds to a 8 ft/sec vertical touchdown velocity. Assuming a tire stroke (1/3 tire radius) and shock absorber efficiencies of 0.85 for the oleo and 0.47 for the tires, results in a stroke of approximately 3.1 inches. This value was increased to 4 inches to account for any uncertainties in loading and provide a margin of safety [Curr88]. The size of the oleo was determined using a typical oleo internal pressure of 1800 psi, an external diameter of 1.3 times the internal diameter, and a length of 2.5 times the stroke, with the external diameter related to the static load for the main wheels and to the dynamic load for the nose wheel [Curr88]. The main gear incorporates a mechanical advantage system to reduce the required oleo stroke for a given wheel stroke, which is included in the oleo sizing computations. The resulting oleo dimensions are: a nose gear outer diameter of 2 inches and length of 10 inches and a main gear outer diameter of 3 inches and length of 10 inches.

7.2.4 – Retraction Geometry

The retraction configuration adopted for the main gear is similar to that used by the Kaman SH-2G Super Seasprite due to its simplicity and small stowed frontal profile. The main gear is designed to retract into the lower fuselage, under the cargo compartment. A positive down lock and mechanical up lock are incorporated to prevent unexpected gear motion. The nose gear retracts under the center instrumentation console located between the flight crew. Refer to Foldout 7.1 for further details.

7.2.5 – Emergency Floatation Gear

The helicopter provides an emergency floatation capability which is required for missions that take place over large bodies of water. The primary purpose of the emergency flotation gear is to enable the helicopter to remain afloat long enough for the occupants to egress the vehicle safely in the event of a forced landing. Inflatable floats are installed due to their light weight and compactness. The inflatable floats, which can be stowed or folded at the landing gear, use a storage charge of air for rapid inflation.

Foldout 7.1

Section 8 – Crew Station Design

A key aspect of any aircraft design is its interface with the crew. Therefore in this section, the design features of the Raven's crew station that have been optimized to enable the crew to function efficiently in SAR missions will be presented.

8.1 – Crew Station Features

The main features of the cockpit include programmable Global Positioning System (GPS) search patterns, a limited cabin crew hover control, a retractable searchlight and Forward Looking Infra-Red (FLIR) radar, FLIR video overlay of displays, a data loader port for uploading mission information, Night Vision Goggle (NVG) compatibility, and a synthetic vision system interfaced with a helmet mounted display. The programmable GPS search pattern feature allows more eyes to participate in the search. Furthermore, it also increases search pattern consistency, ensuring full area coverage irrespective of weather conditions. The ability for the searchlight and FLIR to be retracted reduces the helicopter drag, which allows for an increased cruise speed (the searchlight and FLIR are usually only required on station). Flight plans and mission information can be transferred onto the helicopter using a digital dataloader either via disk or via an upload from a data stream whilst enroute to the search area. The cockpit is NVG compatible through the use of colored lighting and dimmers.

8.2 – Cockpit Layout

8.2.1 – Doors/Ingress/Egress

Hinged doors on either side of the cockpit provide access to and from the station. The collective stick on the copilot's side telescopes to allow improved cockpit ingress and egress. Large sliding doors on either side of the fuselage provide access to and from the cabin, with the port side door being used primarily for patient/litter removal (the hoist is located on the starboard side). The sliding doors can be opened or closed from inside or outside the helicopter and can be jettisoned in an emergency.

8.2.2 – Pilot/Copilot Stations

The cockpit provides seating for a pilot and co-pilot. The pilot station is located on the starboard side of the cockpit, with the copilot station located on the port side (both pilot stations have access to a full complement of aircraft flight controls and instruments). The cockpit configuration and instrumentation has been designed to reduce crew workload. The cockpit layout consists of crashworthy pilot seats, an instrument panel, an overhead console, a center console, and pilot controls. A digital 'glass' cockpit was selected in order to reduce crew workload and enhance mission flexibility.

The instrument panel (refer to Foldout 8.1) consists of four large Multi-Function Displays (MFD's), as well as a standby attitude indicator, altimeter, airspeed indicator, and vertical velocity indicator. A center MFD (for additional displays), two backup radios, two analog clocks, two radar altitude gauges, a standby compass, two master alert switches and two warning light panels are also included. The radios can be controlled via the center display and keypad, or via the backup radio display/dials. An analog backup clock is used in preference to a digital clock so that the pilots can visually note the position of the second hand, and pictorially see the seconds elapse during flight in Instrument Meteorological Conditions (IMC). Vents are also provided for cockpit environmental control. The warning light panels installed on the instrument panel provide visual indications of engine or drive train lubrication system failure, hydraulic system failure, APU failure, generator failure, and low fuel warning (these warnings are generated by the HUMS). Pedal adjustment handles are located at the base of the instrument panel to allow for different pilot leg lengths. In addition, the pilot crew seats are fully adjustable to accommodate different body sizes.

The overhead console (refer to Foldout 8.1) contains aircraft system controls including circuit breaker panes, fire-extinguisher controls, engine controls, a fuel control panel, an aircraft power panel, an engine start panel, anti-ice controls, pitot heat switches, APU controls, pilot/copilot volume controls and two radio/InterCommunication Select (ICS) panels. The center console (refer to Foldout 8.1) contains computer data unit keypads, two keypad entry displays, windshield wiper controls,

console/instrument light controls, external light controls, environmental controls, a crew hover control selector, and the main hoist control panel. The computer data unit controls the navigation, mission displays, avionics systems, AFCS, and communication systems. The parking brake handle and undercarriage control levers are located next to the center console.

For this design a center cyclic stick controller was selected in preference to a side stick controller (which would require increased control sensitivity). A center cyclic stick was selected because most pilots have been trained with and are more comfortable using them, which minimizes the need to retrain the flight crew. The primary function of the cyclic control is to provide cyclic inputs to the rotor, however it was also designed with controls for pilot activated hoist release/cable shear (shielded switch), hoist fixed speed control (roller), stick trim (button), trim release (button), moding cursor control (coolie hat), and ICS call (trigger). The collective stick has controls to turn the searchlight and FLIR on and off, to control the direction of the searchlight/FLIR (coolie hat), and to operate the searchlight/FLIR stow mechanism.

8.3 – Cabin Layout

Special consideration was given to the cabin layout in order to optimize the SAR mission performance of the vehicle. In SAR vehicles the cabin must provide the crew with the capability to rapidly store and access an abundance of equipment such as litters, rescue baskets, and medical equipment. The final layout adopted provides the crew with a logical workstation that addresses human factors. Additionally, the cabin provides adequate space for a litter (required for the transport of injured patients) and ease of access to the extensive emergency medical supplies. The cabin layout is displayed in Figure 8.1.

Figure 8.1 – Cabin Layout

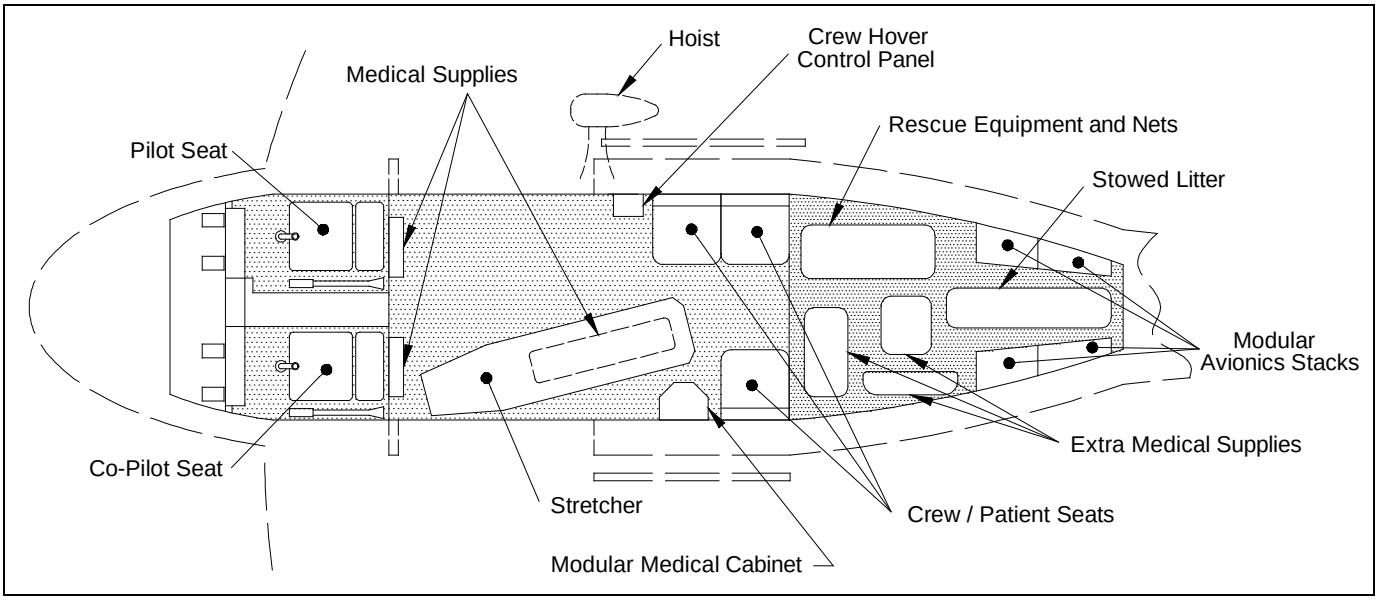

The cabin area includes a crew chief station, three crew/patient seats, a litter, and EMS/SAR equipment. The starboard side of the cabin is uncluttered to facilitate operation of the hoist and ingress of patients/pararescuers. The cabin also includes a crew hover control panel with FLIR display, which is used for search assistance and to provide the cabin crew with the capability to position the helicopter during hoist and rescue operations. The crew hover controller has limited control authority and must be initially activated from the cockpit. The crew control panel is located to the right of the starboard cabin door and includes hoist controls, an ICS trigger switch, cabin dome light controls, a rescue light switch, a hoist shear switch, and radio/ICS controls.

The three utility seats for the cabin occupants were selected for their lightweight, crashworthiness, and ability to be rapidly stowed and removed. The seat material has low elasticity and thus minimizes dynamic overshoot, resulting in minimal rebound

during a crash. Two cross straps provide additional support to the sitting platform during crash pulse attenuation. In addition, the seat uses a four-point occupant restraint subsystem including a lap belt, two shoulder harness straps and a single point attachment-release buckle [Mart01]. A storage area (cargo compartment) for cabin equipment and supplies is located aft of the cabin seating, with the avionics bay also accessible from this location. The avionics bay is modular, in that the components plug into standard power and data line adapters, which improves installation and removal and enhances system flexibility.

8.4 – Cockpit Systems

8.4.1 – Cockpit Instruments/Setup

The Cockpit Management System (CMS) is the primary interface between the flight crew, the aircraft systems, and the avionics. The CMS replaces traditional primary flight instruments and system indicators with an electronic cockpit display system. The CMS provides controls to manipulate and efficiently display the information necessary for the aircrew to operate the helicopter throughout all mission stages. The controls and displays of the CMS are arranged in the cockpit such that both flight crew can fly the aircraft and monitor all phases of the operation. The CMS provides control and display of the flight data and systems operation for communications/identification, navigation, flight director and guidance, mission management, component status and Warning/Caution/Advisory (WCA) alerts. The CMS is a fully redundant system and consists of the 4 MFD's, the center display, the 2 keypads, a memory loader system, 1553B multiplex data buses, aircraft interface units, and electronic display units. Dual components and a liberated architecture ensure that system operation will not be compromised by a single failure.

In a liberated cockpit architecture, each MFD has a separate processor which allows it to pull the required information off the data bus itself rather than having it go through a main mission computer (as in conventional federated architectures). The benefit of such a system is that it allows for individual chip failures (effecting only one MFD) without sacrificing the mission capability of the aircraft. The increased redundancy of this type of system far outweighs the increased cost of having separate processors on each display, particularly for SAR missions.

The primary components in the cockpit are the four color flat panel MFD's. All the MFD's are identical and interchangeable, simplifying vehicle maintenance and logistics requirements. The MFD displays have no set panel that they must be displayed on so the pilots retain total configuration authority. The MFD screens (refer to Foldout 8.1) are ringed by a bezel that contains function keys. Most of the keys are soft coded such that they change function with the display rather than being hard coded for a specific function. The advantage of this design is that it is easily adapted to different missions, displays, and sensor add-ons through a simple software change. The key legends associated with each key appear on the screen adjacent to the keys to describe the current functions. The bezel keys can be coded to either function in a round-robin manner or as a toggle switch or function select. If the function related to a bezel softkey is not available, the key function is crossed out. The hard coded bezel keys are used to control display and symbol brightness, contrast, and symbol intensity. They can also be used to access a complete list of cautions and advisories, acknowledge system faults, and declutter the display.

The operator can select different MFD modes by depressing the bezel key associated with the desired function or by using the moding cursor. Control of the moding cursor is provided by a dedicated switch on both of the cyclic sticks and does not require the pilot's hands to be removed from the controls. A dial is also located in the MFD bezel in order to switch between day, night, and off modes. The dial progresses from OFF to NIGHT to DAY so that the dial does not pass through the display's day brightness setting on its way to the night brightness setting, which would adversely affect the pilots' night vision. All MFD formats are NVG compatible.

The main pages on the MFD's include the flight displays, navigation pages, horizontal situation display pages, sensor pages, FLIR page, system status pages and the WCA page. The main displays that will be presented to the pilot are the primary flight display, the vertical situation display, and the hover page (these will be available in a round robin manner). A FLIR video overlay

is also available for the main flight displays. Furthermore, the MFD's give the pilots access to the communications systems, VOR/ILS frequencies, TACAN channels, barometric pressure input, system time entry, GPS time update, and heading reference (magnetic or true) settings. For navigation, the pilots have the option of having a full color sectional map displayed on one of the MFD screens with GPS position indicator, instead of the standard navigation sticks, way point symbols, and terrain markers.

The primary flight display (refer to Foldout 8.1) consists of an attitude indicator, airspeed indicator, barometric altitude indicator, radar altitude indicator, vertical velocity indicator, barometric pressure, compass, turn coordinator, fuel quantity display, and rotor and engine data. It also includes a pictorial representation of analog gauges for ease of rate identification. The primary flight display was designed to reduce screen clutter in order to minimize pilot eyestrain. The addition of a declutter button to remove predefined information from the display also helps to reduce pilot fatigue, especially when operating with NVG's.

Another technique used to aid the pilot is a difference in tickmark and step size. One example of this is the radar altitude scale, which covers 1000 feet in altitude, however roughly one-fourth of the scale is dedicated to altitudes less than 50 feet, due to the required precision in altitude knowledge at these heights. The scale then continues to 1000 feet at decreasing step sizes. Other aspects of the display that are designed to assist the pilot are the legs on the attitude indicator bars, which help identify which way is 'up', as well as a blue 'sky' and brown 'ground'. In addition, the barometric altitude and airspeed are represented by moving tape scales to show the rate of change of the parameter along with a stationary text box to denote the actual value. The vertical velocity tape remains stationary with a moving cursor. The turn coordinator is located at the base of the display, since it is a primary instrument for flight in IMC. It is frequently used in conjunction with a sideslip indicator, which is a physical gauge located below the outboard MFD's.

Key legends, WCA's and other text messages are displayed in certain defined areas on the screen. The top three lines on the display are dedicated to warning representation, whilst the bottom three lines are dedicated to cautions and advisories. Warnings remain displayed until the condition that caused the warning no longer exists. WCA's are displayed on all four MFD's simultaneously. Other WCA information is conveyed to the crew via verbal messages generated for warnings such as fires, gearbox failures, stall, and low rotor rpm. The MFD's are color coded for ease of distinction between functions, status, and text and follow the standard WCA color conventions for warnings and cautions.

The center display is used as an additional screen to display aircraft status information. Its primary uses are to show information associated with the currently displayed warnings and cautions, as well as for data entry and to display fuel status and other items of interest to the pilot. Displays include analog gauge symbols for engine speed, mean gas temperature and oil pressure indication for the engines, hydraulic pressure, and oil temperature/pressure for the main gearbox. These separate indicators are coded so that warning conditions (high and low) are shown in red, cautionary conditions (high and low) are shown in yellow, and normal operating conditions are shown in green. Gauges are shown pictorially for simplified rate identification and for determining values at a glance. Text boxes are also used to highlight the actual gauge value.

Two keypads are installed on the center console below the center display to allow the pilot/copilot to enter alphanumeric data and information for control of the helicopter systems (two display units are also located above the keypads to simplify data entry). The keypads are optimally positioned to keep the pilots from having to stretch or bend their elbow back behind the seat to gain access. The optimum position for data entry is to have the upper arm remain perpendicular to the cockpit floor and have the keypad fall directly below the hand. The keys were also sized to be large enough to be operated with gloved hands.

8.4.2 – Synthetic Vision System

Another aspect of the crew station design that will improve the crew/vehicle interface is the ability to present data to the pilots via a Helmet Mounted Display (HMD). The basic approach of this type of system is a synthetic vision or virtual reality system that is interfaced with the helmet and vehicle sensors to enable the pilot to see in whatever direction is desired. The cameras and

sensors digitize the external images and put together a database that slues as the pilot's head moves. The system also has the option to interface with a virtual reality database/display of what the scene should look like and look for anomalies. Furthermore, it has the ability to show a projection of the last known location of the victims and have the search pattern superimposed on the helmet display so that the pilot can see where the helicopter is going and what path is being followed. The HMD system can be interfaced with the radar, avionics, sensors, tracking software, and searchlight/FLIR via a display unit on the pilot's helmet. Two examples of this type of system are the Flying Infrared for Low-Level Operations (FLILO) system and the Synthetic Vision System (SVS) for SAR helicopters. The cost of this system is currently unknown, therefore the entire system will be offered as an option that will improve the crew interface, but that is not necessary to ensure adequate mission performance.

8.5 – Cabin Systems

The hoist control panel (refer to Figure 8.2) is located to the left of the starboard cabin door. It contains controls for the hoist power and up/down function, and also contains cable foul sensor lights and a cable position indicator. A tethered portable hoist control (up/down and cable shear) is also available near the crew station, along with a crew safety belt to be worn whilst leaning out the cabin door and manning the hoist. The externally mounted rescue hoist is located over the starboard cabin door along with a manually controlled searchlight. Cabin locations are also provided for fire extinguishers, a crash axe, a SAR flare/marker rack, relief tube, and map cases.

Figure 8.2 – Hoist / Hover Control Panels

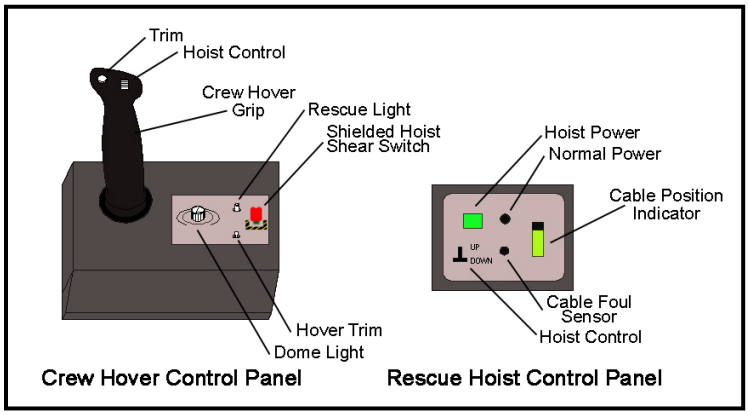

Another important consideration in designing the cabin was in regards to the cabin lighting. The helicopter needs to have sufficient external lighting to conduct a search from both the cockpit and the cabin door. This was addressed with the addition of a pilot controlled nose searchlight and a manually controlled cabin searchlight mounted internally above the starboard door. Furthermore, special internal cabin lighting is required to have the option to be NVG compatible, hence the cabin lighting was selected to be infrared for search and blue-green for internal lighting (the cabin lighting also helps facilitate patient medical care).

8.6 – Methodology

The crew station design was developed through extensive research into current/future systems and through discussions with SAR pilots and pararescuers. The designs were also discussed in great detail with crew station experts such as Ben Johnson (Naval Air Systems Command – crew systems) and Mike Fallon (Naval Air Systems Command – flight dynamics).

Section 9 – Mission Subsystems

The Raven is equipped with an extensive range of SAR and EMS equipment to enhance its mission capabilities. In this section the mission subsystems onboard the Raven will be presented.

9.1 – Mission Equipment Package (MEP)

The comprehensive mission equipment package integrated into the Raven consists of mission systems equipment, rescue/survival gear, medical/Emergency Medical Services (EMS) equipment, crew safety gear, and communications and navigation equipment. All of this equipment was deemed to be necessary to enable the vehicle to adequately perform the specified SAR mission/s at night and in adverse weather conditions.

Foldout 8.1

9.1.1 – Mission Systems Equipment

The mission systems equipment primarily includes NVG filters and dimmers, a weather/search radar, a Forward Looking Infra-Red (FLIR) camera/sensor, a cabin FLIR display, a data loader, a GPS system, two searchlights, and IFR equipment. The NVG's, radar, and FLIR are used simultaneously (at night) to enhance search and rescue operations. The radar is used to monitor the weather as well as to search for metal objects in the water. The NVG's can be used to help locate light sources since they are able to magnify light up to 30,000 times [Fall01]. The FLIR is used to monitor for infrared or heat signatures (Figure 9.1 – courtesy of FLIR Systems [Flir01]). This is especially useful in SAR missions over water due to the fact that the heat signature of the victims will stand out. FLIR's are also very useful over land, however land retains heat better than water which makes locating people more of a challenge. The FLIR includes a video display with a zoom lens to facilitate identification of objects identified as the possible target. All of these systems help to greatly increase the area of coverage for the search.

Figure 9.1 – FLIR

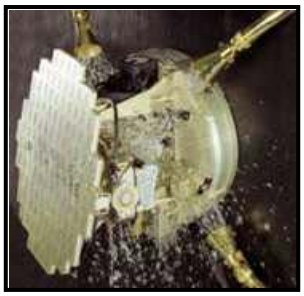

Figure 9.2 – Phased Array Radar

Standard radars generally require installation such that they can rotate to get a 360-degree field-of-view, which is problematic when trying to minimize drag. In view of this, a phased array antenna was selected due to its ability to generate a radar image without requiring the antenna to rotate. The phased array radar on the Raven is located in the nose and is used for weather detection, as well as for searching for downed ships, aircraft, and personnel (Figure 9.2 – courtesy of Honeywell [Hone01]) [Fall01]. A searchlight is also located in the nose of the aircraft and has the ability to be stowed (as does the FLIR). It has the capability to generate normal white light or an infrared beam for NVG use. A second hand controlled searchlight is internally hinged above the starboard cabin door such that it can be swiveled out and used by the hoist operator to assist in hoist rescues and with the search (Figure 9.3 – courtesy of Spectrolab [Spec01]).

A data loader is used to help reduce mission start times – the data can be downloaded directly from a disk carried with the crew from their point of origin or can be updated via uplinks from a data stream whilst enroute to the search area. From this information the pilot can then select a search pattern and either fly the pattern manually, or have the flight control system automatically fly the pattern. The automatic search patterns are executed via GPS positioning. The GPS system is also used for navigation to assist the crew in flying to known locations.

Figure 9.3 – Searchlight

9.1.2 – Rescue/Survival Gear

The rescue/survival gear includes a general rescue equipment bag filled with supplies such as a quick splice, a cable grip, chemlight straps, a rescue litter sling assembly, and a rescue litter trail line and weight. Also included are two crew safety belts, life preservers, a Stokes litter, rescue baskets, and a rescue hoist.

Figure 9.4 – Rescue Net

As previously mentioned, the crew safety belts are used when the cabin door is opened (particularly during hoist operations) to ensure that the crew do not fall out of the helicopter. Life preservers are provided for the crew and passengers following CFR Part 14 regulations for over-water operations. The Stokes litter and rescue baskets are carried to allow for versatility in different rescue environments. A Stokes litter is usually required for the more technically challenging rescues that include severely injured patients, whereas the Billy Pugh rescue nets are used for water rescues and less technical land rescues (Figure 9.4 – courtesy of Bell Helicopter

[Bell01]). The X-873 net is used to rescue 2 people – it has a flotation collar and has folding hinges for more compact storage. The RES-1500 stretcher rescue net is used for rescues requiring a backboard. These nets were chosen for their versatility and excellent safety attributes [Life01].

The Raven is to be equipped with an electric Breeze-Eastern HS-29900 hoist or some future variant of this model (Figure 9.5 – courtesy of Breeze-Eastern [Bree01]). An electric hoist was chosen over a hydraulic hoist due to the fact that it is easier to install and retrofit, has a faster top speed, can have its control 'logic' embedded into the control system, has good reliability and facilitates a reduced maintenance burden [Idle01]. The hoist is equipped with a cable length of 295 ft, a maximum cable speed of 350 ft/min and a 600 lb maximum load capacity. The hoist also incorporates a slip clutch to limit cable peak loads, a cable foul sensor to alert the crew of a mis-wrapping cable, pilot triggered and aft cabin triggered cable shears, and a cable payout sensor so that the crew knows exactly how much cable remains available. Other safely features of the hoist include having NVG compatible displays, a mechanical fail-safe brake, a bi-directional cable tension control, an over-temperature indicator, redundant cable cut switches, and a cable cut test circuit [Idle01].

Figure 9.5 – Hoist

9.1.3 – Medical/EMS Equipment

The medical/EMS equipment includes two level A medical kits, wool blankets to keep passengers warm, a pivoting patient litter (with base cabinet) to facilitate patient egress via the port cabin door, a well equipped modular medical cabinet, and extensive medical supplies for patient treatment.

9.1.4 – Crew Safety Gear

The crew safety gear is comprised of heavy duty gloves, life vests, crashworthy cabin utility seats and general crew survival equipment for crash scenarios. Life vests are supplied for all the crew and passengers. Helicopter Emergency Egress Devices (HEED bottles) are provided for the crew and are stored in their flight suit pockets. The HEED system is a compact, lightweight (1.3 pounds), and reliable breathing system designed to enhance the survivability of the aircrew by protecting them from the dangers of drowning in the event of a water ditching [Life01]. Other survival equipment includes a life raft and a survival kit, which contains items such as water purification tablets, food rations, a portable medical kit, waterproof matches, and a mirror. Marine location marker dispenser assemblies are located on both sides of the forward fuselage, below the cockpit. Each dispenser assembly holds marine location markers to mark the location of survivors for other searchers and can be used in the event the helicopter crashes or is forced to make an emergency water landing. Smoke flares are also available to better mark the rescue location as well as electronic sea markers, which can be used to alert other rescue crews of the rescue site location.

9.1.5 – Communications and Navigation Equipment

The communication systems include cockpit-to-cabin, aircraft-to-ship, aircraft-to-rescue operations, aircraft-to-waterborne crew, and over the horizon systems. The navigation and avionics systems and equipment were chosen to assist the crew in accomplishing the primary SAR mission. An intercom system is required to facilitate hands off communication for the aft crew stations and provide situation awareness for the cockpit. Voice activated headsets are used for inter-cabin communication and a voice activated throat microphone and earpiece are supplied to the pararescuer for communication with the airborne crew. Chemlights are also provided in case of a pararescuer communication system failure or to minimize the amount of voice traffic being relayed to the helicopter crew. Furthermore, cockpit-to-cabin communication is provided via an intercom system to ensure that all passengers and crew can hear instructions from the cockpit.

9.2 – Weight and Cost Estimate

The MEP component weights were estimated based on actual components that are currently (or soon to be) in use by military and civil SAR rotorcraft. The weights of the major MEP components are listed below in Table 9.1. The total weight of the MEP was estimated to be 1052 lbs (including a 15% reduction factor – refer to Section 12). The cost of the individual MEP components was not available from the suppliers and we were unable to find any secondary means of generating these estimates. However, a preliminary estimate of the entire MEP cost was determined to be approximately US $1.09 million (in 2000 dollars), based on existing SAR rotorcraft.

Table 9.1 – MEP Component Weights (major items only)

Component	Weight (lbs)	Component	Weight (lbs)
RADAR	30	Life preservers	22
FLIR	81	Rescue hoist	150
Searchlight	68	Medical kits (×2)	30
IFR equipment	80	Pivoting litter with base cabinet	59
X-873 rescue basket	38	Modular medical cabinet	70
RES-1500 stretcher rescue net	20	Cabinet supplies	30
Stokes litter	31	Additional medical supplies	86

Section 10 – Flight Control System

The unique swashplateless rotor control system adopted by the Raven requires a new Flight Control System (FCS) to be developed in order to ensure optimum handling qualities. In this section of the report, a comprehensive description of the FCS will be given, together with the stability and control characteristics of the vehicle.

10.1 – Flight Control System Design

The key system requirements for the design of the flight control system include: (i) Redundant flight control system, (ii) Flight safety reliability (i.e. 1 failure in 10^7 flight hours), (iii) Fault detection and isolation, and (iv) Handling qualities compliance with ADS-33E-ERF for utility helicopters.

10.1.1 – FCS Overview

The Raven is controlled in flight by varying the pitch of the main rotor and tail rotor (fan) blades. The pilot changes blade pitch indirectly through conventional flight controls, i.e. the collective pitch lever, cyclic stick, and directional pedals. Beyond the pilot controls, the flight control system for the Raven is a triple redundant, digital, fly-by-wire system. Blade pitch modulation is accomplished through an interconnection of mechanical and electrical components along with the incorporation of a unique "integral trailing edge flap modulation" method of main rotor control. These automatically controlled flaps are embedded in the trailing edge of each main rotor blade. They produce pitching moment changes, which impel the main rotor blade to free fly against the feathering spring to achieve aerodynamic equilibrium, thereby producing the desired collective and cyclic blade lift. A benefit to this embedded flap design is that it provides crisp and responsive control on a stable platform with very low vibration. Additionally, the required control forces are very low, and control can be obtained with minimal power. Signals to the embedded flaps and servos for the tail rotor are generated by two major subsystems: the Primary Flight Control System (PFCS) and the Automatic Flight Control System (AFCS). The PFCS is a digital resemblance of a conventional mechanical linkage system traditionally used in helicopters. The PFCS incorporates three levels of redundancy. The AFCS provides command shaping, control mixing, stability augmentation, and a suite of mission modes and holds.

10.1.2 – Description of Fly-by-Wire Architecture

The Raven Fly-By-Wire (FBW) flight control system was designed to maximize safety and reliability by partitioning flight-critical and mission-critical control laws. Figure 10.1 provides a high level description of the Raven FCS architecture. The PFCS processors provide flight critical control laws and the AFCS processor provides enhanced flying qualities for mission performance. The PFCS and AFCS are separated functionally as well as physically in that the PFCS has three separate processors and the AFCS has one. This redundancy in hardware is a significant safety and reliability feature of the design. Other safety and reliability design features include redundancy in system processing, minimization of sensor inputs, reduced control law complexity, and isolation of the AFCS in the event of multiple system faults. The Flight Control Computers (FCC's) provide digital algorithms for fault detection as well as reconfiguration routines that provide redundancy management capability. To reduce coupling, the PFCS performs mixing of the cockpit commands and the AFCS throughout the entire range of airspeed. Utilizing a fully populated mixing matrix to formulate main rotor and tail rotor commands, the Raven FCS provides highly desirable control response in all axes over a wide range of flight conditions.

Figure 10.1 – Flight Control Architecture [Tisc96]

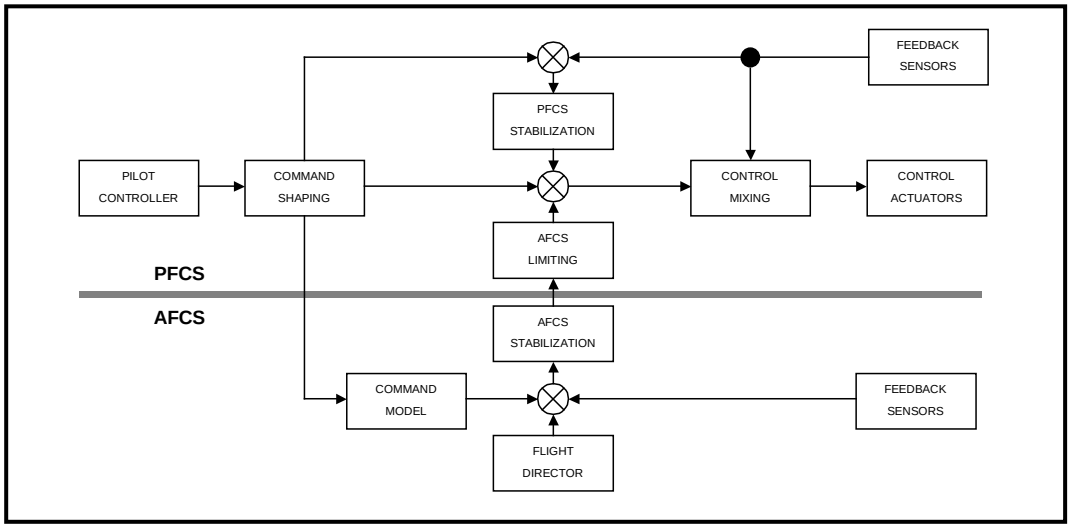

The Raven fly-by-wire FCS utilizes explicit model following control laws. In this design, a cancellation of the inherent aircraft response is accomplished in the PFCS by a command shaping function. The command model, located in the AFCS, is used to generate the desired state response of the aircraft. The desired response is then compared to the sensed states to form state errors for stability and command response augmentation. This FCS architecture provides consistent and predictable response, independently designed stability and command response characteristics, and robust full time feedback stabilization (which allows for gust rejection during maneuvers).

The fly-by-wire FCS also incorporates the attitude-command model following control law approach. The core AFCS in the longitudinal and lateral axis is designed to a rate command, attitude hold system that is selectable to velocity command, position hold in hover, attitude command, attitude hold in low-speed, and attitude command airspeed hold in high speed forward flight. Directionally, the FCS is designed to a rate command, heading hold system with automatic turn coordination.

10.1.3 – Fly-by-Wire Advantages

In comparison to a conventional flight control system, there are several advantages in using a FBW system. With a digital system, the flight controls can be easily made to accomplish complex tasks, with variances for an entire range of configurations and conditions. Due to the absence of mechanical linkages, which are subject to wear and manufacturing variation, a digital FBW system achieves significantly tighter tolerances and reduced accuracy errors. A digital system is also much more

conducive to accurate modeling, which is especially critical in the design phase, and can be developed to overcome shortfalls discovered in testing in less time and at less cost. Finally, the digital flight control system can be equipped with self-monitoring algorithms for added safety and early fault detection. A shortfall of this system, compared to a conventional system, is that physical detection of inaccurate connections is difficult, which makes safe and reliable software a key issue when selecting a digital fly-by-wire design [Dones00].

10.1.4 – Flight Control Computer Description

The Raven fly-by-wire flight control system is similar in design to both the V-22 and RAH-66 digital FCS [Tisc96 & Bosz99]. The flight control computers, which are the key components of the flight control system, are also similar (Figure 10.2). This system contains three FCC's that perform flight critical operations and one that is dedicated to mission critical operations. Of the three FCC's that perform flight critical operations, one is an input/output processor (IOP), whilst the remaining two are Primary Flight Control Processors (PFCP), tied to PFCS functions. The Automatic Flight Control Processor (AFCP) is tied to mission critical AFCS functions.

Figure 10.2 – Internal FCC Architecture [Bosz99]

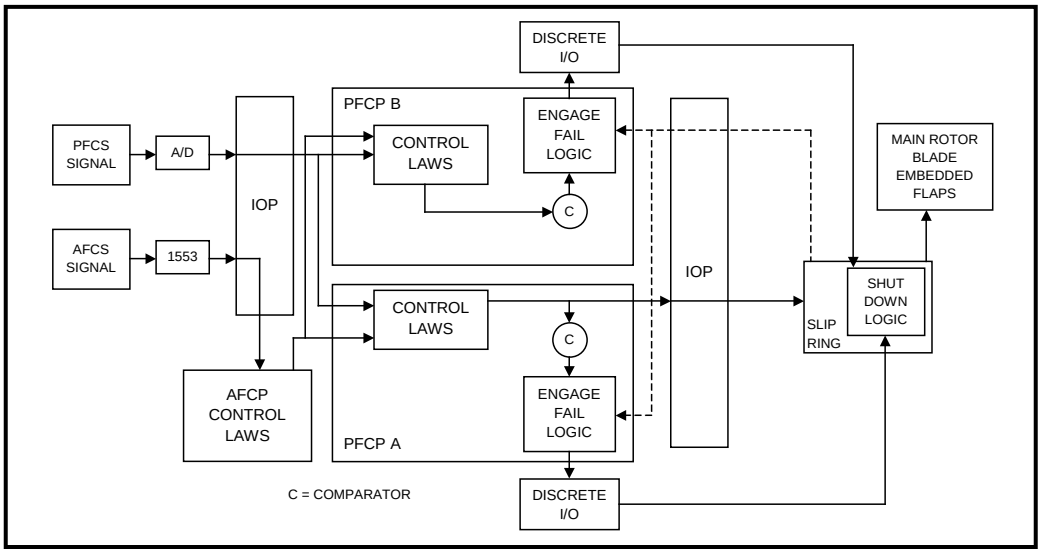

Both PFCP's perform identical, in-line computations, then pass the information through the IOP to the servo electronics. Output signals are fed back into the IOP and passed to the PFCP's. Both PFCP's compare their generated commands to the returned signals. A "mis-compare" automatically shuts down the appropriate function. The FCC's also have the ability to communicate directly with each other by way of serial data buses. This ability adds a redundancy feature to the FCS whilst also allowing for more efficient system processing.

10.1.5 – Failure Management, Fault Isolation, and Reliability

By isolating FCS functions based on flight/mission criticality, an increased level of safety can be incorporated into the design. PFCS functions are considered the most critical and have internal redundancy and self-checks designed into the system. AFCS functions, which are higher-order control and autopilot capabilities, are less critical. The PFCS utilizes more redundant sensors than the AFCS, and the PFCS is protected from potential AFCS anomalies by strict PFCS monitoring of the AFCS. The PFCS has the ability to shut down the AFCS if two PFCS flight control computers detect similar AFCS failures. Additionally, the AFCS is given only limited authority by the PFCS (similar to conventional helicopter flight control systems). The pilot can also counteract any rogue AFCS inputs, such as a hardover, by either overpowering the input with the stick, or disabling the AFCS through a cockpit control. Similar systems in the RAH-66 Comanche boast flight safety reliability of 0.9999998 for a 1-hour mission, fault detection of 97% and isolation of 96% effectiveness [Bocz99].

10.1.6 – Sensors, Inceptors, and Actuators

The angular rate sensors utilized in this design are based in the aircraft body axis. Attitude sensors are inertially based for large amplitude maneuvers. Additionally the design incorporates the use of air data sensors, which are useful for airspeed feedback in the AFCS. Main rotor control is accomplished through the use of blade pitch modulation generated by embedded trailing edge flaps (described in detail in Section 5). Tail rotor actuation uses a servo capable of 6.5 inches of stroke, 7 inches per second rate, and a maximum output force of 400 pounds. The side-by-side cockpit features conventional center stick cyclic controllers, collective levers, and pedal-type directional controllers.

10.1.7 – Software Development

There are four stages to the control law design process. For the purpose of this proposal, the design of the Raven FCS was limited to the first stage only (i.e. preliminary design). The preliminary design stage begins with the development of design criteria based on air vehicle specification requirements and involves an iterative process in which the air vehicle system model is analyzed and assessed against specifications. This stage also begins the analysis of handling quality requirements, structural loads, and aeroservoelastic stability (refer to Section 10.2.4). The next stage of software development is the detailed design stage, where an iterative process is applied that utilizes extensive analysis and piloted simulation to assess control law design over a wide range of conditions and mission task elements. Following this stage, a detailed control law development effort will ensue, focusing on handling qualities, as well as system and structural requirements. The fourth and final stage involves verification and validation followed by acceptance testing.

10.2 – Stability and Control Analysis

While it was difficult within the scope of this design task to develop a comprehensive model of the Raven, a simplified model, based on the techniques presented by Padfield [Padf96], was developed to enable a stability and control analysis to be performed. The analytical techniques presented by Padfield are suitable in the preliminary stages of a design and provide a means to generate reasonably accurate approximations based on the primary vehicle design attributes. Using these methods, and by comparison with similar aircraft, it was possible to obtain a realistic approximation of the handling qualities characteristics of the Raven. In addition, one can utilize these approximations to anticipate the resulting problematic realms of stability and control, and in turn, design augmentation solutions. Much of the stability and control analysis presented in this proposal is based on comparison with known stability and control characteristics from existing helicopters. To this end, the primary design characteristics of the Raven were brought into consideration when determining the stability and control derivative estimates. In some cases, accurate approximations were determined directly from the Raven's design characteristics, such as rotor stiffness, tail size, rotor diameter, or frontal area. In other cases estimates were formed by similarity with existing designs.

It appears, based on existing designs, that the conventional method of determining rotor stiffness is not sufficient for this particular rotor design. Normally, stiffness is thought to be inversely proportional to Lock number. This implies that inertial effects are more dominant than aerodynamic effects. For this design however (which utilizes embedded trailing edge flaps to generate pitch modulation) the aerodynamic aspects of the rotor are clearly more dominant. Using conventional methods, the stiffness number (which is defined as the ratio of hub stiffness to aerodynamic moment) was found to be only 0.12. By comparison the Puma, which is thought to be a relatively sluggish helicopter, has a stiffness number of 0.04, whilst the crisp, responsive Lynx is 0.216 and the very stiff BO-105 is 0.39 [Padf96]. Based on the Kaman H-2 (which has a similar rotor design and is known to have excellent flying qualities and be very responsive to control inputs) it appears that this estimate of 0.12 is not truly representative of the Raven design [Toma99]. Therefore, whilst this stiffness number is used in the analysis of stability, control, and flying qualities, further analysis is required to determine a more accurate stiffness representation.

10.2.1 – Key Stability Derivative Estimation

The key stability and control derivatives are displayed in Table 10.1 (note that estimates are given in hover and cruise at sea level conditions). The force derivatives are normalized by the design gross weight (8330 lbs) and the moment derivatives are normalized by the moments of inertia (1184 slug-ft^2, 11600 slug-ft^2, and 10476 slug-ft^2 for I_{xx}, I_{yy}, and I_{zz}, respectively).

Table 10.1 – Key Stability and Control Derivatives

Derivative	Hover	Cruise	Units	Derivative	Hover	Cruise	Units
X_u	-0.15	1.08	1/sec	M_u	0.003	0.005	rad/(sec-ft)
X_w	0	0.02	1/sec	M_w	-0.005	-0.008	rad/(sec-ft)
X_q	1.6	1.6	ft/rad-sec	M_q	-0.5	-1.2	1/sec
$X_{\theta 1s}$	-32.2	-25	(ft/sec^2)/rad	$M_{\theta 1s}$	6.0	7.0	1/ sec^2
$X_{\theta 1c}$	0	-10	(ft/sec^2)/rad	N_v	0.009	0.02	ft/rad-sec
Z_u	0	-0.001	1/sec	N_r	0.33	1.0	1/sec
Z_w	-0.3	-1.0	1/sec	N_p	-0.05	-0.5	1/sec
$Z_{\theta 1s}$	0	90	(ft/sec^2)/rad	$N_{\theta 1c}$	0.03	0.04	1/ sec^2
$Z_{\theta 1c}$	-200	-200	(ft/sec^2)/rad	$N_{\theta T}$	-8.0	-8.0	1/ sec^2
Y_v	-0.05	-0.15	1/sec	L_v	0	-0.5	1/ sec^2
Y_r	0.6	0.6	ft/rad-sec	L_r	0.07	0.8	1/sec
Y_p	-1.9	-1.9	ft/rad-sec	L_p	-2.0	-2.0	1/sec
$Y_{\theta 1c}$	32.2	32.2	(ft/sec^2)/rad	$L_{\theta 1c}$	-20	-20	1/ sec^2
$Y_{\theta T}$	15	15	(ft/sec^2)/rad	$L_{\theta T}$	0	0	1/ sec^2

A few derivatives are particularly noteworthy and deserve special mention. Speed stability, M_u, is a function of the moment of inertia and the variation of pitch moment with respect to perturbations in forward velocity. It is a function of the stiffness of the main rotor, the effects of the tail, and the aerodynamics of the fuselage. For the Raven, it was estimated that the speed stability is approximately 0.003 rad/(sec-ft) in hover and 0.005 rad/(sec-ft) in forward flight. Angle of attack stability (sometimes referred to as incidence static stability), M_w, is a function of the amount of flapping hinge offset on the rotor system. If flapping hinge offset is present, and if the CG is not on the mast, then there will be pitching moments generated with a change in vertical speed. This derivative is also a function of hub stiffness and moment of inertia. The Raven has a virtual flapping hinge offset of approximately 0.80 feet at the predominant frequency, and a CG that is slightly forward of the mast. Considering these parameters, angle of attack stability was approximated to be –0.005 rad/(sec-ft) in hover and –0.005 rad/(sec-ft) in forward flight. One of the more significant derivatives with respect to lateral-directional stability is L_v, known as the dihedral effect. Lateral blowback in the main rotor and vertical (horizontal) damping in the tail rotor are the main contributions to this derivative (the height and location of the vertical tail and the aerodynamic shape of the fuselage also contribute). The Raven has a dominant tail structure and therefore the dihedral was estimated to be near zero at hover and -0.5/sec^2 at maximum cruise speed.

10.2.2 – Longitudinal Modes

An estimation of the Phugoid mode of the Raven suggests that the helicopter is slightly unstable in hover. Relatively high pitch damping due to the bearingless rotor design, relatively high speed stability, and a sleek aerodynamic design reduce the level of instability but do not entirely eliminate it. To counter this, the AFCS will incorporate velocity feedback to augment speed stability, since pitch rate feedback would be ineffective and would offer little more assistance than the small forward force damping. As airspeed increases so to does the instability (due mainly to the bearingless rotor design), however the instability can be controlled through use of the airspeed feedback loop in the AFCS. Analysis of the Raven design suggests that the longitudinal short period mode is stable in all regions of the flight envelope. This stability is due largely to the strong heave damping and pitch rate damping.

10.2.3 – Lateral Directional Modes

Dutch roll oscillation was predicted to be neutral in hover and stable at higher airspeeds. Dutch roll depends largely on the coupling of roll and yaw, and the key coupling derivatives are the dihedral effect (L_v) and yaw due-to-roll rate (N_p). Due to the Raven's bearingless design, both of these key derivatives were found to be large and negative. Although a negative value of N_p tends to destabilize the Dutch roll oscillation, this mode is maintained in the negative (stable) region by the strong dihedral effect. However, the dihedral effect is lowest at low airspeeds, and this leads to the neutral effects in hover. Improvements to Dutch roll stability will be implemented in this design with roll rate feedback and directional hold. The spiral mode was also approximated to be stable in all regions of flight. Spiral mode is a comparison between dihedral effect by yaw damping versus directional stability by roll damping. As with Dutch roll, the strong dihedral effect due to the bearingless design is the dominant characteristic in all modes of flight, resulting in stability. Roll subsidence was predicted to be stable due to the strong roll damping of the bearingless rotor.

10.2.4 – Handling Qualities

Control sensitivity and damping characteristics are important handling qualities parameters in hover and low speed flight. It is well understood that pilots want a vehicle responsive enough to be able to achieve some level of attitude change within a certain time after a control input is applied. It is also understood that they want predictability, an acceptable ratio of sensitivity to damping, and an acceptable level of response immediately after control input. In very general terms, all of these conditions can be satisfied with adequate sensitivity ($M_{\theta 1s}$ or $L_{\theta 1c}$) and damping (M_q or L_p), and the correct ratios between the two. Design estimates suggest that the Raven has adequate sensitivity and damping in different flight modes and that the ratios remain relatively constant throughout the flight regime. Response can be augmented through the model following architecture feature of the AFCS, if the requirement is determined in simulation.

Although a complete analysis of the longitudinal static stability cannot be predicted by merely examining the stability derivatives, one can determine relative stability, which is determined by the sign of speed stability (M_u). Therefore the Raven design suggests that positive longitudinal static stability is present. Positive static lateral directional stability is a desirable aircraft characteristic in all modes of flight. This attribute can help to maintain a steady hover with reduced pilot workload and can reduce the pilot workload requirements in cruise flight, especially in IFR conditions. While it is impossible to determine the gradient or level of static stability from the ratio of N_v to $N_{\theta T}$, the negative sign is an indication of stability in this critical flight mode. A negative L_v is an indication that the aircraft will exhibit positive dihedral effect, which helps to control the lateral-directional oscillation, thus reducing the workload during up and away cruise.

The Raven was designed to the bandwidth and phase delay requirements depicted in ADS-33E-PRF for utility helicopters. The next stage of development will verify, through testing of linear models and pilot-in-the loop simulation, the handling qualities in compliance with this design standard.

10.2.5 – Automatic Flight Control System

The AFCS was designed with several features and modes to assist the pilot by reducing workload and improving performance, thereby improving handling qualities. With the AFCS, this FCS was designed to perform to the rate command, attitude hold levels of performance defined by ADS-33E-PRF. In addition to stability augmentation functions such as rate feedback and model following architecture, the AFCS will provide the pilot with the ability to switch to pure attitude command for operations in degraded visual conditions. In hover modes, the Raven is capable of translational rate command from various levels of hold modes. Other modes include airspeed hold, altitude hold (barometric and radar altitude), automatic approach and departure, automatic search mode, and hover holds. The AFCS will contain interfaces to the mission computer to allow for flight director controlled instrument flight and will also be robust enough to allow for further expansion to meet future mission requirements.

Section 11 – Mechanical Subsystems

The primary mechanical subsystems onboard the Raven include the engines and the main transmission. These systems are integral to any helicopter design, and as a result a considerable amount of effort went into their selection and design. In this section the engine and transmission details will be presented.

11.1 – Engine Design

11.1.1 – Engine Selection

In order to meet the performance objectives outlined in the RFP, two scaleable Integrated High Performance Turbine Engine Technology (IHPTET) engines were selected, each with a nominal rating of 866 horsepower. The IHPTET initiative is a joint government and industry effort with the objective of developing advanced engine technologies. To date the program has demonstrated a 22% reduction in Specific Fuel Consumption (SFC), a 63% improvement in power-to-weight ratio, an 18% reduction in production cost and a 3% reduction in maintenance cost relative to 1987 state of the art engine technology [Hirs01]. Table 11.1 compares the pertinent design attributes of a number of existing engines with the scaleable IHPTET engine specified in the RFP (note that this data includes the improvements in SFC and power-to-weight ratio stipulated in the RFP).

Table 11.1 – Engine Data (incorporating IHPTET improvements)

Manufacturer	Model	Takeoff rating (shp)	SFC (lb/hp.hr)	Dry weight (lb)	Power/weight (hp/lb)
IHPTET (scaleable)	~	866	0.305	208	4.16
Pratt & Whitney Canada	PT6B-36B	981	0.436	276	3.56
Turbomeca	Arriel 2C/C1	962	0.401	201	4.78
LHTEC	T800-800	1334	0.338	222	6.02
General Electric	T700-401A	1680	0.350	323	5.20

The results from this table show that the IHPTET engine offers a combination of low specific fuel consumption and low weight that no other existing engine can match. It also offers a very high emergency power setting that is 25% above the takeoff rating, which is critical in enabling the Raven to meet the stringent OEI condition without sacrificing cruise fuel efficiency.

11.1.2 – Engine Performance

To enable the scaleable state-of-the art engine characteristics to be determined, the maximum power required from the engine had to first be established. The OEI requirement specified in the RFP was found to generate the highest power requirements and therefore this condition was used to size the engines. The static, uninstalled engine specifications at sea level, ISA conditions are presented in Table 11.2. The effects of altitude, temperature and flight speed on the total uninstalled power (for both engines) are displayed in Figures 11.1 and 11.2. The effects of temperature and altitude were modeled based on the typical uninstalled engine characteristics presented by Prouty [Prou95], whilst the ram power increase with speed was modeled based on the relationship given in the RFP.

Table 11.2 – IHPTET Engine Specifications (static, uninstalled, ISA, sea level)

Rating	Duration	Power ratio	Power (shp)	SFC (lb/hp.hr)
Emergency (OEI)	30 sec	1.25	1082	0.302
Takeoff (max)	2 min	1	866	0.305
IRP[1]	30 min	0.924	800	0.309
MCP[2] (cruise)	Continuous	0.791	685	0.328
Partial power	~	0.5	433	0.4
Idle	~	0.2	173	1

[1] – Intermediate Rated Power (IRP) [2] – Maximum Continuous Power (MCP)

Figure 11.1 – Uninstalled engine ratings as a function of altitude and temperature

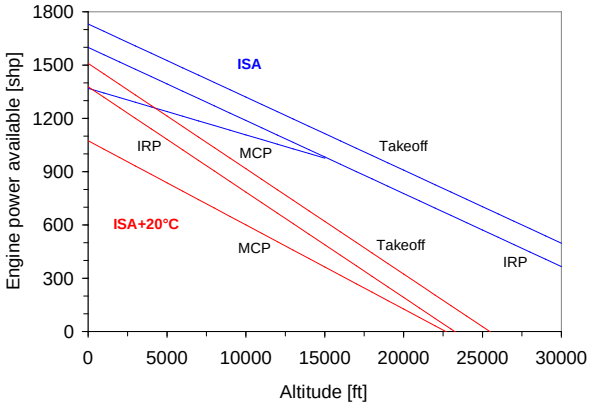

Figure 11.2 – Effect of forward speed on uninstalled engine ratings

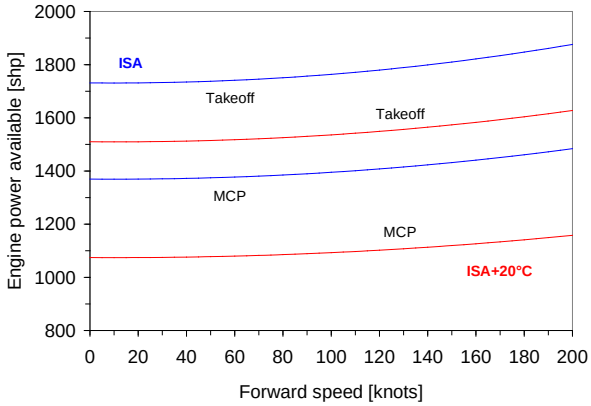

11.1.3 – Engine Characteristics

The engine characteristics were determined using the relationships presented in the RFP, which give an engine weight of approximately 208 lbs. It was however discovered that the relationship given to determine the engine diameter is questionable, since application of this formula yields an engine with a diameter of approximately 6 inches (which is clearly unrealistic). Therefore the engine was sized based on the dimensions of existing engines, resulting in a diameter of 26 inches and length of 31.5 inches. An additional requirement of the engines is the capability to generate different output speeds in hover and cruise. In hover the Raven requires a rotor speed of approximately 339 RPM whereas in cruise the vehicle requires a rotor speed of approximately 353 RPM, an increase of approximately 4% over hover. A variation in rotor speed was deemed necessary to optimize flight in both forward flight and hover. This technology was demonstrated by Mitsubishi Heavy Industries (MHI) on the MH2000 helicopter, which is equipped with MG5-110 turboshaft engines that are capable of operating at two distinct RPM levels. Therefore a variable RPM engine was deemed to be feasible for this design.

11.1.4 – Engine Installation

The engines are installed on the engine deck behind the main gearbox with three A-frames and one sway bar (this location allows for good accessibility for maintenance and inspection). The A-frames are attached to the bulkhead, which transmits the engine loads to the fuselage. The engine output shaft is connected to the main gearbox through a flexible coupling, which can accommodate both axial and angular misalignments. Firewalls are integrated into the design to confine the engines in the event of a fire. The details of the engine/fuselage integration are displayed in Foldout 11.1 (note that the engine/transmission covers can double as work platforms to assist in routine aircraft maintenance).

11.1.5 – Engine Installation Losses

The engine as installed in the helicopter will usually not deliver the same power as it does in the engine manufacturer's test cell. To account for this, an engine power loss due to installation was estimated based on the data presented by Prouty [Prou95] and Stepniewski [Step84]. The total engine installation loss was estimated to be five percent of the uninstalled engine power and consists of losses due to – inlet pressure (1%), compressor bleed (2%), engine mounted accessories (1.5%), and exhaust back pressure (0.5%).

11.1.6 – Oil System

In order to improve reliability and safety, an independent oil system is provided for each engine. The oil system is assumed to be an integral part of the engine. Each system consists of a pump, tank, filter, cooler and two particle detectors. The particle detectors are monitored by the FADEC system (see below).

11.1.7 – Engine Control System (FADEC)

A Full Authority Digital Electronic Control (FADEC) system is integrated into the design to ensure optimum engine performance, enhance flight safety, reduce pilot workload, increase mean time between removals/overhauls, reduce life cycle costs and simplify engine maintenance.

11.1.8 – Particle Separator

In order to minimize the risk of engine damage during extended operations in hostile conditions, a particle separator is supplied as an integral component of the engine design. The particle separator provides continuous engine protection from sand and dust.

11.1.9 – Auxiliary Power Unit (APU)

An APU was integrated into the design to enable reliable unassisted self-starting. The APU is also used to supply power to the cockpit electronics and the environmental control system whilst the vehicle is on the ground.

11.2 – Main Rotor Transmission Design

11.2.1 – Configuration

The Raven incorporates a split-torque transmission design, which is shown in detail in Foldout 11.1. A split-torque transmission was selected in preference to a conventional planetary design due to its advantages in terms of weight, noise and Mean Time Between Removal (MTBR). The main rotor transmission is divided into three stages: an input bevel stage, an intermediate spur stage and an output helical stage. The output from each engine is first inputted to an overrunning spring clutch and then directly into a bevel pinion (the spring clutch can be used to disengage the engines from the rotor system in the event of engine failure). The centerline of the output bevel gear is parallel to the centerline of the main rotor shaft. The shaft angle of the input bevel gear pair is 80 degrees in order to accommodate a 4 degree forward tilt of the main rotor shaft and a 6 degree inclination of the tail drive shaft. The engines are aligned parallel to the tail rotor shaft. The intermediate spur gears transfer torque from the bevel gear to the dual sets of helical pinions. The output bevel gear teeth are opposed helically such that they load share through a balance of axial forces. A summary of the drive system features are given below in Table 11.3.

Table 11.3 – Drive System Design Features

Drive system parameter	Input bevel stage	Intermediate spur stage	Output helical stage
Torque paths	1	2	4
Tooth numbers	57/33	98/27	269/27
Reduction ratios	1.727	3.630	9.963
Diametral pitch	10	10	10
Pressure angle (deg)	20	22.5	20
Helix angle (deg)	20	0	±40
Face width (in)	1.332	1.388	2.173
Pinion speed (RPM)	21150	12245	3373.6
Gear diameter (in)	5.7	9.8	26.9
Pinion diameter (in)	3.3	2.7	2.7
Pinion torque (ft.lb)	268	231.5	420.1
Actual compressive stress (psi)	137×10^3	169×10^3	130×10^3
Actual bending stress (psi)	31.2×10^3	45.7×10^3	46.0×10^3
Center distance (in)	N/A	6.25	14.8

The gears were designed to satisfy strength limits and were developed using the methods presented by Dudley [Dudl54]. As mentioned previously, the RFP stipulates a stringent OEI capability. In order to meet this requirement, the transmission components were designed to transmit a maximum power of 1082 hp (for no more than 30 seconds), which corresponds to the emergency output rating from one engine.

11.2.2 – Structural Integration

Typically, rotor mast loads (including moments, thrust, side loads and torque) are transferred to the helicopter fuselage via the transmission housing. In order to minimize the loads experienced by the housing, an independent truss support, referred to as a standpipe, was incorporated into the design [Kish78]. The primary benefit of the standpipe is that it transfers all loads directly to the fuselage (except for the torque), which reduces the weight and increases the fatigue life of the transmission. The standpipe consists of a bearing housing and four legs, all manufactured from titanium. The bearing housing contains two tapered roller bearings and the rotor shaft. The four legs are attached to the bearing housing and then mounted to the transmission deck using nodal vibration isolators. Torque is carried between the transmission and the rotor shaft by a steel quill shaft that has a flange designed to support the maximum torque loads and react the minimal head moment, thrust and side loads. The quill shaft is mounted between the transmission output quill and the main rotor shaft.

11.2.3 – Transmission Housing

The primary function of the transmission housing is to support and enclose the main transmission components, in addition to reacting the residual loads transferred by the quill shaft. The transmission housing is mounted under the standpipe where it attaches to the bearing housing. The engine inputs are at the mid height of the gearbox, with overlap of the three reduction stages resulting in low height. The main gearbox housing carries only the gear reaction loads due to the use of a standpipe. The housing is to be manufactured from an aluminum alloy (C355T7), which has better corrosion resistance than typically used magnesium-zirconium alloys. Selecting a material for the transmission that has good corrosion resistance is critical for rotorcraft that are expected to operate for extended periods of time in a marine environment.

11.2.4 – Oil System

A combined scavenge and lubrication pump, driven from each bevel gear, scavenges oil from the transmission lower case sump through a chip detector and an oil inlet screen. From the pump, the oil is delivered to an oil filter assembly and an oil cooler and then returns to the main transmission internal lubrication channels and spray jets to lubricate the internal gears. Separate lubrication systems are used for each side of the transmission. A pressure failure in either side shifts a balance valve that directs lubricant from either pump to both sides of the transmission. An oil level sight gage is located on the starboard side of the lower casing of the main transmission where it can be easily inspected. An oil breather is installed in the gearbox to permit the lubrication oil and air to expand or contract with changing temperature.

11.2.5 – Weight Reduction Features

The transmission incorporates the following weight reduction features; an output stage planetary train is replaced by a multipinion split-torque train, the tail drive system power is extracted prior to the main drive system gears and the low height transmission housing supports only gear reaction loads [Whit98].

11.2.6 – Transmission Power Losses

Losses which occur between the engine torquemeter and the rotors must be made up by the engine and are additive to the power required by the rotors. These losses were estimated based on the information presented by Prouty [Prou95] and Stepniewski [Step84]. The transmission losses were determined to be approximately two percent of the power required by the main rotor whereas the accessory losses were estimated to be one percent of the power required by the main rotor (accessory losses include power extraction for items such as engine and transmission cooling blowers, electrical power generation and

hydraulic supplies). Therefore the total losses were estimated to be approximately three percent of the main rotor power required (this was factored into all main rotor power estimates).

11.3 – Tail Rotor Power Transmission

The transmission takeoff for the tail rotor is located between the engine inputs, with half the power requirements split between each bevel pinion (refer to Foldout 11.1). Over-travel stops are designed to engage if either section of the bevel pinion attempts to overrun the other, as would happen in the event of a structural failure. In such cases, all torque to the tail drive shaft is extracted from one input pinion. In the case of single-engine operation the motion limit stops of the summing unit engage before the dead side of the unit can pull its normal share of the torque. The torque is drawn only through the train that connects the bevel pinion with the live engine. A three stage spur gear train with a total reduction ratio of 1:6.58 provides the anti-torque fan with a rotational speed of 3320 RPM, as required. The tail rotor drive shaft is connected to the main gearbox by a flexible coupling. The shaft is divided into four segments, with each segment supported by two bearing blocks and equipped with a grease fitting for lubrication. Flexible couplings are incorporated between each section to accommodate shaft misalignment and fuselage bending. At the end of the tail rotor drive shaft, a pair of self-lubricating bevel gears are used to rotate the tail transmission shaft by 90° to power the fan.

11.4 – Auxiliary systems

Hydraulic pumps are connected to the idle gears located in the drive train connecting the main gearbox to the tail drive shaft. Unlike helicopters that use a conventional swashplate, the hydraulic systems onboard the Raven are used primarily to operate the undercarriage (instead of driving the swashplate actuators). Activation of the hydraulic system is accomplished electrically, however in the event of total electrical power loss, the hydraulics can be activated manually [Bell01]. A blower is required for the environmental control system and is driven by transfer gears connected to the tail drive shaft. Two electric generators, driven from pinions that mesh with the forward second-stage gears, supply power to the on-board electronics, de-icing systems, and magnetic SMA actuators in the blades. Each generator is decoupled from the engine drive path such that it can continue to produce power whilst the main rotor turns.

Section 12 – Weight Analysis

In this section of the report, a detailed component weight breakdown for the Raven will be presented, together with an estimate of the Center-of-Gravity (CG) travel. The methods used in the weight analysis will be discussed, and detailed weight component descriptions will be given.

12.1 – Weight Estimation

The preliminary weight estimate was based upon two primary techniques: a method presented by Prouty [Prou95], which is based upon multiple linear regression techniques, and a method developed by Tishchenko [Tish01], which is based upon the equations developed at the Mil Design Bureau. This second method requires weight coefficients to be established for each component, by using regression analysis techniques to develop a relationship between the component weights and the design parameters that most influence these weights. Two different methods were adopted in preference to one in order to provide a check on the weight estimates made. Since both of the methods adopted rely upon historical data from existing rotorcraft, they do not reflect advanced technologies that are likely to emerge over the next 15 years (such as MicroElectroMechanical Systems or 'MEMS'). Therefore to enable a more representative estimate of the empty weight of the Raven to be made, these methods were supplemented with advanced technology correction factors. The correction factors used were primarily based upon the recommendations made by Shinn [Shin84] and Unsworth [Unsw84], and are discussed in greater detail in the following section.

Foldout 11.1

12.2 – Component Weight Breakdown

The rotorcraft empty weight was divided into groups conforming to MIL-STD-1374 and is presented in Table 12.1. The relevant longitudinal and vertical CG locations are given with respect to a virtual datum point located 238.8 inches ahead and 159.8 inches below the main rotor hub. A detailed MIL-STD-1374 (Part I) weight breakdown is attached at the end of this report. Descriptions of the primary weight components are given after the table.

Table 12.1 – Component Weight Breakdown

Component	Weight (lb)	% Empty weight	Long. CG (in)	Vert. CG (in)
Main rotor	433.4	10.03	238.8	159.8
Fan-in-fin	81.4	1.89	506.4	101.3
Empennage	43.3	1.00	520.2	163.9
Fuselage	652.6	15.10	244.1	76.9
Landing gear	225.7	5.22	245.3	54.1
Nacelles	37.7	0.87	241.3	128.2
Propulsion system	608.2	14.07	278.4	118.6
Drive system	374.2	8.66	261.7	126.2
Control system	232.9	5.39	233.3	103.5
Auxiliary power unit (APU)	88.6	2.05	196.9	128.2
Avionics	650	15.04	295.3	82.7
Electrical systems	159.2	3.68	321.2	66.4
Instruments	29.1	0.67	120.8	67.9
Hydraulics	57.0	1.32	260.9	128.2
Furnishings & equipment	83.0	1.92	172.4	69.3
Air conditioning & anti-ice	86.8	2.01	196.9	128.2
Load and handling	36.5	0.84	255.9	76.9
Internal noise reduction	86.8	2.01	255.9	76.9
Trapped fuel and oil	38.9	0.90	233.8	86.2
Crashworthiness features	161.6	3.74	255.9	76.9
Manufacturing variation	34.7	0.80	255.9	76.9
Weight growth	121.2	2.80	@CG	@CG
Empty weight*	**4323**	**100**	**248.5**	**95.5**
Payload (2 @ 190lbs each)	380	~	228.3	73.1
Crew (4 @ 200 lbs each)	800	~	191.5	76.9
MEP	1052	~	228.7	73.8
Fuel	1710	~	236.2	1250
Transmission & engine oil	65.6	~	241.3	128.2
Design Gross Weight	**8330**	**~**	**237.1**	**79.9**

* – Empty weight is defined as the dry empty weight plus the unusable fuel and trapped transmission and engine oil.

12.2.1 – Main Rotor and Fan-in-Fin

Unsworth and Sutton [Unsw84] show that with an Integrated Technology Rotor (ITR) the weight of the rotor blades can be reduced by approximately 6% and the rotor hub by approximately 30% over 1980's rotor technology. Therefore, the weight of the rotor blades was estimated to be 256 lbs and the weight of the titanium/composite bearingless rotor hub was estimated to be

177 lbs. The weight of the rotor blades includes the weight of the rotor folding modifications, but not the embedded swashplateless controls, which are included in the control system weight (Section 12.2.6). The total weight of the fan-in-fin anti-torque system was estimated to be 81 lbs, which incorporates a reduction factor to account for composite construction and inherent lightweight fan-in-fin attributes (refer to Section 6).

12.2.2 – Fuselage & Empennage

The Army/Bell Advanced Composite Airframe Program (ACAP) demonstrated that use of composite materials can reduce the airframe weight by 22% without sacrificing strength and crashworthiness [Reis86]. Considering advances in the use of composite materials since the inception of the ACAP program in 1986, and the fact that delivery of the first Raven is not anticipated until 2015, a reduction factor of 25% was used, resulting in a fuselage weight estimate of 653 lbs. In addition, approximately 4% of the empty weight (162 lbs) was added to this estimate to account for the additional structure that is used to enhance the crashworthiness of the vehicle. The empennage weight, which includes the horizontal and vertical stabilizers in a T-tail configuration, was estimated to be 43 lbs. The weight of the engine nacelles was estimated to be 38 lbs.

12.2.3 – Landing Gear

The weight of the landing gear was estimated to be 226 lbs, which includes a 13% weight savings due to structural optimization [Shin84]. The main gear, which supports the primary landing loads, was estimated to account for approximately 80% of the total landing gear weight (181 lbs).

12.2.4 – Propulsion System

The propulsion system weight consists of the dry engines, engine installation, propulsion subsystems and fuel systems. The engine weight was determined directly from the IHPTET scaleable state-of-the-art engine characteristics given in the RFP. Based on a nominal engine power rating of 866 hp, each engine was estimated to weigh approximately 208 lbs. The engine installation and propulsion subsystems were estimated to weigh 123 lbs and the fuel systems were estimated to weigh 69 lbs.

12.2.5 – Drive System

The drive system weight consists of the main gearbox, fan-in-fin gearbox and transmission shaft (no intermediate gearbox was required). The weight of the main gearbox was estimated to be 335 lbs, the tail gearbox to be 17 lbs and the transmission shaft to be 23 lbs. The total drive system weight was reduced by approximately 15% to account for composite applications, new tooth forms, higher speed input sections, and improved material characteristics and processing [Unsw84].

12.2.6 – Control Systems

The control system weight is comprised of the flight control system (upper and lower controls minus the swashplate), cockpit controls and the swashplateless control system (which replaces the conventional swashplate). The flight control system, which consists of digital Fly-By-Wire (FBW) controls, was estimated to weigh 157 lbs (including cockpit controls). This estimate includes a 60% reduction in the lower control system weight due to the FBW system [Tish01]. The swashplateless control system was estimated to weigh approximately 76 lbs and consists of all the components that were added to the rotorcraft to replace the swashplate. This estimate accounts for the on-blade actuators, cables, balance weights, additional blade structure (to stiffen the ribs around the actuators) and springs at the hub, and is approximately 50% lower than the weight of a conventional swashplate.

12.2.7 – Instruments & Avionics

The instruments group weight reflects the use of an advanced “glass cockpit”, as presented in Section 8. The MFD displays and other digital equipment are significantly lighter than traditional analog gages and as a result a reduction factor of approximately 50% was used (based on the Comanche), resulting in a weight estimate of 29 lbs. The avionics weight was estimated to be approximately 650 lbs, as suggested in the RFP.

12.2.8 – Electrical Systems & Hydraulics

The electrical system primarily consists of the batteries, electrical cables and two generators. Due to the fact that the design includes an onboard APU to start the main engines, the cold start load requirements of the batteries will be reduced, allowing lightweight batteries to be used. Fiber optic cables were also used to reduce the overall weight of the electrical cabling. The total electrical system weight was estimated to be 159 lbs, which includes a 15% weight reduction to account for the weight savings outlined above. The hydraulic system was estimated to weigh 57 lbs, with weight savings being realized from the use of advanced materials, and by giving special attention to the routing of the hydraulic lines.

12.2.9 – Miscellaneous Components

The remaining weight components consist of the APU, furnishings, air conditioning, anti-ice systems, load and handling group, internal noise reduction features, manufacturing variation and weight growth. The weight of the APU was estimated to be 89 lbs, based on existing rotorcraft and factoring in a similar weight improvement to that specified for the IHPTET engines. The furnishing and equipment weight, which includes only those items necessary to make the vehicle flight worthy, was estimated to be 83 lbs (including 2 crashworthy cockpit seats weighing 28.6 lbs each). The air conditioning and anti-ice systems were estimated to weigh 87 lbs. The special load equipment, which consists of aircraft towing points and jack hard points, was estimated to weigh 37 lbs. The internal noise reduction features were estimated to weigh 87 lbs (or 1% of the gross weight, as specified in the RFP). And finally, to account for manufacturing variation and weight growth, 156 lbs was added to the empty weight (0.4% of the gross weight for manufacturing variation and 3% of the empty weight for weight growth).

12.2.10 – Crew & Payload

The crew and payload requirements were specified in the RFP – 4 crew estimated to weigh approximately 200 lbs each and 2 patients estimated to weigh approximately 190 lbs each. The crew consists of 2 flight crew and 2 pararescuers.

12.2.11 – Mission Equipment Package

The MEP weight was estimated to be 1052 lbs and includes all items that are added to the flight worthy rotorcraft to enable it to perform the specified SAR mission. It is anticipated that the application of advanced technology will result in a weight savings on the order of 15% [Shin84], which has been included in the 1052 lb estimate. A more detailed MEP component breakdown and description is presented in Section 9.

12.2.12 – Fuel & Oil

The total fuel capacity of the vehicle was estimated from the final evaluation mission outlined in Table 2.1. The total fuel required to complete this mission was estimated to be 1732 lbs (259 US gallons of JP4 fuel). This estimate includes an additional 1.3% to account for any unusable fuel that is trapped in the tanks. The fuel is to be primarily stored in two main tanks located under the floor of the cabin between the landing gear wells (each tank supplies a different engine). The vehicle also carries 55.8 lb of engine oil (including 11.2 lb of trapped oil) and 26.2 lb of transmission oil (including 5.3 lb of trapped oil). These oil requirements were estimated by comparing the oil capacities of existing rotorcraft with similarly sized engines [Tayl00].

12.2.13 – Maximum Takeoff Weight

The Raven was designed with a maximum takeoff weight (8680 lbs) that is approximately 350 lbs greater than the design gross weight (8330 lbs). The added weight evolved from a basic desire to give the rotorcraft an added lift capacity to enable it to rescue more people than was specified in the RFP. The need for added lift capacity was highlighted by the recent Coast Guard rescue of 34 sailors from a cruise ship off the coast of Virginia [Guar01]. During that rescue a HH-60J Jayhawk ended up rescuing 26 sailors, well above its normal design capacity of 6 patients. The same requirement for added capacity was also highlighted in the Operation Lichi rescues performed by the South African Air Force in Mozambique. During these rescues a BK-117 was loaded with an astonishing 26 people, which is again well above its design capacity of 7 passengers. As a result of

these 'real world' cases, the structure, transmission and landing gear of the Raven was designed for the maximum takeoff weight, whilst the performance was optimized for the design gross weight. Note also that the fuselage weight estimate of 653 lbs (Section 12.2.2) accounts for an oversized cabin, which is necessary to accommodate the added payload.

12.3 – Weight Efficiency

Based on the preliminary weight estimates, the predicted empty weight fraction (defined as empty weight divided by design gross weight) is approximately 50%, which leaves 50% for fuel, crew and payload. This compares favorably with current helicopters [Tayl00] and appears to be reasonable for a 2001 helicopter design, based on the trends in empty weight fraction as a function of time shown by Scott [Scot91].

12.4 – Weight & Balance

The longitudinal CG locations of the weight components are displayed in Figure 12.1 (the lateral CG locations are not shown since it was assumed that the aircraft's port and starboard sides are loaded symmetrically). In order to obtain a more accurate approximation of the aircraft CG, the group weights displayed in Table 12.1 were broken down further into individual weight components.

Figure 12.1 – Component CG Locations

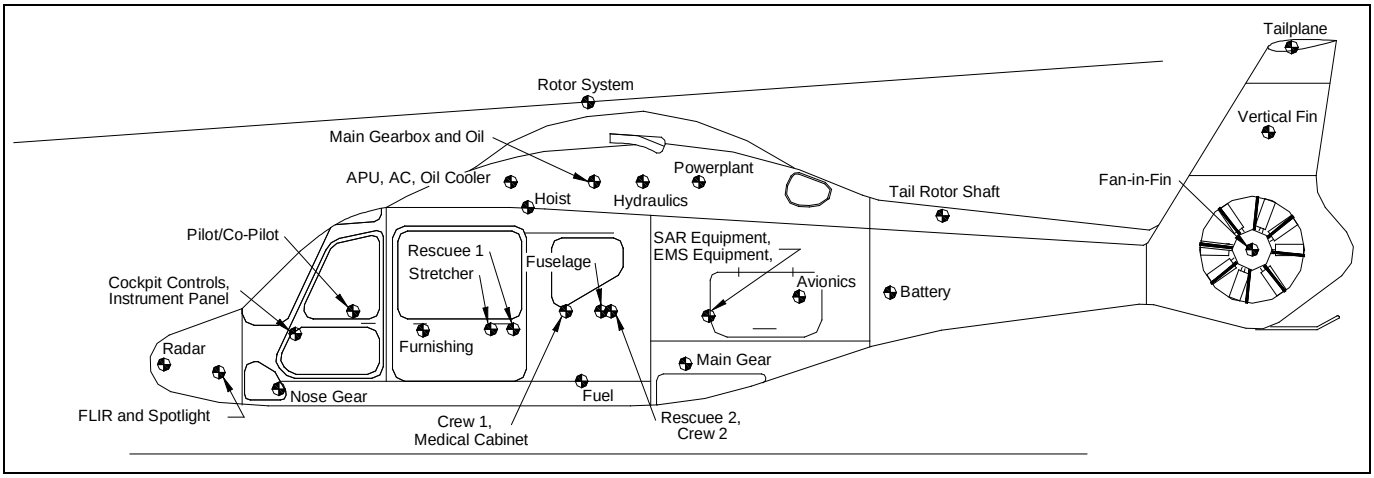

The longitudinal CG location of the fuel tanks was kept close to the total aircraft CG in order to minimize the longitudinal CG travel during flight. In optimizing the aircraft CG location, a number of components were moved in order to obtain a CG position/travel that minimized cyclic requirements and facilitated good handling qualities throughout the mission. The longitudinal CG travel as a function of gross weight is shown in Figure 12.2. The figure shows that the most forward CG position is 5.9 inches ahead of the main rotor shaft (2.6% of the rotor radius), and the most aft CG position (in flight) is 0.8 inches ahead of the rotor shaft (0.3% of the rotor radius). The maximum CG travel in flight is therefore 5.1 inches, or 2.3% of the rotor radius. The empty weight and mission equipped empty weight CG locations are both aft of the rotor shaft by 9.2 inches and 2.1 inches respectively.

Figure 12.2 – Longitudinal CG Travel

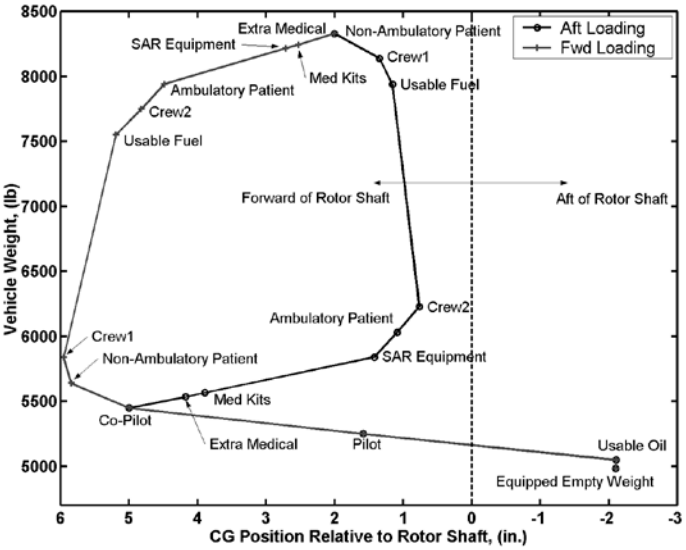

Section 13 – Performance Analysis

The performance analysis focused primarily upon estimating the power requirements of the Raven in hover, climb, and forward flight, over a variety of temperatures and altitudes. This enabled the primary rotor and engine parameters to be sized in order to optimize flight at the design gross weight. A concise summary of the vehicle performance is listed below in Table 13.1. The general performance attributes, including drag and flight performance, are presented throughout this section.

Table 13.1 – Performance Summary (DGW, ISA, sea level conditions unless specified)

Parameter	Estimate
Design gross weight	8330 lb
Nominal cruise speed (500 ft)	160 knots
Maximum cruise speed	170 knots
HOGE[1] ceiling (ISA, takeoff power)	12730 ft
HOGE ceiling (ISA+20°C, takeoff power)	6677 ft
HIGE[2,3] ceiling (ISA, takeoff power)	15327 ft
HIGE ceiling (ISA+20°C, takeoff power)	8683 ft
VROC[4], maximum (ISA, takeoff power)	3071 ft/min
VROC, maximum (ISA+20°C, takeoff power)	2265 ft/min
Climb rate, maximum (ISA, MCP)	2900 ft/min
Range[5], maximum (with standard reserves)	776 nm
Endurance[6], maximum (with standard reserves)	5.7 hrs
Best range speed	150 knots
Best endurance speed	115 knots
OEI[7], HOGE ceiling (ISA, emergency power)	4224 ft
OEI, HIGE ceiling (ISA, emergency power)	8039 ft

[1] – Hover Out-of-Ground-Effect (HOGE)
[2] – Hover In-Ground-Effect (HIGE)
[3] – Estimated at a 5ft wheel height above the ground
[4] – Vertical Rate of Climb (VROC)
[5] – At 500 ft PA, ISA+15°C
[6] – At 500 ft PA, ISA
[7] – One Engine Inoperative (OEI)

13.1 – Drag Estimation

Drag estimation is a key component in the prediction of rotorcraft performance, and as a result requires careful consideration to ensure optimal performance is achieved. For a comprehensive drag estimate to be made, the drag of the vehicle must be estimated in both hover (vertical drag) and forward flight (parasite drag). In industry, the vehicle drag is usually estimated via a combination of experimental data and potential flow theory (i.e. panel methods). However in this preliminary design, such an advanced approach was not available and therefore the methods presented by Prouty [Prou95] and Stepniewski [Step84] were adopted. Both of these methods primarily rely upon estimating the component drags based on experimental results and as a consequence are more suited to the preliminary stages of a design. The breakdown of the parasite drag in forward flight is shown in Table 13.2 (the vertical drag on the fuselage was estimated to be approximately 2.81% of the vehicle gross weight). Note that these percentages compare well with a typical low drag helicopter design given by Leishman [Leis00].

Table 13.2 – Parasite Drag Component Breakdown

Component	Flat Plate Area (ft^2)	% of Total
Basic fuselage	3.35	33.25
Engine nacelles	0.62	6.18
Main rotor hub and shaft	3.65	36.25
Horizontal stabilizer	0.21	2.10
Vertical stabilizer	0.13	1.29
Fan-in-fin	0.30	3.02
Hoist	0.11	1.11
Rotor-fuselage interference	0.79	7.88
Engine exhaust system	0.23	2.27
Miscellaneous	0.67	6.65
Total flat plat drag area	**10.08**	**100**

In order to maximize the speed capability of the Raven a concerted effort was made to minimize the drag, which is evident from the low equivalent flat plate drag area. The low drag characteristics of the Raven are primarily attributable to the following:

- *Fuselage* – the fuselage shape was designed to be smooth, with no abrupt changes to cause flow separation. The upsweep angle of the fuselage was kept small.
- *Engine nacelles and intakes* – the engine nacelles were designed to ensure a smooth and gradual transition to the fuselage. The intakes were based on the advanced low drag intake design developed for the Ka-62.
- *Undercarriage* – the undercarriage is fully retractable.
- *Rotor hub* – the bearingless main rotor hub (with fairing) incorporates fewer parts and contributes less to drag than traditional articulated rotor hubs.
- *Fan-in-fin* – the fan-in-fin minimizes drag due to the shroud (which houses the rotor components) and by being significantly offloaded in forward flight.
- *Empennage* – the 'T-tail' configuration reduces the download in hover by placing the horizontal stabilizer outside of the main rotor wake.
- *SAR equipment* – the FLIR and searchlight are both capable of being retracted into the fuselage. The only primary external disturbance is attributable to the hoist, which is faired (including the struts) to reduce the impact on drag. Special consideration was given to reducing the drag of the SAR equipment to limit the impact on mission performance.

All of these features helped to minimize the vehicle drag in both hover and forward flight. Furthermore, in order to minimize the fuselage drag in cruise and improve passenger comfort, it is generally desirable to have a low fuselage angle of attack. Therefore, based on the vehicle trim analysis (refer to Section 5), the main rotor shaft incidence angle was set at approximately 4 degrees relative to the fuselage, such that the fuselage angle in forward flight is small (this shaft tilt is not large enough to adversely alter the field of view of the pilots in hover).

13.2 – Hover Performance

The hover performance was estimated from the main rotor model (refer to Section 13.3) and includes empirical corrections to account for power losses due to the rotation of the wake, tip vortex interference, and the effect of the ground on induced velocities. The vertical climb performance was estimated by a modified momentum approach that accounts for the power required to climb in excess of that required to hover at the same conditions. The results are displayed in Figures 13.1 - 13.3.

Figure 13.1 – Hover Ceiling OGE

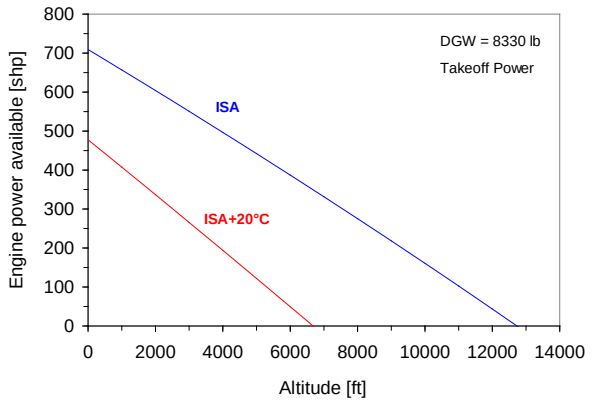

Figure 13.2 – Hover Ceiling IGE

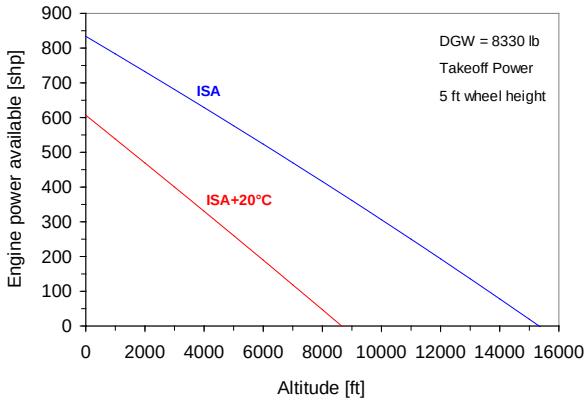

Figure 13.1 shows the hover ceilings out-of-ground-effect and Figure 13.2 shows the hover ceilings in-ground-effect, whilst

Figure 13.3 shows the maximum vertical rate of climb as a function of altitude. The results indicate that the hover and climb performance of the Raven are significantly better than existing SAR aircraft, such as the HH-65A Dolphin (which has a HOGE ceiling of 5340 ft and a HIGE ceiling of 7510 ft). This will allow the Raven to operate in more adverse conditions (such as in mountains at altitude) and perform rescues in locations that the HH-65A cannot. This performance advantage can be traced directly back to the requirement to meet the stringent OEI condition (refer to Table 3.7), which ensures that a large excess power is available in hover. This large excess in power gives the Raven its excellent hot and high hover and vertical climb performance.

Figure 13.3 – Vertical Rate of Climb

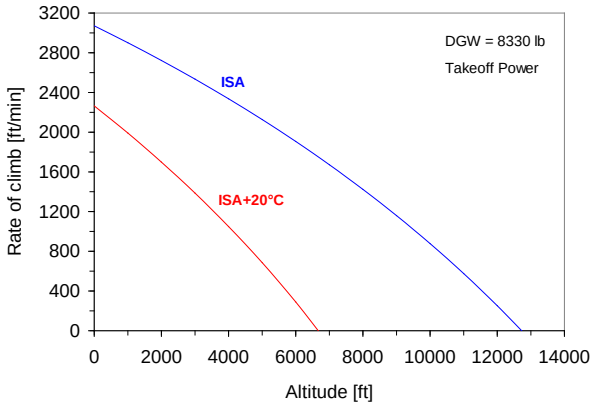

13.3 – Forward Flight Performance

The main and tail rotor powers required as a function of forward speed are displayed in Figure 13.4 (level flight, DGW, ISA, sea level conditions). A propulsive trim model of the helicopter was developed to generate these results. In this model, the rotor blades are assumed to be rigid, with pitch and flap degrees of freedom. The relevant blade pitch deflections and trailing-edge flap control deflections required for trim in level flight were shown in Section 5. The discontinuities shown in Figure 13.4 at 70 knots correspond to a change in rotor tip speed from 695 fps to 725 fps.

Figure 13.4 – Power Required Curve (DGW, ISA, SL)

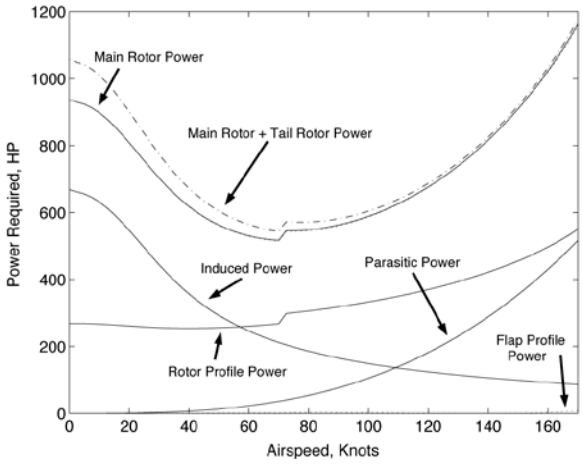

Figure 13.5 shows the equivalent lift-to-drag ratio of the Raven as a function of forward speed. As can be seen from this figure, a maximum lift-to-drag ratio of approximately 4.5 is reached at a flight speed of 115 knots. The fuel consumption of the two engines under cruise conditions is shown in Figure 13.6. At the design gross weight, a best range speed of 155 knots (based on 99% maximum specific range) and a best endurance speed of 120 knots (based on maximum specific endurance) were determined. The weight of fuel required to perform the range mission was estimated to be 1273 lbs and that required for the endurance mission was estimated to be 1500 lbs (refer to Section 3.3.2).

Figure 13.5 – Equivalent Vehicle Lift-to-Drag (ISA, SL)

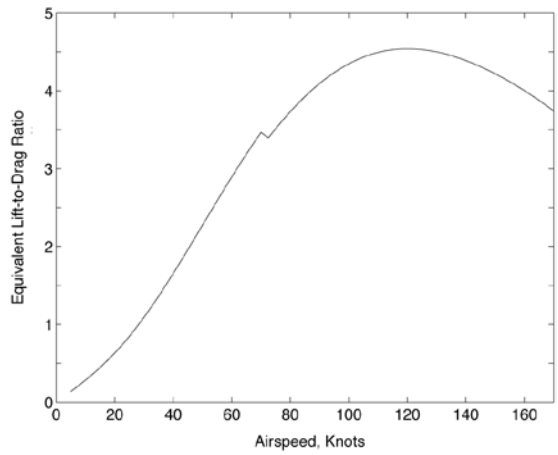

Figure 13.6 – Fuel Consumption

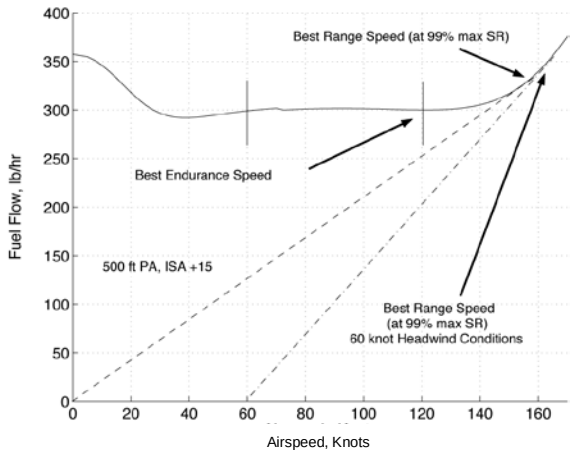

Figure 13.7 shows the payload capability of the helicopter as a function of range. A maximum range of approximately 780 nm was determined (design gross weight, standard reserves) based on the maximum fuel capacity. The maximum possible range with auxiliary tanks was estimated to be 1560 nm (which was determined by replacing all of the payload and mission equipment with fuel). Figure 13.8 shows the payload endurance diagram. A maximum endurance of 5.7 hours was determined (design gross weight, standard reserves) based on the maximum fuel capacity.

Figure 13.7 – Payload/Range Diagram

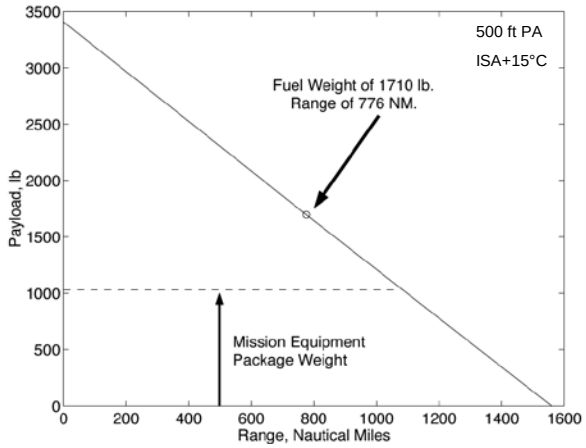

Figure 13.8 – Payload/Endurance Diagram

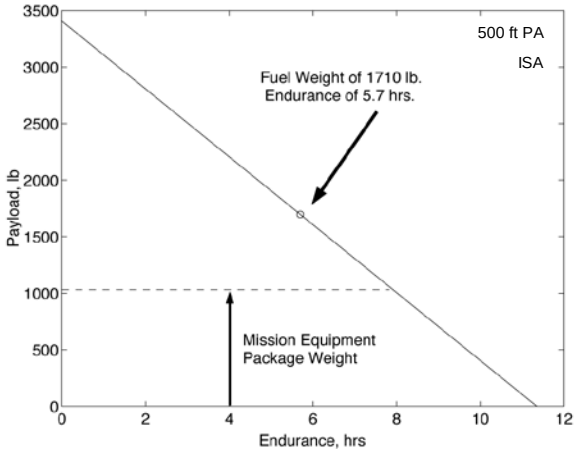

Figure 13.9 shows the maximum rate of climb in forward flight with maximum continuous power under ISA, sea level conditions. The limit shown is based on typical passenger comfort levels for unpressurized cabins. The OEI requirement ensures rates of climb in excess of 1500 fpm at forward flight speeds ranging from 25 to 150 knots, with a maximum rate of climb of approximately 2900 fpm occurring at 70 knots.

Figure 13.9 – Maximum Rate of Climb in Forward Flight

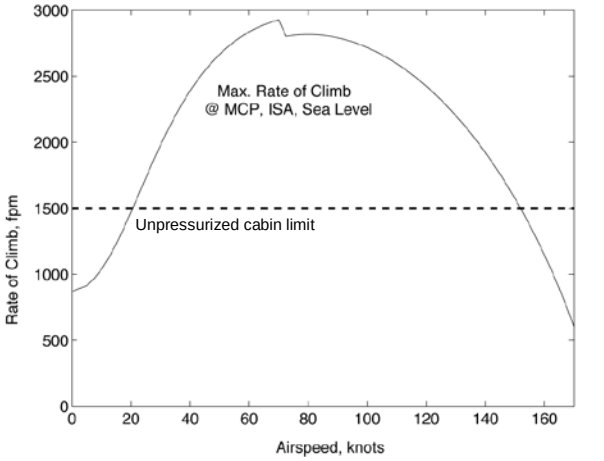

13.3.1 – Primary Mission Performance

The primary evaluation mission profile (refer to Section 2.2.2) was analyzed in great detail to ensure that sufficient fuel would be available. Due to the 300 nm range requirement, the two cruise segments were determined to be the most crucial in terms of fuel requirements. Of the two, the second cruise segment was found to be the most critical due primarily to the large headwinds that were specified. In fact, the 60 knot headwinds significantly increase the fuel requirement, so much so that pressurizing the cabin to enable flight at higher altitudes was given serious consideration. Due to a 20 knot reduction in headwind above 10000 feet the fuel requirements would reduce, however the additional weight and complexity that is associated with pressurizing the cabin were deemed to outweigh this benefit (particularly since a 500 foot ceiling was specified for the first cruise segment). Therefore based on this analysis, a fuel capacity of approximately 1710 lbs (256 US-gallons) was determined to be sufficient to account for all segments of the primary mission including warmup, takeoff, cruise, climb and hover.

13.3.2 – Cruise Maneuver Capability

In accordance with the RFP, the vehicle should be capable of a transient turn capability at cruise speed equal to a standard Rate 1 turn, which corresponds to a 30 degree bank turn (i.e. a load factor of 1.16). Therefore based on this requirement, the

Raven was determined to be capable of a maximum cruise speed of approximately 170 knots at sea level under ISA conditions (at its design gross weight). This estimate was determined by incorporating experimental data into the main rotor model to account for non-linear aerodynamic effects such as stall, reversed flow and drag divergence [Tish01]. With increasing altitude (i.e. decreasing density) stall will occur at lower speeds and hence the maximum cruise speed will decrease. Note that due to the lighter fuel and payload weights throughout the primary mission, the Raven was able to consistently cruise at high speed (between 160-165 knots) and still be able to successfully perform this maneuver.

Section 14 – System Affordability

The affordability of any new aircraft design is undoubtedly a critical factor in determining its potential to succeed or fail. It is therefore of great importance to ensure that a new design is affordable to not only purchase, but also to maintain and operate. In this section, the operational supportability and cost aspects of the design will be presented in order to demonstrate the overall system affordability of the Raven design.

14.1 – Operational Supportability

The operational supportability of a complex system such as a helicopter is a critical factor in determining mission readiness and system affordability. The Raven was developed to minimize supportability by being more efficient and less expensive to operate than existing SAR aircraft. This was achieved by focusing on improving component accessibility, reducing supportability resource requirements and developing an aircraft that could be supported by a streamlined maintenance system.

14.1.1 – Maintenance Design Features

The Raven incorporates a large number of innovative features to help minimize the maintenance requirements of potential operators. The salient design features include:

- *Non-load Bearing Skin Panels* – The airframe skin was designed to be non-load bearing so that access to the aircraft's interior could be optimized. The design consists of access panels, doors and drop down engine cowlings to make servicing the aircraft safer and easier, thereby minimizing mission preparation time. Approximately 50% of the Raven's skin is capable of being hinged or removed.
- *Remove & Replace Modular Avionics* – The aircraft employs a centralized modular avionics architecture with robust avionics modules installed in highly accessible and easily opened avionics bays.
- *Advanced Diagnostic & Prognostic System* – Maintenance diagnostics are simplified through the use of a Portable Intelligent Maintenance Aid (PIMA). The primary function of the unit will be to assist maintenance personnel in isolating aircraft faults and diagnosing problems. The unit will plug directly into the aircraft after each flight to assess system status, alert maintenance personnel to impending problems, and rapidly pinpoint and describe faults. The built-in diagnostic and prognostic subsystems (or HUMS) that the PIMA plugs into will eliminate the cost of separate test equipment and ensure fast maintenance turnarounds.
- *Built-in Maintenance Platforms* – The engine cowlings can double as maintenance platforms for servicing of the engines, APU, transmission and main rotor. These built-in work stations enable access to even the topmost parts of the aircraft without special equipment, such as ladders and stands.
- *Split-torque Transmission* – The aircraft employs a split-torque transmission which enhances transmission reliability and reduces repair times by elimination of complex planetary gearing.
- *Main Rotor Design* – The bearingless main rotor hub eliminates a significant number of components, bearings and seals, improving reliability and easing maintenance. The five bladed main rotor and trailing edge flaps also help to reduce aircraft vibration levels.

- *Fan-in-fin System* – The fan-in-fin system requires fewer gearboxes and a shorter drive train than conventional high mounted tail rotors. The fan assembly is also easily accessible from the ground and the shroud provides for a safer maintenance environment.
- *Keel Beam Structural Design* – The internal keel beam design reduces the numbers of fasteners and structural stiffeners that are required for the airframe, thereby increasing reliability and reducing maintenance requirements.

All of these features will serve to reduce support equipment requirements, manpower requirements and operating costs resulting in a significant improvement in system affordability.

14.2 –Cost Analysis

The Raven includes a large number of cost reduction features that enable it to minimize acquisition and operating costs. In this subsection the primary cost reduction features that were incorporated into the design will be identified, and an initial acquisition and operating cost estimate will be presented.

14.2.1 – Cost Reduction Features

The following features were integrated into the Raven design to ensure a cost effective and affordable design solution:

- *Simple Structural Design* – The primary load carrying keel beam design is simple to manufacture and the hybrid composite/metal airframe and composite main rotor reduces the overall number and variety of parts on the aircraft.
- *Low Risk Technology* – The design incorporates existing, growth or uprated versions of advanced proven technologies (such as the fan-in-fin, main rotor hub, transmission, etc.), significantly reducing development risks and unit costs whilst simultaneously increasing component reliability. Maximizing the use of existing technology will also help to offset the higher development costs associated with the implementation of an advanced swashplateless control system.
- *Easy Access* – All of the vehicles maintenance areas have been designed to be easily accessible without the use of special equipment by incorporating built-in maintenance platforms and a large number of access panels and doors.
- *Easy & Efficient Maintenance* – Aircraft maintenance procedures have been streamlined with an integrated electronic diagnostic and prognostic system combined with remove and replace modular avionics. A Health and Usage Monitoring System (HUMS) is also integrated into the design, enhancing maintenance predictability. All of these features significantly reduce operating costs by reducing the maintenance required per flight hour to one fourth of the time required by current helicopters [Tara98] and by facilitating fewer parts, tools and ground support equipment.
- *Future Growth* – The rotorcraft has been designed to exploit future growth opportunities (oversized undercarriage, maximum takeoff weight is greater than design gross weight, etc.) thereby minimizing future redesign, development, test, and certification, and making retrofit of product improvements easier and less costly.
- *Electric Technology* – The design primarily uses electric components that are generally more reliable and less maintenance intensive than hydraulic and pneumatic components, and can be integrated much more easily into the HUMS.

14.2.2 – Acquisition Cost

The manufacturing and acquisition cost estimates are primarily based upon trends in historical data. Two fundamental methods were used to estimate base purchase price:

1. *Harris and Scully method* [Harr97] – a price estimating relationship that is based upon a linear regression statistical analysis of approximately 120 rotorcraft. This relatively simple empirical relationship is a function of empty weight, installed power, number of rotor blades, engine type, engine number, number of main rotors and type of landing gear. This global method is suitable for use in the preliminary stages of a design due to the small number of inputs required.

2. *Bell Helicopter method* [Bell98] – a set of more detailed cost estimating relationships that are based upon historical cost data and use component weights, total production quantity and production rate as primary cost drivers. Additional variables are used to account for differences in manufacturing techniques and materials used. The original form of the relationships were modified and adjusted to more accurately reflect existing cost trends [Heli93] as well as to account for the manufacture of the new swashplateless technologies proposed. Since this method requires detailed component weight breakdowns as primary inputs, it is better suited to the later stages of a preliminary design.

The primary component manufacturing costs are displayed in Table 14.1 (all cost estimates are for the year 2000). Note that to generate year 2000 cost estimates an average inflation rate of approximately 2.2% was used, based on the changes in the consumer price index and gross domestic product implicit price deflator [Appl01].

Table 14.1 – Component Manufacturing Cost Breakdown

Component	Cost (US$)
Rotor system*	476881
Fuselage	523113
Engine installation	711089
Drive system	384719
Manufacturing Cost	**3106775**
Tooling Amortization & Profit	1242710
Base Price (US $ million)	**4.35**

14.2.3 – Operating Costs

According to the NASA Rotorcraft Economics Workshop held in 1996 [Lesl96], an aircraft's operating costs can be divided into two main categories: Direct Operating Costs (DOC's) and Indirect Operating Costs (IOC's). These costs can be broken down further as: *cash* DOC's (maintenance, flight crew, fuel and oil); *ownership* DOC's (depreciation, hull insurance, and finance); *aircraft related* IOC's (ground property, control and communications, ground handling, etc.); and *passenger related* IOC's (liability insurance, amenities, commissions, etc.). The DOC's are usually incurred per flight hour whereas the IOC's are generally independent of flying hours (it is however common practice to express IOC's as an annual cost). Also, given that the primary mission for the Raven is SAR, the IOC's will be dominated by the aircraft related expenses (most of the passenger related expenses are generally not incurred in SAR operations).

In preliminary design it is usually quite difficult to accurately determine aircraft operating expenses, due to the fact that much of the required data (such as crew costs, financing, insurance, etc.) is heavily dependent upon the individual operators. The only operating cost component that is usually quantifiable in the preliminary stages of a design is the fuel cost per flight hour, since this relies primarily upon knowledge of the aircraft's performance. Therefore with this in mind, a method was developed that is based primarily upon the historical data presented at the NASA Rotorcraft Economics Workshop. Using this method enabled the Raven's operating costs to be estimated (Table 14.2).

Table 14.2 – Operating Cost Breakdown

		Operating Cost	Estimate
DOC (94%)	Cash DOC (26%)	Fuel and oil (18%)	76.2 $/fh
		Flight crew (25%)	105.8 $/fh
		Maintenance (57%)	241.2 $/fh
		Cash DOC ($/fh)	**423.1**
	Ownership DOC (74%)	Depreciation (39%)	469.7
		Insurance (30%)	361.3
		Finance (31%)	373.3
		Ownership DOC ($/fh)	**1204.2**
IOC (6%)	**Aircraft related (94%)**	~	195282 $/yr
	Passenger related (6%)	~	12465 $/yr
		DOC ($/flight-hour)	**1627.4**
		IOC ($/year)	**207747**
Total operating costs (US $million/year)			**3.46**

The following information is applicable to the estimates contained in Table 14.2:

- The cost analysis was based upon the 600 nm range mission requirement defined in the RFP.
- Fuel costs vary considerably based on where the fuel is purchased geographically and whether it is purchased at retail price or in bulk. A cost of approximately 1.5 $/US-gal was used in this analysis, which is based on a combination of current

prices, the price defined by Leslie [Lesl96] and the average increase in fuel costs from 1996 to 2000.

- The DOC estimates were based on the data presented by Leslie [Lesl96]. In order to account for the advanced health monitoring, diagnostic and prognostic systems, the maintenance DOC's were reduced by approximately 25%.
- The breakdown of the maintenance DOC's is: engine (22%), on-condition maintenance (20%), scheduled retirement (5%), unscheduled maintenance (2%), scheduled overhaul (4%), and scheduled inspection (4%).
- The IOC estimates were based on the data presented by Scott [Scot96] – with modifications to account for the fact that the primary mission is SAR and not passenger transportation.
- The IOC and total operating costs were estimated by assuming an annual usage of approximately 2000 flight hours per aircraft, as stated in the RFP.

14.2.4 – Cost Comparison

To demonstrate the affordability of the Raven design proposal, the cost estimates were compared with existing rotorcraft of similar weight and performance (Table 14.3 - data taken from Jane's [Tayl00]).

Table 14.3 – Cost Comparison of Existing Rotorcraft

Parameter	TW258	412EP	BA609	EC135	A109K2	MD902
Gross weight (lb)	8330	11900	16000	6250	6283	6250
Fuel weight (lb)	1710	2209	2476	1182	1325	1078
Range (nm)	600	402	750	340	434	293
Cruise speed (kts)	160	122	275	138	143	134
Base price (US $ million)	4.35	5.23	9.00	4.79	3.45	2.66
Cash DOC (US $/fh)	423	756	773	448	412	460

This table clearly highlights the affordable and competitive nature of the TW258 design proposal. In fact the DOC is remarkably low for the high performance levels offered (due primarily to a reduction in maintenance costs), which should ensure its future success in a highly competitive marketplace. If "goodness" for a civil helicopter is defined as long term economic viability [Olso93], then the Raven is a great helicopter!

14.2.5 – Analysis Limitations

The methods employed to predict the Raven's acquisition and operating costs are primarily based upon historical trends and as a result have several inherent limitations. In the analysis carried out the impact of new advanced technologies (such as the swashplateless control system) and lean manufacturing techniques have not been directly captured, since they are not reflected in historical cost data. The software development costs, which are generally independent of aircraft weight, are also not explicitly included in the cost estimates. For an advanced technology rotorcraft with a glass cockpit, swashplateless rotor, digital flight control system and health-and-usage monitoring system, software development costs can potentially be high. And finally, the additional research and development costs involved with the proposed swashplateless control concepts have not been directly factored into the estimates, since they are extremely difficult to quantify at the preliminary design stage. However in the absence of a more detailed cost database, and prior to further concept definition in the detailed design stage, the economic model developed in this section was used to provide an initial estimate of the vehicles acquisition and operating costs.

Section 15 – Multimission Capability

Throughout this report the Raven has been demonstrated to be a highly effective SAR design solution. However the design attributes that enable it to perform so well in SAR missions, such as long range, large internal capacity, high speed and low operating costs, also serve to enhance its multimission capability. Due to the fact that acquisition cost is proportional to

production quantity, it makes economic sense to develop a vehicle that is capable of performing a wide variety of different missions. Therefore a brief selection of the alternative missions that the Raven is capable of performing are discussed below.

15.1 – Passenger/VIP Transport

The large cabin can accommodate up to 8 people, with a separate area in the rear fuselage for luggage, leaving an uncluttered interior. The high maximum takeoff weight allows for this additional payload without the need for an expensive redesign of the undercarriage and transmission. The Raven offers a high cruise speed combined with low levels of noise and vibration, whilst large access doors and low floor level allow for easy access and boarding. Furthermore, the inherently low operating costs of the Raven ensure a high level of operator satisfaction. A VIP layout is also available which takes full advantage of the spacious cabin interior by providing luxurious seating for 4 people.

15.2 – Emergency Medical Service

The high cruise speed, large cabin and long range make the Raven ideally suited to dedicated EMS missions. The cabin can be rapidly reequipped to accommodate multiple stretcher patients and more extensive medical equipment (to resemble a mini-operating theatre environment), whilst still providing ample working space for two medical attendants. Loading and unloading of patients and equipment is made easy by the large cabin doors on either side of the fuselage.

Figure 15.1 – VIP / Passenger / EMS Cabin Layouts

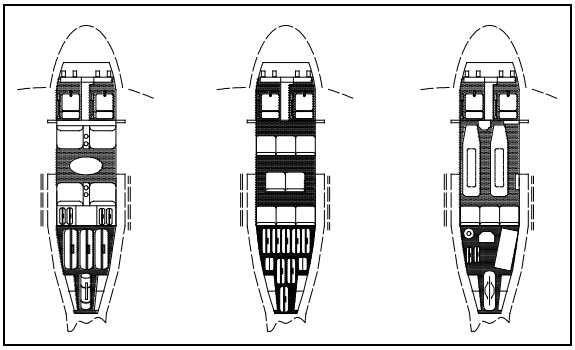

Section 16 – Conclusion

Our intention in this report has been to clearly demonstrate the thorough and systematic approach that was taken to develop the Raven SAR helicopter. The design, as presented, offers prospective customers a revolutionary rotor control system that is affordable, reliable and easy to maintain. Furthermore, the Raven is responsive to the unique demands of SAR operators by offering unsurpassed mission performance at an affordable price. Some of the more salient features of the design include:

- *Configuration* – the configuration was selected as a result of a comprehensive configuration trade study. This study concluded decisively that the pure helicopter was the most effective SAR design solution. Furthermore, a fan-in-fin anti-torque system was selected due to its inherent safety features and efficient performance in adverse weather conditions.
- *Swashplateless rotor* – the swashplateless control system incorporates torsionally soft main rotor blades with embedded trailing edge flaps that are actuated by magnetic shape memory alloys. This system was developed as the result of an extensive swashplateless control study that concluded in favor of embedded trailing edge moment flaps as the most cost effective and reliable swashplate replacement.
- *Crew station* – the crew station design optimizes cabin space and enhances situational awareness for demanding SAR missions, thereby enabling the crew to operate as efficiently as possible. The cabin and cockpit designs, which serve to reduce crew workload, were developed after extensive consultation with SAR pilots and pararescuers.
- *Flight control system* – the flight control system ensures a predictable response, enabling helicopter pilots to fly the vehicle without requiring special training. The system was developed to complement the unique swashplateless rotor and to ensure that optimum handling qualities were achieved.

The end result of this comprehensive design study is a vehicle that meets or exceeds all of the performance requirements and expectations specified in the RFP. The Raven provides an innovative SAR design solution in a safe and reliable package that is capable of meeting all of the demands of current and future customers well into the 21st century. Put simply, the Raven is the perfect helicopter for the perfect storm.

References

[Abbo58] – Abbot, I. H. and Von Doenhoff, A. E., *Theory of Wing Sections*, Dover Publications, New York, 1958.

[Adap01] – Adaptamat, *Adaptive Material Technologies*, http://www.adaptamat.com, 1st June, 2001.

[Alex86] – Alex, F. W. and McCoubrey, G. A., "Design and Structural Evaluation of the SH-2F Composite Main Rotor Blade", *Journal of the American Helicopter Society*, April, 1986, pp. 345-359.

[Amun01] – Amuneal Manufacturing Corporation, http://www.amuneal.com, 12th June, 2001.

[Anon96] – Anon, "Handling Qualities Requirements for Military Rotorcraft", *U.S. Army AMCOM Aeronautical Design Standard - ADS-33E-PRF*, May, 1996.

[Appl01] – Applied Reasoning, *The Financial Forecast* Center, http://www.neatideas.com/info/inflation.htm, 3rd April, 2001.

[Bell01] – Bell Helicopter Textron, *Bell Helicopter Textron*, http://www.bellhelicopter.com, 1st June, 2001.

[Bell98] – Bell Helicopter Textron, "16th Annual Student Design Competition Request For Proposal", *American Helicopter Society International*, 1998.

[Bern00] – Bernhard, A., "Smart Helicopter Rotor with Active Blade Tips (SABT)", *Ph.D. Dissertation, Aerospace Engineering, University of Maryland*, College Park, March 2000.

[Bocz99] – Boczar, B., Borgstrom, D., and Everett, P., "Key Aspects and Attributes of the RAH-66 Comanche Flight Control System", *Proceedings of the 55th Annual American Helicopter Society Forum*, Montreal, Canada, 25-27 May, 1999.

[Bous83] – Bousman, W. G. and Ormiston, R. A., "Design Considerations for Bearingless Rotor Hubs", *Proceedings of the 39th Annual American Helicopter Society Forum,* May, 1983, pp. 509-536.

[Bree01] – Breeze-Eastern, "Breeze-Eastern: Helicopter Rescue Hoists, Cargo Hooks & Winches", http://www.breeze-eastern.com, 20th April, 2001.

[Chen96] – Chen, P. C., "Development of a Smart Rotor with Induced-Strain Actuation of Blade Twist", *Ph.D. Dissertation, Department of Aerospace Engineering*, University of Maryland, College Park, 1996.

[Chop92] – Chopra, I., "Smart Structures Technology: Innovations and Applications to Rotorcraft Systems", *Smart Structures URI Progress Report to ARO Contract DAAL03-92-G-0121*, 1992.

[Chop00] – Chopra, I., "Status of Application of Smart Structure Technology to Rotorcraft Systems", *Journal of the American Helicopter Society*, October, 2001, pp. 228-252.

[Chop01] – Chopra, I., "Review of State-of-Art of Smart Structures and Integrated Systems", *42nd AIAA/ASME/ASCE/AHS/ASC Structures, Structural Dynamics and Materials Conference*, Seattle, WA, 16-19 April, 2001.

[Clem92] – Clemmons, M. G., "Antitorque Safety and the RAH-66 Fantail", *Proceedings of the 48th Annual American Helicopter Society Forum*, June, 1992, pp. 169-175.

[Curr88] – Currey, N. S., *Aircraft Landing Gear Design: Principles and Practices,* AIAA Education Series, Reston, VA, 1988.

[Dudl54] – Dudley, D. W., *Practical Gear Design*, General Electric Company, 1954.

[Desj91] – Desjardins, R. A., Noehren, W. L., and Bertolazzi, A. N., "Design and Flight Test Evaluation of the Fantail Antitorque System", *Proceedings of the 47th Annual American Helicopter Society Forum*, May, 1991, pp. 857-867.

[DeTo91] – DeTore, J. and Conway, S., "Technology Needs for High Speed Rotorcraft (3)", *NASA Contractor Report 177592* –

Bell Helicopter Textron, Fort Worth, Texas, October, 1991.

[Done00] – Dones, F., Dryfoos, J., McCorvey, D., and Hindson, W., "An Advanced Fly-By-Wire Flight Control System Designed for Airborne Research – Concept to Reality", *Proceedings of the 56th Annual American Helicopter Society Forum*, 2-4 May, 2000.

[Fall01] – Fallon, M., "Flying Qualities Engineer / CH-46 Pilot", NAVAIR – *private communication*, March – May, 2001.

[Feld00] – Feld, W. M., *Lean Manufacturing: Tools, Techniques, and How to Use Them - APICS Series on Resource Management*, St. Lucie Press, 2000.

[Fink00] – Fink, D. A., Hawkey, T. J., and Gaudreau, M. P. J., "An Electromagnetic Actuator for Individual Blade Control", *Proceedings of the 56th Annual American Helicopter Society Forum*, May 2-4, 2000.

[Flir01] – Flir Systems, *Flir Systems*, http://www.flir.com, 4th April, 2001.

[Garf75] – Garfinkle, M., "Directional Control System for Helicopters", *United States Patent No. 3,921,939*, 25th November, 1975.

[Guar01] – Guardiano, J. R., "Coast Guard Jayhawk Crew Executes the Perfect Rescue", *Rotor & Wing*, February 2001, p. 10.

[Harr97] – Harris, F. D. and Scully, M. P., "Helicopters Cost Too Much", *Proceedings of the 53rd Annual American Helicopter Society Forum*, April, 1997, pp. 1575-1608.

[Heli93] – HeliBooks, *Helicopter Equipment Lists and Prices (HELP) – Volume III, Edition 1*, Helibooks Ltd. Illinois, 1993.

[Hirs01] – Hirschberg, M., "On The Vertical Horizon: IHPTET - Power for the Future", http://www.vtol.org/IHPTET.HTM, 8th June, 2001.

[Hone01] – Honeywell, Inc., "Honeywell BCAS: Primus 800", http://www.cas.honeywell.com/bcas/products/primus_880_environment.cfm, 29th April, 2001.

[Idle01] – Idleman, C., "Marketing Manager, Breeze-Eastern", *private communication*, 25th - 30th, May, 2001.

[Jile00] – Jiles, D., *Introduction to Magnetism and Magnetic Materials – 2nd Edition*, Chapman and Hall, 2000.

[John01] – Johnson, B., "Human Factors Engineer, Crew Station Analysis and Design", NAVAIR – private communication, May, 2001.

[John80] – Johnson, W., *Helicopter Theory*, Dover Publications, New York, 1980.

[Kasj91] – Kasjanikov, V. A., "Kamov Ka-62 – The New Soviet Helicopter for the 1990's", *Vertiflite*, September/October, 1991, pp. 54-58.

[Keys91] – Keys, C., Sheffler, M., Weiner, S., and Heminway, R., "LH Wind Tunnel Testing: Key to Advanced Aerodynamic Design", *Proceedings of the 47th Annual American Helicopter Society Forum*, May, 1991, pp. 77-87.

[Kish78] – Kish, J., "Advanced Overrunning Clutch Technology", *Society of Automotive Engineers - Technical Report 781039*, November, 1978.

[Kora00] – Koratkar, N. A., and Chopra, I., "Wind Tunnel Testing of a Mach-scaled Rotor Model with Trailing Edge Flaps", *Proceedings of the 56th Annual American Helicopter Society Forum*, Virginia Beach, VA, May 2-4, 2000.

[Kuma97] – Kumagai, H. and Deardon, J. D., "Contactless Magnetic Slip Ring", *United States Patent No. 5,691,687*, Nov25, 1997.

[Lee98] – Lee, T. and Chopra, I., "Design and Testing of a Trailing Edge Flap Actuator with a Piezostack for a Rotor Blade",

SPIE Conference on Smart Structures and Intelligent Systems Vol. 3329, March, 1998.

[Leis00] – Leishman, J. G., *Principles of Helicopter Aerodynamics*, Cambridge University Press, New York, 2000.

[Lesl96] – Leslie, P., "Short Haul Civil Tiltrotor and Bell Model 412 Cost Drivers", *NASA / Industry / Operator Rotorcraft Economics Workshop – NASA Ames Research Center*, Moffett Field, CA, May 1996.

[Life01] – Life Support International, "Search & Rescue Equipment", http://www.lifesupportintl.com/, 20th April, 2001.

[Lord01] – Lord Corporation, http://www.lord.com, 1st June, 2001.

[Lynn69] – Lynn, R. R., Robinson, F. D., Batra, N. N., and Duhon, J. M., "Tail Rotor Design Part I – Aerodynamics", *Proceedings of the 25th Annual American Helicopter Society Forum*, May, 1969.

[Mart01] – Martin-Baker Aircraft Company Limited, "Martin-Baker Aircraft Company – Utility Seat", http://www.martin-baker.com/utilseat.html, 2nd April, 2001.

[Matt84] – Matthys, C. G. and Scroggs, E. E., "Technology Impact on Helicopter, Tilt Rotor, and Tilt Fold Rotor Concepts", *Proceedings of the 40th Annual American Helicopter Society Forum*, 1984, pp. 229-236.

[McMa01] – McMaster - Carr Supply Company, http://www.mcmaster.com, 1st June, 2001.

[Mich71] – Michaelson, O. E., "Comparison of Outflows from a Helicopter, Tilt Wing and Jet Lift Hovering Aircraft", *Canadair/General Dynamics - AIAA Paper Number 71-992*, 1971.

[Mide01] – Mide Technology Corporation, http://www.mide.com/expertise/matsys/compare.html, 1st June, 2001.

[Moui86] – Mouille, R. and d'Ambra, F., "The Fenestron – a Shrouded Tail Rotor Concept for Helicopters", *Proceedings of the 38th Annual American Helicopter Society Forum*, May, 1986, pp. 597-606.

[Moui75] – Mouille, R., "New Concepts for Helicopter Main Rotors", *Proceedings of the 39th American Helicopter Society Forum*, May, 1975, pp 1-8.

[Naka01] – Nakadate, M., Taguchi, H., and Takakim, J., "Design and Test Evaluation of FBR Bearingless Main Rotor", *Journal of The American Helicopter Society*, April, 2001, pp 107-116.

[Niwa98] – Niwa, Y., "The Development of the New Observation Helicopter (XOH-1)", *Proceedings of the 54th American Helicopter Society Forum*, May, 1998, pp. 1285-1297.

[Olso93] – Olson, J. R., "Reducing Helicopter Operating Costs", *Vertiflite*, Jan/Feb, 1993, pp. 10-16.

[Ormi01] – Ormiston, R. A., "Aeroelastic Considerations for Rotorcraft Primary Control with On Blade Elevons", *Proceedings of the 57th Annual American Helicopter Society Forum*, May, 2001.

[Padf96] – Padfield, G. D., *Helicopter Flight Dynamics: The Theory and Application of Flying Qualities and Simulation Modeling*, AIAA, Washington, D.C., 1996.

[Pago01] – Pagounis, E., "Adaptamat", *Private Communication*, 18th May, 2001.

[Paul01] – Paulstra-Vibrachoc, *Vibration and Shock Handbook*, France, 1st June, 2001.

[Prec98] – Prechtl, E. F. and Hall, S. R., "An X-Frame Actuator Servo-Flap Actuation System for Rotor Control", *SPIE Conference on Smart Structures and Intelligent Systems, Vol. 3329*, March, 1998.

[Prou95] – Prouty, R. W., *Helicopter Performance, Stability, and Control*, Krieger Publishing Company, Florida, 1995.

[Raym00] – Raymer, D. P., *Aircraft Design: A Conceptual Approach - Third Edition*, AIAA Education Series, Washington D.C.,

2000.

[Reis86] – Reisdorfer, D. and Thomas, M. L., "Static Test and Flight Test of the Army/Bell ACAP Helicopter", *Proceedings of the 42nd Annual American Helicopter Society Forum*, June, 1986, pp. 865-872.

[Rocc01] – Rocconella, B. and Wei, F., "Wind Tunnel Model Testing of the Improved K-MAX Servo-Flap Blade Section", *Proceedings of the 57th Annual American Helicopter Society Forum*, May, 2001.

[Roge98] – Rogers, J. P., and Hagood, N. W., "Development of an Integral Twist-Actuated Rotor Blade for Individual Blade Control", *MIT AMSL 98-6*, October, 1998.

[Roge01] – Roget, B. and Chopra, I., "Trailing-Edge Flap Control Methodology for Vibration Reduction of Helicopter with Dissimilar Blades", *Proceedings of the 42nd AIAA/ASME/AHS Adaptive Structures Forum*, Seattle, WA, April 16-18, 2001.

[Rosk90] – Roskam, J., *Part VIII: Airplane Cost Estimation: Design, Development, Manufacturing and Operating*, Roskam Aviation, Kansas, 1990.

[Ruth91] – Rutherford, J., O'Rourke, M., Martin, C., Lovenguth, M., and Mitchell, C., "Technology Needs for High Speed Rotorcraft", *NASA Contractor Report 177578 – McDonnell Douglas Helicopter Company*, Mesa, Arizona, April, 1991.

[Scha67] – Schane, M. C., "Effect of Downwash on Man", *US Army Aeromedical Research Unit – Report Number 68-3 USAARV*, 1967.

[Scot96] – Scott, M. W., "Economic Analysis of SHCT Tiltrotor", *NASA / Industry / Operator Rotorcraft Economics Workshop – NASA Ames Research Center*, Moffett Field, California, May, 1996.

[Scot91] – Scott, M. W., "Technology Needs for High Speed Rotorcraft (2)", *NASA Contractor Report 177590 – SikorskyAircraft*, Connecticut, August, 1991.

[Shen00] – Shen, J., and Chopra, I., "Aeroelastic Modeling of Trailing-Edge Flaps with Smart Material Actuators", *Proceedings of the 41st Structures, Structural Dynamics and Materials Conference and Adaptive Structures Forum*, Atlanta, GA, April 3-6, 2000.

[Shen01] – Shen, J. and Chopra, I., "Aeroelastic Stability of Smart Trailing-Edge Flap Helicopter Rotors", *Proceedings of the 42nd Structures, Structural Dynamics and Materials Conference and Adaptive Structures Forum*, Seattle, WA, April 16-19, 2001.

[Shin84] – Shinn, R. A., "Impact of Emerging Technology on the Weight of Future Rotorcraft", *Proceedings of the 40th Annual American Helicopter Society Forum*, 1984, pp. 219-227.

[Sima01] – Simard, P., Ferrie, F. P., Link, N. K., and Kruk, R., "Synthetic Vision System for Search and Rescue Helicopters", http://www.cim.mcgill.ca/research/1999AnnualReport/html/node70.html, 16th June, 2001.

[Siro01] – Sirohi, J. and I. Chopra., "Development of Piezoelectric Hydraulic Hybrid Actuators", *SPIE Conference on Smart Structures and Intelligent Systems*, March, 2001.

[Spec01] – Spectrolab, Inc., "Spectrolab Products – SX-16 Nightsun with Infrared In-Flight Changeover", http://www.spectrolab.com/prd/prd.htm, Sylmar, California, 2001.

[Spen98] – Spencer, M. G., Sanner, R. M., Chopra, I., "Development of Neural Network Controller for Smart Structure Activated Rotor Blades", *Proceedings of the 39th AIAA/ASME/ASCE/AHS/ASC Structures, Structural Dynamics and Materials Conference and AIAA/ASME/AHS Adaptive Structures Forum*, Longbeach, CA, April 1998.

[Spen00] – Spencer, M. G., "Development of a Real Time Adaptive Neural Network Controller for Active Rotorcraft Vibration Reduction", *Ph.D. Dissertation, Department of Aerospace Engineering*, University of Maryland, May, 2000.

[Step84] – Stepniewski, W. Z. and Keys, C. N., *Rotary-Wing Aerodynamics*, Dover Publications, New York. 1984.

[Stra95] – Straub, F. K., "A Feasibility Study of Using Smart Materials for Rotorcraft", *Journal of Smart Materials and Structures, Volume 5*, 1995, pp. 1-10.

[Stra99] – Straub, F. K. and Charles, B. D., "Aeroelastic Analysis of Rotors with Trailing-Edge Flaps Using Comprehensive Codes", *Proceedings of the 55th Annual American Helicopter Society Forum*, Montreal, Canada, May 25-27, 1999.

[Tara98] – Tarascio, M. J., "An Advanced Rotorcraft Design Concept for Project Air 87 – Volume Two", *RMIT University Undergraduate Thesis*, Melbourne, Australia, 1998.

[Tayl00] – Taylor, J. W. R., *Jane's All The World Aircraft – 2000/2001*, Jane's Publishing Company, London, England, 2000.

[Tisc96] – Tischler, M. B., *Advances in Aircraft Flight Control*, Taylor and Frances, Philadelphia, Pennsylvania, 1996.

[Tish01] – Tishchenko, M. N. and Nagaraj, V. T., *ENAE 634 Helicopter Design Lecture Notes*, University of Maryland, College Park, 2001.

[Toma99] – Tomashofski, C. and Tischler, M., "Flight Test Identification of SH-2G Dynamics in Support of Digital Flight Control System Development", *Presented at the 55th Annual American Helicopter Society Forum*, May, 1999.

[TREC64] – TRECOM, "Downwash Impingement Criteria for VTOL Aircraft", *US Army Transportation Research Command – TRECOM Report 64*-48, 1964.

[Unsw84] – Unsworth, D. K. and Sutton, J. G., "An Assessment of the Impact of Technology on VTOL Weight Prediction", *Proceedings of the 40th Annual American Helicopter Society Forum*, 1984, pp. 253-262.

[Vuil86] – Vuillet, A. and Morelli, F., "New Aerodynamic Design of the Fenestron for Improved Performance", *Proceedings of the 12th European Rotorcraft Forum*, September, 1986.

[Vuil89] – Vuillet, A., "Operational Advantages and Power Efficiency of the Fenestron as Compared to a Conventional Tail Rotor", *Vertiflite*, July/August, 1989, pp. 24-29.

[Wang99] – Wang, B., "A Computational Study of Trailing-Edge Flap Aerodynamics and Acoustics", *Master of Science Thesis, Department of Aerospace Engineering, University of Maryland*, College Park, June, 1999.

[Whit98] – White, G., "Design Study of a Split-Torque Helicopter Transmission", *Proceedings of the Institution of Mechanical Engineering*, Volume 212, Number G2. 1998.

[Wrig91] – Wright, G. P., Driscoll, J. T., and Nickerson, J. D., "Handling Qualities of the H-76 Fantail Demonstrator", *Proceedings of the 47th Annual American Helicopter Society Forum*, May, 1991, pp. 123-135.

MIL-STD-1374 Weight Breakdown

MIL-STD-1374 PART I – TAB
NAME: UMD
DATE: 22 JUNE 2001

PAGE: 1
MODEL: Raven
REPORT

GROUP WEIGHT STATEMENT

AIRCRAFT

(INCLUDING ROTORCRAFT)

ESTIMATED – CALCULATED - ACTUAL

CONTRACT NUMBER	N/A
AIRCRAFT GOVERNMENT NO.	N/A
AIRCRAFT CONTRACTOR NO.	N/A
MANUFACTURED BY	N/A

	MAIN	AUX
ENGINE QUANTITY	2	
ENGINE MANUFACTURED BY	N/A	N/A
ENGINE MODEL	N/A	N/A
ENGINE TYPE	N/A	N/A

PROPELLER QUANTITY	N/A
PROPELLER MANUFACTURED BY	N/A
PROPELLER MODEL	N/A

PAGES REMOVED — PAGE NO.
NONE

MIL-STD-1374 PART I – TAB
NAME: UMD
DATE: 22 JUNE 2001

PAGE: 2
MODEL: Raven
REPORT

1	WING GROUP						
2	BASIC STRUCTURE - CENTER SECTION						
3	- INTERMEDIATE PANEL						
4	- OUTER PANEL						
5	- GLOVE						
6	SECONDARY STRUCTURE						
7	AILERONS – INCL. BALANCE WEIGHT						
8	FLAPS - TRAILING EDGE						
9	- LEADING EDGE						
10	SLATS						
11	SPOILERS						
12							
13							
14	ROTOR GROUP						(433.4)
15	BLADE ASSEMBLY					256.2	
16	HUB AND HINGE					177.2	
17							
18	EMPENNAGE GROUP						(124.7)
19	BASIC STRUCTURE					43.3	
20	SECONDARY STRUCTURE						
21	CONTROL SURFACES						
22	BLADES					14.1	
23	HUB & HINGE					67.3	
24	ROTOR / FAN DUCT & ROTOR SUPTS						
25							
26							
27	FUSELAGE GROUP	(NOTE: INCLUDES CRASHWORTHINESS FEATURES)					(814.2)
28	BASIC STRUCTURE					814.2	
29	SECONDARY STRUCTURE						
30	ENCLOSURES, FLOORING, ETC.						
31	DOORS, RAMPS, PANELS & MISC.						
32							
33							
34	ALIGHTING GEAR GROUP - TYPE						(225.7)
35	LOCATION						
36	MAIN					180.5	
37	NOSE/TAIL					45.2	
38	ARRESTING GEAR						
39	CATAPULTING GEAR						
40							
41							
42	ENGINE SECTION OR NACELLE GROUP						(37.7)
43	BODY - INTERNAL					37.7	
44	- EXTERNAL						
45	WING - INTERNAL						
46	- EXTERNAL						
47							
48							
49	AIR INDUCTION GROUP	(NOTE: INCLUDED IN NACELLE GROUP ABOVE)					
50	DUCTS						
51	RAMPS, FLOGS, SPIKES						
52	DOORS, PANELS, MISC						
53							
54							
55							
56							
57	TOTAL STRUCTURE						1635.7

MIL-STD-1374 PART I – TAB
NAME: UMD
DATE: 22 JUNE 2001

PAGE: 3
MODEL: Raven
REPORT

58	PROPULSION GROUP						(608.2)
59	ENGINE					415.9	
60	ENGINE INSTALLATION					45.8	
61							
62	ACCESSORY GEAR BOXES & DRIVE					77.2	
63	EXHAUST SYSTEMS						
64	ENGINE COOLING						
65	WATER INJECTION						
66	ENGINE CONTROLS						
67	STARTING SYSTEM						
68	PROPELLER INSTALLATION						
69	SMOKE ABATEMENT						
70	LUBRICATING SYSTEM						
71	FUEL SYSTEM					69.3	
72	TANKS – PROTECTED						
73	TANKS – UNPROTECTED						
74	PLUMBING						
75							
76	DRIVE SYSTEM						(374.2)
77	GEARBOXES, LUB SYS & ROTOR BRK					351.4	
78	TRANSMISSION DRIVE					22.8	
79	ROTOR SHAFTS						
80							
81	FLIGHT CONTROLS GROUP						(232.9)
82	COCKPIT CONTROLS					10.9	
83	SYSTEMS CONTROLS					76.0	
84	AUTOMATIC FLIGHT CONTROL SYSTEM					146.0	
85							
86	AUXILIARY POWER PLANT GROUP						(88.6)
87	INSTRUMENTS GROUP						(29.1)
88	HYDRAULIC & PNEUMATIC GROUP						(57.0)
89							
90	ELECTRICAL GROUP						(159.2)
91							
92	AVIONICS GROUP						(650.0)
93	EQUIPMENT						
94	INSTALLATION						
95							
96	ARMAMENT GROUP						
97	FURNISHINGS & EQUIPMENT GROUP						(1135)
98	ACCOMMODATION FOR PERSONNEL					134.4	
99	MISCELLANEOUS EQUIPMENT					460.9	
100	EMERGENCY EQUIPMENT					539.7	
101							
102							
103	AIR CONDITIONING GROUP						(56.8)
104	ANTI-ICING GROUP						(30.0)
105							
106	PHOTOGRAPHIC GROUP						
107	LOAD & HANDLING GROUP						(36.5)
108	AIRCRAFT HANDLING						
109	LOADING HANDLING						
110	BALLAST						
111	MANUFACTURING VARIATION	(NOTE: INCLUDES 3% WEIGHT GROWTH)					(155.9)
112	TOTAL CONTRACTOR CONTROLLED						
113	TOTAL GFAI						
114	TOTAL WEIGHT EMPTY (PAGES 2 & 3)						5249.1

MIL-STD-1374 PART I – TAB
NAME: UMD
DATE: 22 JUNE 2001

PAGE: 4
MODEL: Raven
REPORT

115	LOAD CONDITION						
116							
117	CREW (NO. 4)						(800.0)
118	PASSENGERS (NO. 2)						(380.0)
119	FUEL LOCATION TYPE						(1735.9)
120	UNUSABLE JP-4					25.9	
121	INTERNAL JP-4					1710.0	
122							
123							
124							
125							
126							
127							
128	OIL						(78.6)
129	TRAPPED					13.0	
130	ENGINE					65.6	
131							
132	FUEL TANKS (LOCATION)						
133	WATER INJECTION FLUID (GALS)						
134							
135	BAGGAGE	NOTE: ALL BAGGAGE AND CARGO INCLUDED IN EMERGENCY EQUIPMENT					
136	CARGO						
137							
138	GUN INSTALLATIONS						
139	GUNS LOC FIX. OR FLEX. QTY CAL.						
140	AMMO						
141	SUPPORTS*						
142							
143	CHAFF (QTY)						
144	FLARES (QTY)						
145							
146	WEAPONS INSTALL **						
147							
148							
149							
150							
151							
152							
153							
154							
155							
156	SURVIVAL KITS						
157	LIFE RAFTS						
158	OXYGEN						
159	MISC.						
160	INTERNAL NOISE RED. TREATMENTS						(86.8)
161							
162							
163							
164							
165							
166							
167							
168							
169	TOTAL USEFUL LOAD						3081.3
170	WEIGHT EMPTY						5249.1
171	GROSS WEIGHT						8330.4

* IF REMOVABLE AND SPECIFIED AS USEFUL LOAD

** LIST STORES, MISSILES, SONOBUOYS, ETC. AND PYLONS, RACKS, LAUNCHERS, CHUTES, ETC. THAT ARE NOT PART OF WEIGHT EMPTY. LIST NOMENCLATURE, LOCATION, AND QUANTITY FOR ALL ITEMS SHOWN INCLUDING INSTALLATION.

NOTE: THE EMPTY WEIGHT AND THE USEFUL LOAD PRESENTED HEREIN DIFFER FROM THOSE PRESENTED IN SECTION 12 OF THIS DOCUMENT DUE TO DIFFERENCES IN THE CLASSIFICATION OF THE COMPONENTS. FOR EXAMPLE, THE MISSION EQUIPMENT PACKAGE IS PRESENTED HERE AS PART OF THE EMPTY WEIGHT.

Table 3.1 – Candidate Configurations

 **Conventional**	 **NOTAR**	 **Fenestron**
 **Vectored Thrust Ducted Propeller (VTDP)**	 **Tandem**	 **Compound**
 **Coaxial**	 **Advancing Blade Concept (ABC)**	 **Reaction drive**
 **Synchropter**	 **Tiltrotor**	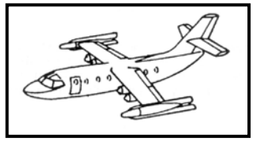 **Folding tiltrotor**
 **Tiltwing**	 **Canard Rotor Wing (CRW)**	 **Verticraft**

Table 3.3 – Configuration Evaluation Matrix

Evaluation Criteria	WEIGHTING	Conventional[1]	NOTAR[2]	Fan-in-fin[2]	VDR[3]	Tandem	Compound[4]	VTDP[5]	Coaxial	ABC[6]	Reaction drive	Synchropter	Tiltrotor	VDTR[7]	Folding tiltrotor	Tiltwing	CRW[8]	Verticraft
Compact design	**1**	2	2	2	2	1	2	2	2.5	3	2	2.5	1	1	1	1	2	2
High speed cruise	**2**	1	1	1	1.5	1	2	2	1	1.5	1	1	3	3	3	3	3	3
Range	**3**	2	2	2	2	2	2.5	2.5	2	2	1	2	3	3	3	3	3	3
Endurance	**3**	2	2	2	2	2	2	1.5	2	2	1	2	3	3	3	3	3	3
Crosswind performance	**3**	1.5	1	2	1.5	2.5	1.5	2	2.5	2.5	1.5	2.5	1	1	1	1	1.5	1.5
Hover efficiency (PL)[9]	**2**	3	3	3	3	2.5	2	1	3	3	1	3	1	2	1	1	1	1.5
Hover downwash (DL)[10]	**3**	3	3	3	3	3	2	2	3	3	3	3	1	2	1	1	3	2.5
CG range	**2**	1	1	1	1	3	1	2	1	1	1	1.5	2	2	2	2	1	1
Operational safety	**3**	1	3	3	1	2	1	3	3	3	2.5	1	2	2	2	2	2	2
Handling qualities (VTOL)	**3**	3	3	3	3	2.5	2.5	2.5	2.5	2.5	1.5	2.5	2	2	2	1.5	1.5	1.5
Affordability	**2**	3	3	3	2	2.5	2	2	2.5	1.5	1	2.5	1.5	1	1	1.5	1	1
Design complexity	**3**	3	3	3	1.5	2.5	2	1.5	2	1.5	1	2.5	1.5	1	1	1	1	1
Acoustic signature	**1**	2	3	2.5	2	2	2	2.5	2	2	1	2	2	2	2	2	1	2
Internal volume	**3**	2	2	2	2	2.5	2	2	2	2	2	2	2.5	2.5	2.5	2	2	2
Swashplateless technology	**1**	3	3	3	1	2	3	3	1.5	1.5	1	2	1.5	1	1	1.5	1	1
Multimission capability	**1**	2	2	2	2	1.5	2.5	2.5	2	2	1	1.5	2	2.5	2	2	2	2
TOTAL	**108**	77.5	83	85.5	70	81.5	70	75	80	78	53.5	76.5	69.5	72	66.5	65	69	69.5
RANKING	**~**	**6**	**2**	**1**	**11**	**3**	**10**	**8**	**4**	**5**	**17**	**7**	**12**	**9**	**15**	**16**	**14**	**13**

[1] – Single main rotor / tail rotor configuration (SMRTR)
[2] – Single main rotor configuration
[3] – Variable Diameter Rotor (VDR) – SMRTR
[4] – SMRTR with open pusher propeller and wing
[5] – Vectored Thrust Ducted Propeller (VTDP) - SMRTR
[6] – Advancing Blade Concept (ABC)
[7] – Variable Diameter Tiltrotor (VDTR)
[8] – Canard Rotor Wing (CRW)
[9] – Power Loading (PL)
[10] – Disk Loading (DL)

Section 4 – Raven Design Features and Performance Summary

The primary design features and performance specifications of the Raven are summarized and presented in this section. The general design specifications are displayed in Table 4.1. An inboard profile diagram showing the general arrangement of the major subsystems is displayed in Figure 4.1. A three view diagram of the final configuration is displayed in Foldout 4.1.

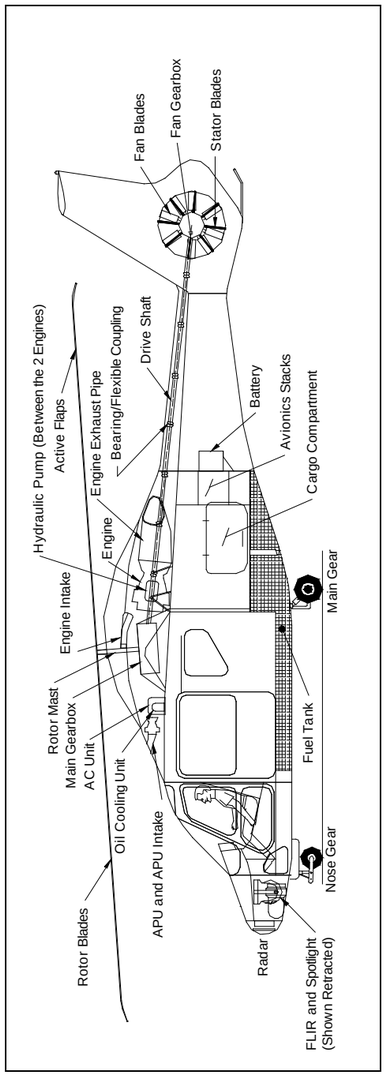

Figure 4.1 – Inboard Profile Diagram

Table 4.1 – General Design Specifications

General Details	
Designation	TW-258 Raven
Type	Twin turboshaft SAR helicopter
Accommodation	4 crew / 2 passengers
Acquisition cost	US $ 4.35 million (2000)
Direct operating cost[1]	US $ 423 per flight hour (2000)

Weights & Loadings	
Design gross weight	8330 lb (3778 kg)
Maximum takeoff weight	8680 lb (3937 kg)
Empty weight	4323 lb (1961 kg)
Fuel weight	1710 lb (776 kg)
Payload weight[2]	1432 lb (650 kg)
Disk loading, maximum	7.1 lb/ft^2 (34.7 kg/m^2)
Main Rotor Specifications	
Diameter	39.2 ft (11.9 m)
Number of blades	5
Chord	1.08 ft (0.329 m)
Tip speed[3]	695 – 725 ft/s (212 – 221 m/s)
Twist	-12.5 deg (linear)
Sweep (leading edge)	25 deg (from 90% radius)
Anhedral	8 deg (from 95% radius)
Shaft tilt	4 deg (forward)
Root cutout	30%
Airfoil sections	RAE9648 (root - 60%) VR-12 (60% - 90%) SSC-A09 (90% - tip)
Fan-in-fin Specifications	
Diameter	3.7 ft (1.1 m)
Number of blades	8
Blade chord	0.39 ft (0.12 m)
Rotational speed	3320 RPM
Twist	-7 deg
Blade spacing	35/55 deg
Root cutout	38%
Airfoil sections	OAF102 / OAF117 / OAF128

Performance Specifications	
Nominal cruise speed (@ 500ft)	160 knots (296 km/hr)
Maximum cruise speed (@ SL)	170 knots (315 km/hr)
HOGE ceiling[4]	12730 ft (3880 m)
HIGE ceiling[4]	15327 ft (4672 m)
OEI, HOGE ceiling[5]	4224 ft (1287 m)
VROC[4], maximum	3071 ft/min (936 m/min)
Climb rate[6], maximum	2900 ft/min (884 m/min)
Range[7], maximum	776 nm (1437 km)
Endurance[8], maximum	5.7 hrs
Engine Specifications	
Number of engines	2
Emergency power	1082 hp (807 kW)
Takeoff power	866 hp (646 kW)
Intermediate rated power	800 hp (597 kW)
Maximum continuous power	685 hp (511 kW)
Dimensions	
Length (overall, rotors turning)	44.5 ft (13.6 m)
Height (overall)	13.9 ft (4.24 m)
Fuselage width (maximum)	6.5 ft (1.98 m)
Horizontal stabilizer span	6.5 ft (1.98 m)
Wheelbase	24.1 ft (7.34 m)
Wheeltrack	6.4 ft (1.95 m)
Cabin width (maximum, internal)	5.5 ft (1.68 m)
Cabin length (internal)	8.9 ft (2.71 m)
Cabin height (internal)	5.7 ft (1.74 m)
Cargo compartment volume	130 ft^3 (3.68 m^3)
Cabin door height	5.1 ft (1.55 m)
Cabin door width	4.5 ft (1.37 m)

[1] – Direct operating costs include fuel, flight crew and maintenance only.
[2] – Including MEP weight
[3] – Hover and cruise setting
[4] – ISA, takeoff power
[5] – ISA, emergency power
[6] – ISA, maximum continuous power
[7] – Standard reserves at 500 ft PA, ISA+15°C
[8] – Standard reserves at 500 ft PA, ISA

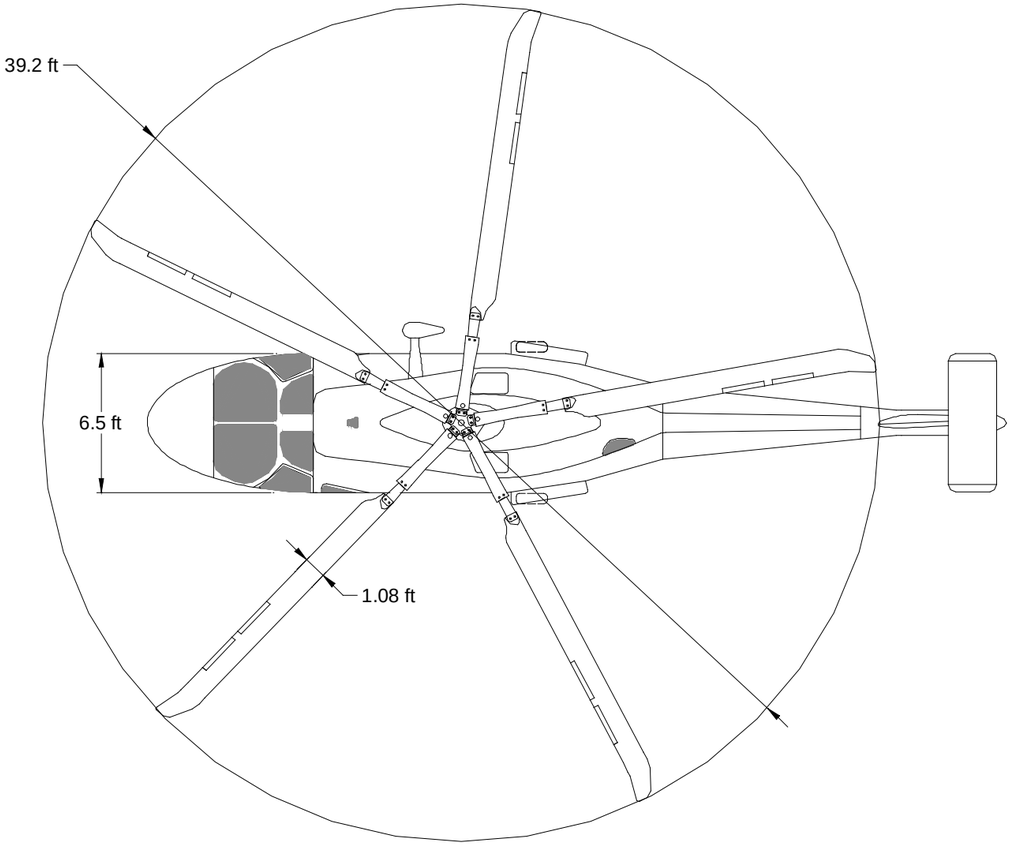

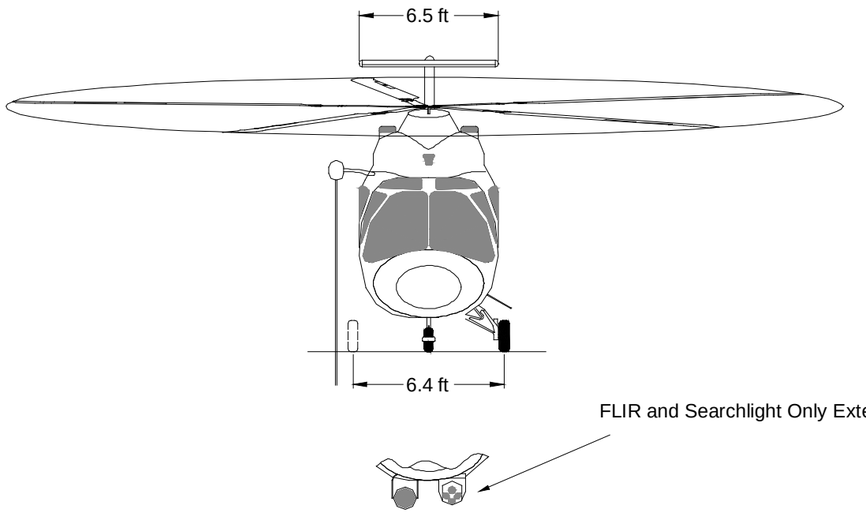

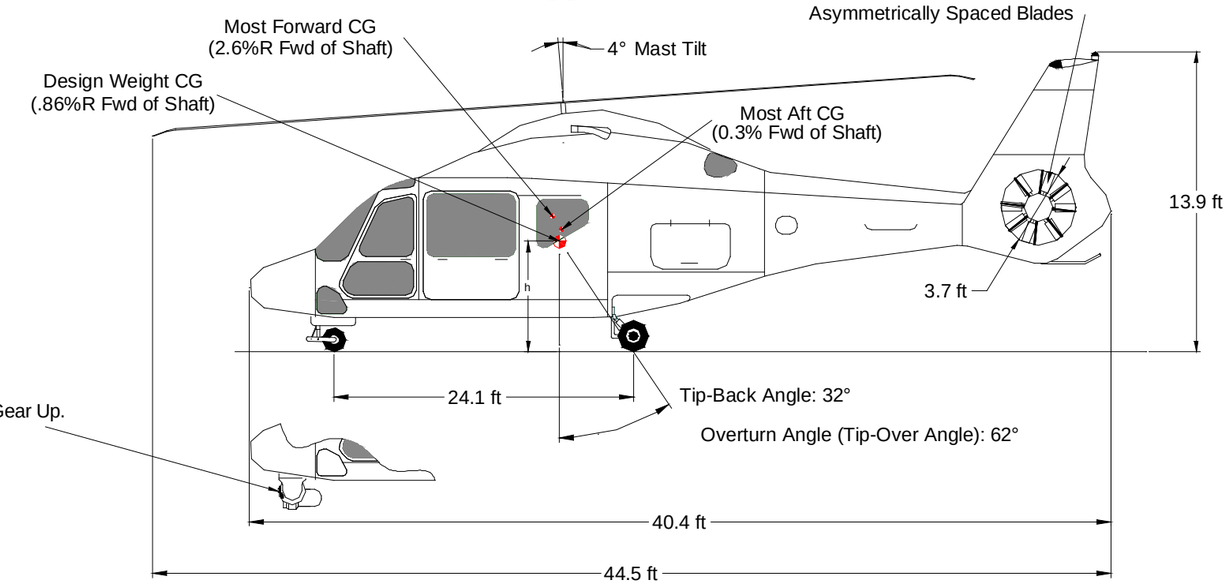

FOLDOUT 4.1: 3-VIEW DRAWING

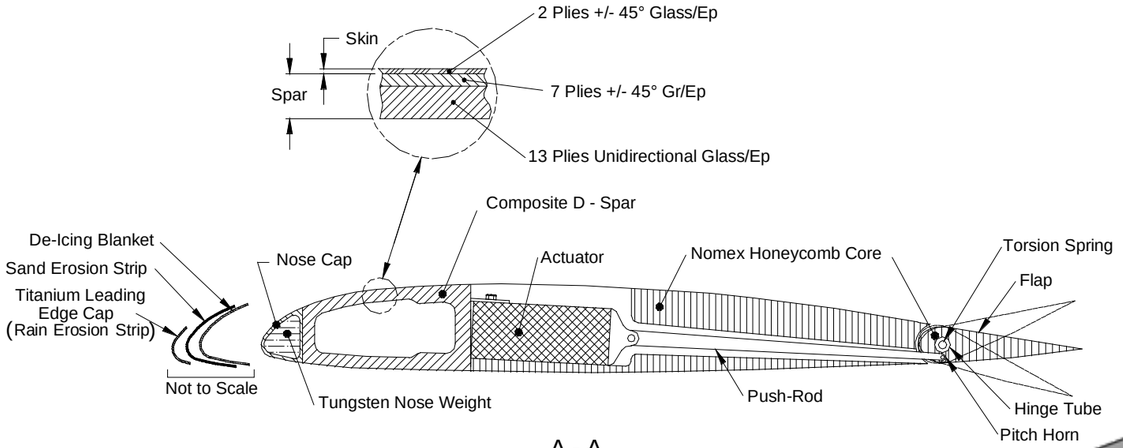

A - A

Detail B

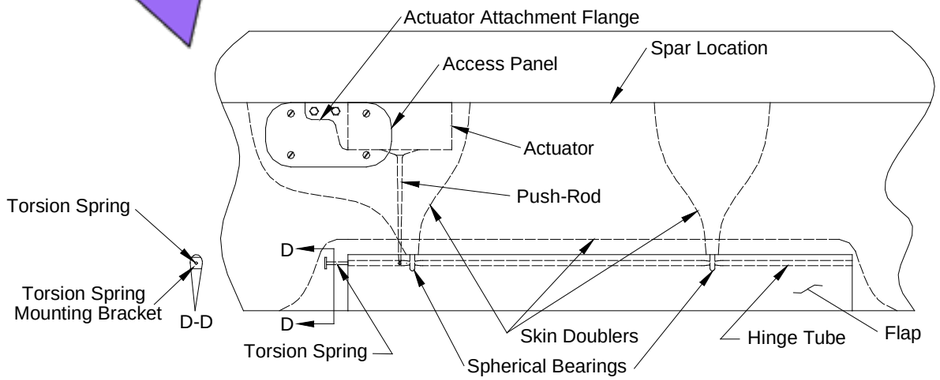

Detail C

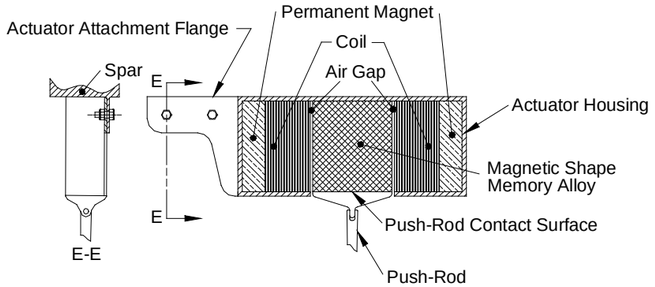

FOLDOUT 5.1: ROTOR BLADE

Blade Planform

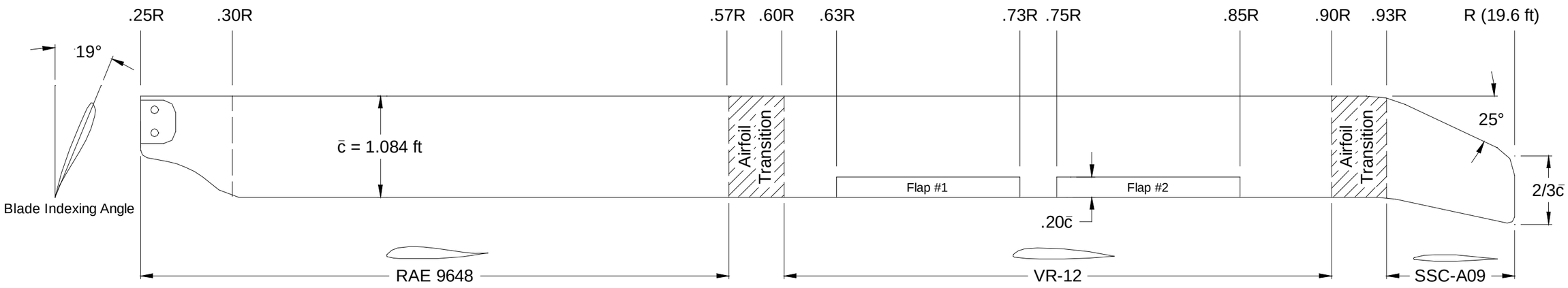

Note: 12.5° Twist Over Entire Blade Span

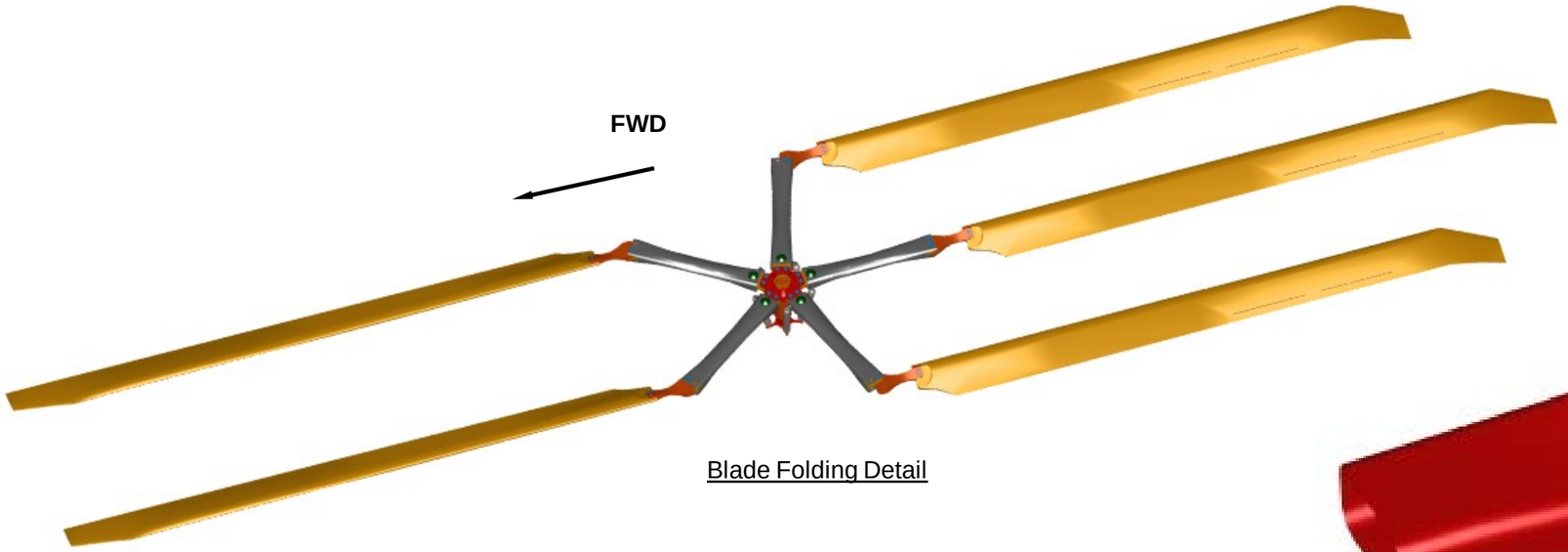

Blade Folding Detail

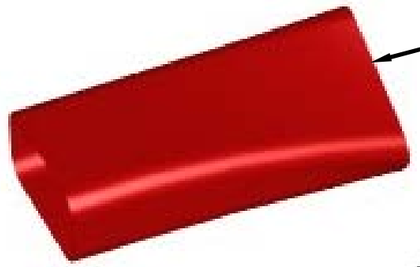

Indexing Splice Fairing

Hub Fairing

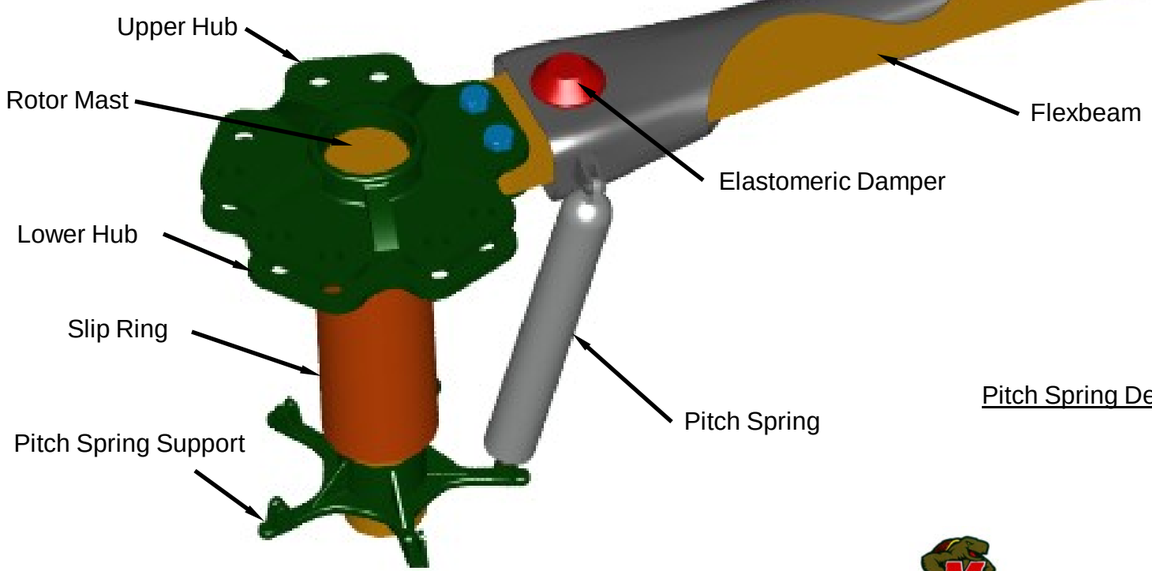

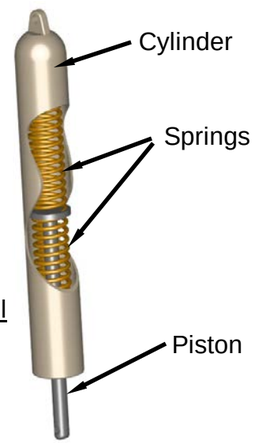

Pitch Spring Detail

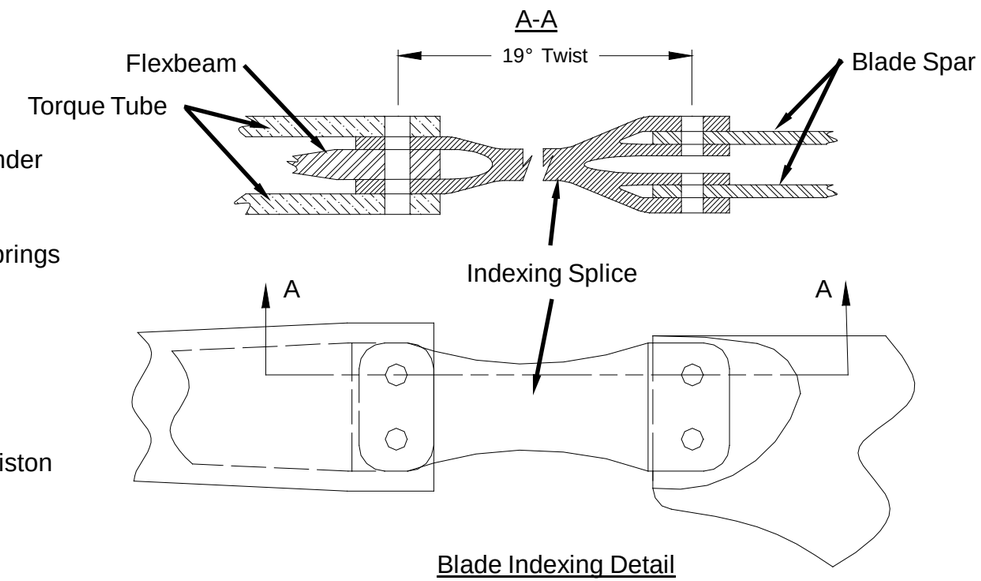

Blade Indexing Detail

Not to Scale

FOLDOUT 5.2: ROTOR HUB

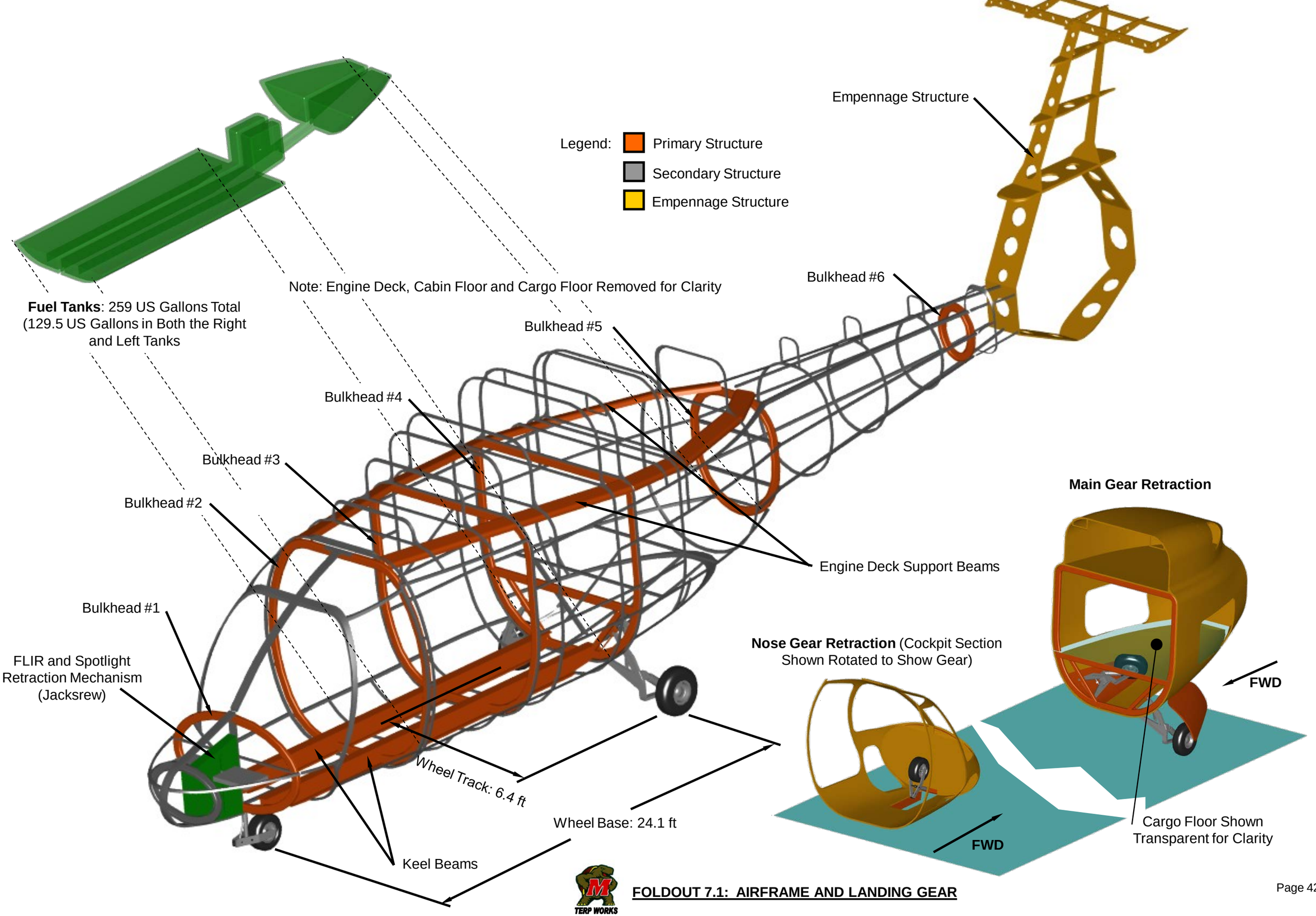
Empennage Structure
Legend:
Primary Structure
Secondary Structure
Empennage Structure
Bulkhead #6
Note: Engine Deck, Cabin Floor and Cargo Floor Removed for Clarity
Fuel Tanks: 259 US Gallons Total
(129.5 US Gallons in Both the Right
and Left Tanks
Bulkhead #5
Bulkhead #4
Bulkhead #3
Bulkhead #2
Bulkhead #1
FLIR and Spotlight
Retraction Mechanism
(Jacksrew)
Engine Deck Support Beams
Wheel Track: 6.4 ft
Wheel Base: 24.1 ft
Keel Beams
Main Gear Retraction
Nose Gear Retraction (Cockpit Section
Shown Rotated to Show Gear)
FWD
FWD
Cargo Floor Shown
Transparent for Clarity

Over Head Console

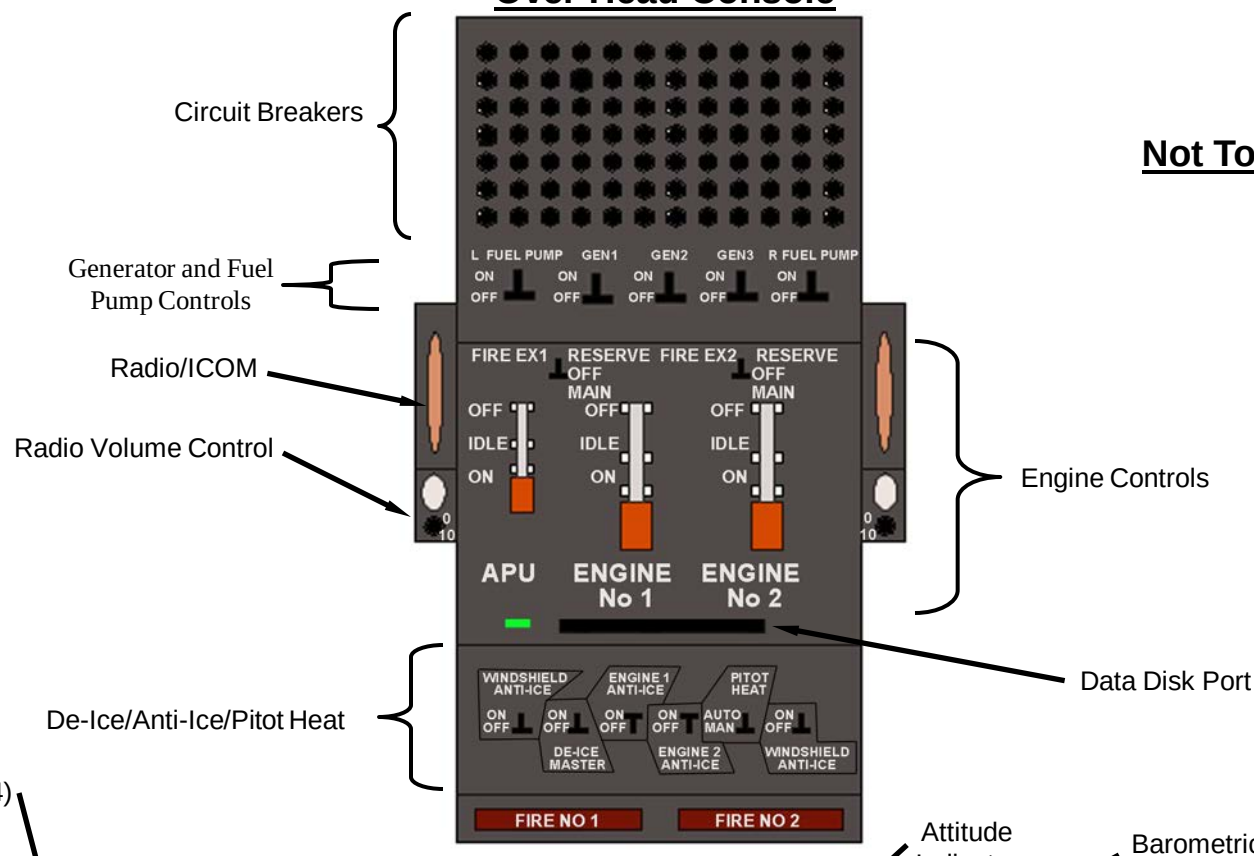

Not To Scale

Instrument Panel

Center Console

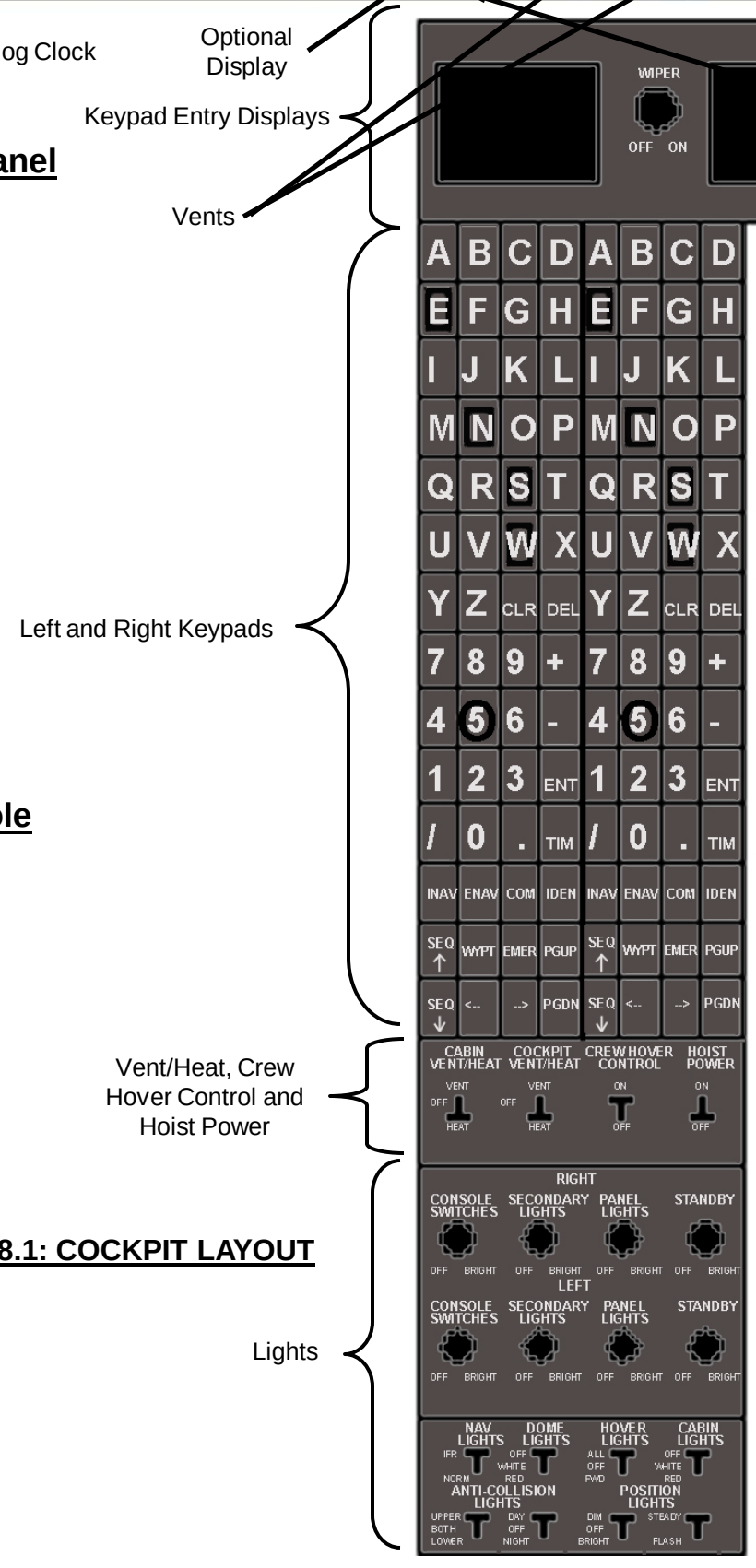

Multi-Function Display (MFD)

Main Page on MFD

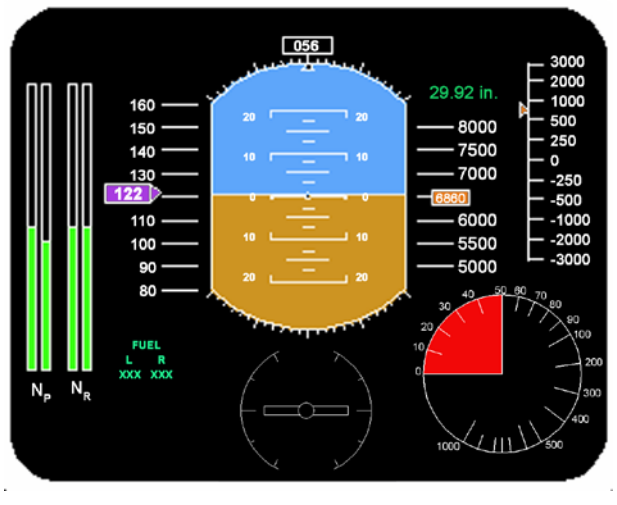

FOLDOUT 8.1: COCKPIT LAYOUT